

Journal of Energy Challenges and Mechanics

ISSN 2056-9386

<http://www.nscj.co.uk/JECM/>

Volume 1, Issue 3
November 2014



Featured article:

Future energy needs and engineering reality

Michael J Kelly

Electrical Engineering Division, Department of Engineering, University of Cambridge, 9 JJ Thomson Avenue, Cambridge CB3 0FA, UK

Journal of Energy Challenges and Mechanics, volume 1, pages 113-118.



North Sea Conference & Journal LTD
2 Charlestown Walk, Cove Bay, AB12 3EZ, Aberdeen, Scotland, United Kingdom
<http://www.nscj.co.uk/JECM/> | jecm@nscj.co.uk | +44(0)1224 875635



TABLE OF CONTENTS

pages

ECM Series Interview: Prof. Michael Kelly FRS FREng, University of Cambridge –
Dr. Henry Tan, University of Aberdeen ([video](#))

[Article 1](#): Future energy needs and engineering reality 113-
Michael J Kelly 118
*Electrical Engineering Division, Department of Engineering, University of
Cambridge, 9 JJ Thomson Avenue, Cambridge CB3 0FA, UK*

[Article 2](#): Developments in the sustainable production of algal biofuels 119-
André DuPont 126
*Program Advisor, United States Environmental Protection Agency, Washington,
DC 20460, USA*

[Article 3](#): Design and performance analysis of a piezoelectric generator by Von 127-
Karman vortexes for underwater energy harvesting 132
Andrea Perelli^{1}, Osvaldo Faggioni^{1,2}, Maurizio Soldani² and Rodolfo Zunino¹*
*¹Department of Naval, Electric, Electronic and Telecommunication Engineering,
University of Genoa, ITALY*
²Istituto Nazionale di Geofisica e Vulcanologia, Rome, ITALY

[Article 4](#): Research on the local and total stability criterion of high arch dam 133-
Guojian Shao, Jiashou Zhuo* 138
Department of Engineering Mechanics, Hohai University, Nanjing 210098, China

[Article 5](#): Defining ecological and economical hydropower operations: a 139-
framework for managing dam releases to meet multiple conflicting objectives 146
Elise R. Irwin
*U.S. Geological Survey, Alabama Cooperative Fish and Wildlife Research Unit,
Auburn University, Auburn, Alabama, 36849 USA*



- [Article 6](#): Numerical simulation of wave loads over a large container ship on mooring state 147-154
Qiu Jin^{}, Tingqiu Li, Zaiqing Li, Jianjian Xin*
WUT-UoS High Performance Ship Technology Joint Centre, Departments of Naval Architecture, Ocean and Structural Engineering, School of Transportation, Wuhan University of Technology, P. R. China.
- [Article 7](#): Effect of PV module frame boundaries on cell stresses in solar cells 155-162
Johannes Schicker^{1}, Christina Hirschl¹, Roman Leidl²*
¹CTR Carinthian Tech Research AG, Europastraße 4/1, 9524 Villach, Austria
²AIT Austrian Institute of Technology, A-1220 Vienna, Austria
- [Article 8](#): Policy Impact on Concentrated Solar Power Technology Deployment: Experience of Global Environment Facility 163-172
Ming Yang^{1}, Hang Yin²*
¹Senior Climate Change Specialist, Global Environment Facility, Washington DC, USA
²Intern, Global Environment Facility, Washington DC, USA



Future energy needs and engineering reality

未来能源需求与工程实际

Michael J Kelly

Electrical Engineering Division, Department of Engineering, University of Cambridge, 9 JJ Thomson Avenue, Cambridge CB3 0FA, UK

mjk1@cam.ac.uk

Accepted for publication on 8th September 2014

Abstract - The need to decarbonize the world economy in short order is the persistent claim of those who think that recent climate change is man-made and the future prospects for mankind are alarming in the absence of action to decarbonize. The statements about what must be done are almost always devoid of any assessment of the engineering reality of what is proposed, and make no reference to lessons on technology change from recent history. In this paper I want to recall some of these lessons and add comments that are further to those made in a previous publication on this topic.

Keywords – Energy policy, global warming, decarbonization, renewable energy

I. INTRODUCTION

The Intergovernmental Panel on Climate Change summarises the current physical scientific understanding of the changing climate every seven years, and complements this with studies of possible impacts and actions in mitigation, the fifth and most recent assessment being published earlier this year [1]. The strength of this case in terms of forward projections is not the subject of this paper but rather the consequences of actions that might be taken in mitigation. There is a difference between policy advice and policy advocacy that seems to have been lost in most of the public debate and in many professional circles where policy is framed. Policy advice puts four scenarios before those (elected politicians) that make the decisions, the up-sides and the down-sides of both doing something and doing nothing on any given issue. We have many scientists who claim to give advice when they are advocating. If you look at, for example, the latest joint report from the Royal Society of London and the National Academy of Sciences [2], you will not see any sections that deal explicitly with the upsides of doing nothing or the down-sides of any proposals to mitigate emissions of carbon dioxide. In the absence of such balance, it is those elements of alarm that are extreme (two or more standard

deviations from the norm in statistical parlance) that get the press coverage.

I have encountered a strong ‘leave it to the engineers’ meme among the climate scientist community – we do the science, they will have to sort out the consequences. If the community was to learn that engineering will not be able to 80% mitigate CO₂ emissions by 2050 without inflicting massive harm on the global economy and mankind in general, it might improve the quality of the public debate. Furthermore, if it was also to learn that it is personal behaviour change that would have the maximum impact over the next 20 years, the members might show leadership in making that change, for example by less frequent flying, and less use of the internet and supercomputers.

More generally, popular writers such as Thomas L Friedman [3], with his ‘Hot, Flat and Crowded’, describe the problems of the world in a neo-Malthusian sense, and then set about suggesting changes to society, which are reasonable but challenging, but in the background lurks the need for a radical break-through discovery of a source of cheap, plentiful, clean, green electrons. When we consider that nuclear fission is the only new breakthrough source of energy in the last 200 years, and we have sought for fusion based energy for 60 years without success, a sober sense of reality about the immediate prospects of a breakthrough is essential here.

At the time of the IPCC publications, I prepared a paper ‘Technology Introduction in the Context of Decarbonization: Lessons from Recent History’. I sent it to a number of professional societies and academies, but it was picked up and published [4] by the Global Warming Policy Foundation. The paper was peer and Peer reviewed both before its publication and since. No-one has seriously challenged any of the scientific or engineering arguments I made therein, or the numbers that I quoted. In this paper I will summarise the same points, but only report material that is supplementary to that

provided in the original paper. I summarise ten lessons, and make three concrete suggestions about the way forward. In the final section I deal with other issues that are germane to the general arguments. The lessons below are interrelated as one can see from the frequent cross-referencing.

1. RELEVANT LESSONS FROM RECENT HISTORY

1.1. New energy technologies improve the lot of mankind

Many premier journals report breathlessly each week of another breakthrough that will cure cancer, or solve the energy problem. However in the transition from science to a technology, and from a technology to a product for which there is a willing market, there are many hurdles of which the originating scientist remains rather ignorant, too often blithely so. The attrition rate is very high, and simple successes in new technologies in the modern day occur when an as yet unmet societal need is suddenly met. That need may or may not have been predicted. The role of liquid crystals in making electronics portable is a case in point: the long term goal of a flat screen television took another 30 years of intensive development after the first liquid crystal display was sold. The mobile phone was foreseen as a convenient way of communicating by voice, but not by text or picture. The smart phone performs the functions of over 20 disparate and bulky items of only 20 years ago! Any new energy technology is going to have to go with the flow of human development. Where the new technology will replace an existing one, as would be the case of a new energy technology for transport, domestic energy or industrial processes, there will be the added challenge of dislodging an incumbent: the new technology will have to be sharply superior to overcome the problem of stranded assets associated with the existing technology.

1.2. The scale of the decarbonisation problem is unprecedented

Over 90% of all the energy provided world-wide for modern civilization as we know it since 1800 has been provided by burning fossil fuels. Nuclear, hydro and geothermal power, together with the historical burning of wood and straw, provide of order 15%. Even today the first generation renewables provide less than 1% of the world's energy. Furthermore since the mid-1980s, the level of fossil fuel energy and low carbon energy have been growing such that in spite of all the efforts, renewables are not making a dent in the share of total energy coming from fossil fuels which remains stubbornly at about 85% [5]. The implication of this is that the current level of activities will get us nowhere near the 80% decarbonisation targets for 2050 being advocated by the IPCC and others.

1.3. Tackle megacities first

Over half the world will live in cities by 2050, and nearly all the schemes for renewable energies being so strongly advocated in the EU and US are inappropriate for mega-cities. Think about Hong Kong, with a population now 7.2M of confined onto an area of just over 1000km², and a density of

6500 people per sq km. Much of the land not used for buildings is very steep hills, covered in dense shrub and is prioritised as green space. None of the present generation of renewable energy technologies is going to be able to contribute anything significant towards powering Hong Kong in 2050: there is not enough land area or shallow ocean. Only fossil fuels (with or without carbon capture) and nuclear power will be available at the right scale. These have the energy density of fuels needed for city living. It is one thing to conceive of a low density city like Phoenix AZ becoming a solar city, it is quite another for any of the dense megacities around the world.

1.4. Only deploy new energy technologies when they are mature and economic

It is 40 years since the first oil crises in the 1970s provided the impetus that has led to the present generation of wind and solar energy, as examples of renewable energy. Twenty-five years ago, there was an initial roll out of these technologies in the Mohave Desert, and today there are many square kilometres of industrial dereliction of abandoned solar and wind farms that could not generate a revenue to maintain themselves in operation without subsidy [6]. The windmills were small and the solar panels not as good as today. The clear lesson is that they were neither economic nor mature.

Will they ever mature and become economic? If one compares the energy density of the land used to generate energy, one comes up against a stark contrast. The nuclear reactor at Sizewell B occupies an area that is of order 0.1km² within which a continuous 1.3GW of electricity is generated using nuclear fuel, and energy density exceeding 10GW/km². A coal fired power plant can generate comparable energy in the same area, but there is a factor of 1-10 million between the energy density of fossil fuels and of nuclear fuels. In stark contrast, the typical biomass, wind and solar energy density is at the level of 1-20MW per square kilometre, a factor of order 10³-10⁴ less [7]. Over one thousand square kilometres or one quarter of the Fen Country in the East of England, presently growing food, would be needed to produce even 1GW of electricity [4]. These are huge factors that will not be impacted by lengthening the blades of windmills, or increasing the efficiency of solar cells by a few percent. Anywhere that land is at a premium, and that is around most large cities in terms of foodstuffs, these technologies will not change the world in 40 years, let alone 400. If the costs of access, construction and maintenance remain high (see next section), the question of economic competitiveness will be a very tough one ever to resolve.

1.5. Salutory lessons from the first round of renewables technologies

A recent quantitative analysis of the solar energy installations in Spain gives a very sober perspective on the energy rate-of-return of solar energy [8]. Because of legislation associated with subsidies, much clean data is available in the public domain for analysis. It is possible to take the intense period of solar installation up to the year 2009 when no solar installation took place in Spain in view of the

global financial crash. It is possible to get reliable estimates of all the costs in getting those solar panels installed and maintained over a 25 year lifetime; this includes the infrastructure of roads and cables needed to install the panels and collect the electricity, washing the panels four times a year and six times if they are near dusty road, the costs of surveillance and security, interest on the loans on capital raised, the cost of manufacturing and transport of the panels, the relevant duties payable, and the cost of renting the large tracks of land involved. These total costs can be converted into an equivalent total energy using the ratio of the GDP in Spain to the total energy consumed by the Spanish economy. This gives the energy invested into the sector. When the actual metered energy generated to date is extended over the 25 year design life, the result is the energy out. The ratio of energy out to energy in, called the energy return on investment (EROI), is 2.5. Thus 40% of all the energy to be generated is already used in fossil fuel equivalents to produce the solar energy system in the first place. A parallel exercise shows that at this level, if all Spain's energy were to come from solar energy in future, there would not be enough energy or revenues left over to support a modern society for which it is estimated that an EROI of order 10 is required from the main source of energy in the economy. Note that even if the solar panels were free (they were only 33% of the costs in the Spanish example), the remaining costs are considerable, and they all scale with the large areas of land needed. Furthermore, if one adds in the extra cost of installing batteries to store the electricity between peak generation and peak demand, the energy input goes up by more than the extra energy, and the energy return on investment decreases still further [9]. The reason that these figures are profoundly disappointing is an EROI of over 10 is needed to support a modern society that includes functions such as higher education and the arts [8]. The comparable fossil fuel EROI is about 30, with hydropower at 49 and nuclear power at 75 [10]!

The same analysis can be applied, *mutatis mutandis*, to wind energy and to cultivated biomass, where the same intrinsic energy diluteness at source is the insurmountable challenge. The conclusion is that a substantial element of fossil fuel energy will be needed in 2050 to maintain a civilized society in Spain or elsewhere.

1.6. Subsidies for premature rollout are a recipe for disaster

One theory of technology introduction is to use subsidies to encourage manufacturers to go down the learning curve and cut the costs of manufacture in the process, so that subsidies can be allowed to wither without undue impact: Friedman [3] describes this in the context of catalytic converters for automobile. In the international energy markets this so far has been a recipe for disaster. The cuts to subsidies caused by the financial crash have caused the bankruptcies of companies across the world working in renewable energies, without any stable conglomerates being formed as had happened in earlier technology introductions, as with the telephone, railroad etc. The scale of the present energy challenge and the total reliance on reliable and affordable energy, let alone sustainable energy, is such that subsidies have been too small and ephemeral.

Unlike high-technology interventions where 5-10 years of intervention will see the required take up, infrastructure technology like energy has timescales of order 40 years, and few countries have stable multi-party multi-government support that lasts that long.

1.7. Technology developments are not usually pre-programmable

Writers such as Friedman [3] and others hope for a technology breakthrough that will provide a new clean cheap and sustainable source of electrons for an electrically powered world. If that should emerge over the next decades, it will be a bonus. When 'necessity is the mother of invention' is cited in the present context, it is a mistake. The solutions to earlier necessities were largely brought about by the timely deployment of newly known science. Radical new technologies over the last 200 years have followed on from scientific discovery, typically in a timescale of 40 years for automobile, telephone etc. This time, apart from nuclear fusion, there is simply no new science in any primitive form that is offering access to untold sources of energy. Nuclear fusion has been under investigation for 60 years, and it is not clear that faster progress would have been made if the budget for that research had been doubled. There are lengthy timescales for building the equipment, and global collaboration has gone about as fast as possible. Even if there was a radical breakthrough tomorrow, the level of further engineering and technical development required to provide a stable, reliable and affordable source of electricity is still decades away in terms of contributing (say) 10% of the world's energy needs. It would be irresponsible with nuclear technology to promise anything faster, even if the effort were increased. The current battery technology has struggled to provide energy for portable electronics - battery life is still measured as a few hours between recharge - and there is no question of batteries supporting (say) Hong Kong in any form of load balancing mode.

1.8. Nothing will happen if the population is not trusting

There were a number of millennium development goals devised and adopted by the UN for completion in the period 2000-2015. Some have been achieved, others have not. This is the only basis on which the global population has experience of solving pressing problems facing humanity as a whole. While environmental degradation is one problem, all the progress that has been made has come from advanced economically sound countries cleaning up past mistakes and preventing future ones. The lack of clarity with which long-term climate change will really make major impacts does not seem to generate the public appetite for much larger scale public intervention. When some of the more alarmist views have not come to pass over the 20-30 years since they were first made in terms of vanishing Pacific Islands or millions of climate refugees, the impetus to achieve a global agreement to circumscribe personal behaviour in the cause of reducing CO₂ emissions is simply not there. A recent call for a global

regulator 'with teeth' to curb air-travel did not get fulsome or widespread support [11].

1.9. Finance is limited, so actions at scale must be prioritised

I have estimated that one could retrofit all the UK building stock over 40 years at the cost of £1.7T, £40Bpa [4]. This would require an army of workers of order 1M, i.e. comparable with the health service, and a very large increase in the supply chains. Using state of the art technologies of today, but leaving the interventions to be future-proof, the result would be to halve the energy consumption in buildings (both domestic and non-domestic), and reduce the nation's carbon foot print by 23%. The payback time in terms of savings in energy bills is too long to justify raising the money on the capital markets so that some state intervention would be needed. This intervention would compete with the Government's ability to raise funds for supporting a renewal of the current energy infrastructure for which £200B over the next decade is the widely quoted figure. How to factor such enormous sums into national budgets while trying to maintain contemporary commerce, manufacture, agriculture, defence and logistics is a square that has not been circled. What is the appropriate fraction of the national budget to be spent on energy over the coming decades, given it has been about 8% over recent years?

1.10. If the climate imperative weakens, so does the decarbonisation

In the early days of climate change 25 years ago, the scientific community pointed to rising globally averaged surface temperatures as the clearest evidence of a problem. Since the start of the present hiatus in the globally averaged surface temperature, now 17 years old, the rhetoric has used other signals of climate change such as rising sea levels, ocean acidification, extreme weather events, melting polar icecaps etc., as the evidence. Since sea level rise has not been accelerating, and severe weather events not become more common (although the damage is because there are more of us in the way with more possessions at risk), the rhetoric is under challenge by the accumulating real-world data. Last year over 70 peer-reviewed papers came to the conclusion that the sun was playing a greater role in the climate change of the last 50 years, and this year this trend is continuing, with the possibility of a return to a little ice-age by mid-century being predicted [12]. There would be a supreme irony if that were to happen, as every ton of human generated CO₂ in the atmosphere would be called upon to help feed 9B people in 2050 rather than the 1B people during the last little ice age.

The IPCC's most recent (5th) assessment report [1] has pulled back on the severity of some of their more catastrophic projections in the face of clear evidence that their climate models are running systematically hotter than the earth itself. If the temperature hiatus lasts another decade, we will be approaching 30 years without a temperature rise while the level of human-induced CO₂ will have increased by over 50%, then anyone respecting the canons of science as the explanation of nature will demand a going back to the drawing

board as far as the current understanding of the atmospheric temperature systems is concerned.

These ten lessons together indicate profound shortcomings in the understanding of the engineering realities associated with decarbonisation, and in many cases the poor return on investment represents an opportunity cost that has inhibited possible human development in other quarters, as outlined in 2.3 below.

II. THREE PRACTICAL PROPOSITIONS:

2.1. Work within business as usual with a focus on the efficient use of energy

Since energy costs money, it has always been an imperative to reduce energy use, and that is likely to continue and especially if fuel continues to become more expensive. In the case of several energy-intensive industries such as metals, ceramics and cement, there are limits to the potential energy savings set by basic thermodynamics.

2.2. Derisk infrastructure projects

Since energy is expensive, and energy infrastructure is supposed to last for decades, we cannot afford to get it wrong. Small scale deployment for trialling new technologies is appropriate, but a hasty roll-out leaves stranded assets there to attract the mockery of passers-by for decades to come [6]. By definition such unused assets have an opportunity cost, and we need much care to avoid mistakes. The imperatives of climate change are not sufficient to overrule this principle. How much of the investment over the last 30 years in greening the economy will be written off? We simply must be much more sophisticated in our approach to decarbonisation than we have been to date.

2.3. Public attitudes and personal behaviour are much the most effective place to work now

Colleagues in Cambridge have estimated that people in the UK could live a civilized life on about half the energy usage per person per day [13], provided the citizens were more overtly energy conscious and came to regard energy profligacy as deeply antisocial. Cars could be much smaller and lighter if we asked for them to be: so far we like the acceleration and safety associated with large and heavy vehicles and the demand for fuel seems remarkably price inelastic. Public attitudes and behaviour have changed in issues like smoking in public confined spaces, drink-driving and wearing seat-belts. In the short term, the energy, cost and other savings from behaviour change dwarf anything made possible by new technology. Even IT is now an energy intensive operation, with each google search using enough energy to boil water for a medium size cup of coffee, at over a trillion searches a year and growing at 10-15% in recent years [14]. Exemplary changes in personal lifestyles should be undertaken by the advocates of decarbonisation as a sign of their commitment.

III. OTHER GENERIC ISSUES

3.1 Demographics

No-one yet factors in the demographic consideration of peak population predicted for the period 2050-70 so that much new infrastructure may be needed for only 100 years at most. Some predictions indicate a population back at 7B by 2100, and we will have unused assets for 2B people on our hands [15]. How is it best to prepare infrastructure with a finite lifetime in mind? There are parts of Eastern Europe where the population has been in absolute decline for 20 years now, and towns are being abandoned and villages razed. Current fertility trends if continued would have the Italian population down to 8M by 2100 and that of Germany down to the present population of Berlin! [16].

3.2 Decarbonization as a Focussed Global Project

Suppose the world were to agree to provide £1T per year for a decade to be spent on mitigating climate change by reducing carbon emission. This is about enough to capture all the CO₂ from existing coal-fired power stations. It is questionable whether it could be done in ten years. What would we notice in terms of future climates? The answer is simply that no one knows. The same £10T would enable the poorest 1B in the world to receive £10K each, and one could expect to see some very tangible change after ten years in terms of the elimination of world poverty on the (admitted large) assumption of global good governance. Mitigation of future climate change is not a sufficient justification for any large scale engineering project in the absence of foreseeable and measureable outcomes. The insurance premium argument does not work – the risk remains uninsured.

3.3 A Day of Reckoning

In the absence of a temperature rise in the next few years, there should be a day of reckoning about the way that the current stress on climate mitigation came to the fore in the public debate - even more so if the sun heralds a little ice age, where the global temperature cools and the world struggles to feed 9B in 30-40 years. We will ask how it was possible that we prepared for the wrong 'catastrophe'. Work to reduce resource use and waste is an intrinsically good thing, but the large-scale mis-investment in averting something that only ever might have happened, should not go unreviewed and without sanctions. At the very least, the key scientists will have to be ever more circumspect in their pronouncements, and that would be a welcome return to the canons of normal as opposed to post-normal science that prevailed until recently, and still prevails in engineering disciplines, where individual engineers can be held legally liable for the consequences of their actions and professional judgements. The same discipline should apply to those who advocate spending public money on major projects. The lack of continued incisive debate, closed off by expressions such as 'the science is settled' has done untold damage to the reputation of sciences which, as a class, will be vilified as rent seekers. The first

debate on this whole subject at the Royal Society in London was held only two months ago [17] under the title 'What is the right level of response to anthropogenic induced climate change?'

3.4 Adaptation

Professor John Holdren the US Presidential Scientific Advisor is quoted [18] as saying: "What this means," he said, "is that we have to figure out how to meet transport needs with less oil and economic aspirations with less carbon dioxide. There are only three options: Mitigate, adapt, suffer." The Dutch down the centuries have been exemplary as they have coped with rising sea levels: they have adapted as and when necessary. Again, the Thames barrier has saved London from flooding and the height of the barrier will be increased in 20 years in good time to cover the medium term future. Here the problem is not global warming but that the East of England as a whole is sinking. These are the entirely positive and practical solutions that apply to most of the problems that have been adduced as the result of our use of fossil fuels to energize modern civilization. Moreover, adaptation is a trait of humanity down the ages, with the few exceptions proving the rule.

IV. CONCLUSION

The major actions currently taken in the name of decarbonizing the world economy are ineffective and unlikely ever to succeed. We need a debate that is altogether more sophisticated, open and humble, and policies that might succeed rather than being guaranteed to fail. I end with a classic example: two of the three aluminium smelters in the UK have closed because of higher energy prices, and the UK imports aluminium from coal-fired smelters in China, with a net addition to the global CO₂ emissions – total madness!

ACKNOWLEDGEMENTS

I wish to thank the many people with whom I have debated these topics, and who have provided me with material. I wish to thank the organisers of the 2nd International Symposium on Energy Challenges and Mechanics for the opportunity to present these views to a group of 130 international energy researchers from 40 countries, who did not provide any counterevidence to the major points I made.

REFERENCES

- [1] <http://www.ipcc.ch/report/ar5/index.shtml>
- [2] https://royalsociety.org/~media/Royal_Society_Content/policy/projects/climate-evidence-causes/climate-change-evidence-causes.pdf

This paper purports to be purely a scientific description in the form of answers to 18 questions. Taking one in

particular, we note the last sentence as a totally inadequate counterbalance!

17: Are climate changes of a few degrees a cause for concern?

Yes. Even though an increase of a few degrees in global average temperature does not sound like much, global average temperature during the last ice age was only about 4 to 5 °C (7 to 9 °F) colder than now. Global warming of just a few degrees will be associated with widespread changes in regional and local temperature and precipitation as well as with increases in some types of extreme weather events. These and other changes (such as sea level rise and storm surge) will have serious impacts on human societies and the natural world.

Both theory and direct observations have confirmed that global warming is associated with greater warming over land than oceans, moistening of the atmosphere, shifts in regional precipitation patterns and increases in extreme weather events, ocean acidification, melting glaciers, and rising sea levels (which increases the risk of coastal inundation and storm surge). Already, record high temperatures are on average significantly outpacing record low temperatures, wet areas are becoming wetter as dry areas are becoming drier, heavy rainstorms have become heavier, and snow packs (an important source of freshwater for many regions) are decreasing.

These impacts are expected to increase with greater warming and will threaten food production, freshwater supplies, coastal infrastructure, and especially the welfare of the huge population currently living in low-lying areas. Even though certain regions may realise some local benefit from the warming, the long-term consequences overall will be disruptive.

- [3] T.L. Friedman, 'Hot Flat and Crowded – Why we need a green revolution and how it can renew America'
- [4] <http://www.thegwpf.org/content/uploads/2014/03/Kelly-lessons.pdf>
- [5] <http://rogerpielkejr.blogspot.co.uk/2014/06/treading-water.html>
- [6] Google the phrases 'abandoned solar farm' and 'abandoned wind farm'
- [7] Concerning the areal efficiency of renewable energy harvesting, see D.J.C. MacKay, *Sustainable Energy: Without the Hot Air*, UIT Cambridge, 2009. Available from <http://www.withouthotair.com>.
- [8] P.A. Prieto and C.A.S. Hall: 'Spain's Photovoltaic Revolution: The Energy Return on Investment', Springer 2013.
- [9] <http://theenergycollective.com/barrybrook/471651/catch-22-energy-storage>
- [10] D. Weißbach, G. Ruprecht, A. Huke, K. Czerski, S. Gottlieb, and A. Hussein, 'Energy intensities, EROIs (energy returned on invested), and energy payback times of electricity generating power plants', *Energy* 2013; 52: 210-221.
- [11] <http://wattsupwiththat.com/2014/08/12/southampton-university-we-need-a-air-travel-regulator-with-teeth/>
- [12] <http://bit.ly/1bpzysw> and Vahrenholt F and Luning S, 'The Neglected Sun', Stacey International, 2013.
- [13] Bajzelj B, Allwood MJ and Cullen JM, 'Designing climate change mitigation plans that add up', *Env. Sci Tech* 2013; 47: 8062–8069.
- [14] <http://www.internetlivestats.com/google-search-statistics/>
- [15] Wolfgang Lutz et al, 'The end of world population growth', *Nature* 412 543-5, 2001.
- [16] Fred Pearce 'Peoplequake', *Transworld*, 2011: p 294.
- [17] http://www.foundation.org.uk/Events/pdf/20140616_Summary.pdf
- [18] <http://slice.mit.edu/2010/10/26/johnholdren/>



Developments in the sustainable production of algal biofuels

藻类生物燃料可持续生产之发展

André DuPont

Program Advisor, United States Environmental Protection Agency, Washington, DC 20460, USA

Andy.dupont@gmail.com

Accepted for publication on 23rd September 2014

Abstract - Many recent scientific developments have made the commercial production of algal-based biofuels more economically feasible and adaptable as a drop-in fuel for consumers. These new innovations make the principles of sustainability more significant because of the need to conserve natural resources in the production of biofuels. This paper highlights new scientific discoveries that could significantly improve the production rate for algae biofuel production facilities. This paper will emphasize the concept of designing facilities that blend in with naturally occurring topography to enhance land management principles that are critical for acceptance of this technology where public opinion is important. The scientific, engineering and environmental community will find that sustainable management of algae-based facilities will provide a healthier economic model for the long-term growth for this emerging industry when good public trust is part of the design concept.

Furthermore, this paper will review fundamental scientific guidelines that can improve sustainable biofuel development in emerging markets throughout North and South America, Europe, the Middle East, Asia and many countries that have large populations and thriving communities near the seacoast. A comparison of different technologies and their reported economic structure will show critical factors that make algae biofuel production more publicly acceptable for industrialized and developing countries. Public perception of this nascent technology could be greatly enhanced by using the guidance of sustainability in creating biofuel facilities that could be economically competitive with conventional petroleum fuels.

Keywords - Sustainability, economics, design, guidelines

Disclaimer: This document is an independent, non-federal publication, and the views expressed in the document do not necessarily represent the views of the United States Government or any of its agencies. The Federal employee participating in the affairs of this publication does so in a private capacity, not on behalf of the Federal Government.

I. ECONOMICS FACTORS

The information provided is for educational purposes only and reflects observations that are available to the general public. This document merely provides suggestions on the principles of sustainability that may improve the development of biofuel production.

The first critical step in establishing a new production facility for algal biofuels is to establish the market demand for both consumer and military use. The market price and demand in the United States varies by the type of consumer. The United States Department of Defense has a great interest in the development of biofuels because of the overall cost of managing fuel cost to support worldwide operations.

For the military in a conflict situation, the purchase cost of petroleum products is almost incidental when compared to the cost of transporting fuel to the location where it is needed in a war zone. The cost of shipping and danger of shipping the fuel is far higher than the purchase cost. Because of the urgent need to provide liquid fuel in war zones, the military is tremendous financial resources to encourage the development of biofuels that can be produced closer to the intended location of use. Also, biofuels are tested for quality and compatibility with existing engines. Because of all these factors, the U.S. Department of Defense will continue to purchase biofuel for testing at very high prices to encourage the development of infrastructure to produce biofuels that can be dropped into conventional jet engines and many types of land vehicles.

However, for the typical American consumer, the most important factor is reducing fuel cost for their current vehicles. Low cost is the predominant factor for most consumers. Ethanol production from fermentation of corn is the most common biofuel in the United States. Many farmers grow corn

in the Midwest of the U.S. and the conversion of corn to ethanol is the primary biofuel available in the U.S. Ethanol is considered a drop-in fuel and widely supported by the American public and automobile industry. Currently, automobiles in the United States can use two different types of ethanol mixture for gasoline-powered vehicles. The blend of 10% ethanol blend with 90% gasoline is the most standard fuel mixture. In addition, the “Flex Fuel” blend of 85% ethanol and 15% gasoline blend is available in many locations.

Algal biofuels will certainly become more important in the future, but their costs to consumers will be crucial in developing a sustainable regional biofuel market. From this concept we can better understand the true financial and economic benefit of algal biofuels. To begin this process, let us review the price of biofuels that have been reported in the U.S. The table shown below indicates both the low and high cost of biofuels recently reported. To illuminate the significant difference between the consumer goals and military use requirements, notice the great variation in the reported price of biofuel in Table (1) below.

TABLE 1, REPORTED PRICES OF U.S. BIOFUELS

Biofuel type	Consumer	Product Type	Price (US \$)
Generic (Catalina, Waste vegetable oil, algal biofuel, pyrolysis of wood, many others.)	Military	Various Biofuels (quality assured for specific use)	\$ 59.00/ U.S. gallon ¹ £ 9,20 /liter
Algal Biofuel	General Consumer and Military	Ethanol	\$ 1.27/U.S. gallon ² £ 0,198 /liter

The price variation is very substantial between military requirements and general requirements. The high cost of biofuel at £ 9,20/liter (\$59/gallon) represents a variety of biofuel development technologies. The biofuels for military utilization are from an unspecified source. Because of stringent Air Force requirements, liquid biofuel is quality assured and tested as a drop-in fuel for military application. The low cost of £ 0,198 /liter (\$ 1.27/U.S. Gallon) represents biofuel production from one small research facility located in sub-tropical climate of Florida. It is noteworthy to mention that the United States Government has funded the development of biofuel production for the last few years and it is important to emphasize the dedication of many accomplished scientists that have contributed their time and energy on the development of biofuels for both the military and public sector.

Many stakeholders will question the great price differences between military grade and consumer cost for different biofuels. The higher price for military biofuel includes development cost and the cost of quality assurance that is required for military jet engines and diesel vehicles. The lower cost of public sector biofuels centers on the production of low cost ethanol and may not include the cost of quality assurance that is needed for military applications. Biofuel production hinges on the type of raw materials; labor cost production; and

the selection of process. The development of algae based biofuel depends also on the type of reactor, type of algae strain, availability of low cost nutrients, and environmental conditions. The lower production cost of biofuels for the general public is focused on drop-in fuels that are accepted by an established market.

II. BIOREACTOR DESIGN DEVELOPMENTS



Fig. 1, Algae growing in an open raceway pond³

The most common approach of cultivating algae for biofuel production is centered on facilities that use open raceway ponds as depicted in Fig. 1. In many cases, raceway ponds grow algae with a high lipid content that can be refined to biodiesel. In this commercial production mode, the growth rate of algae is a major component of the overall reactor or process design. Other skilled researchers are focused on developing cutting-edge biofuel reactors for full-scale commercial production.⁴ Recently, the Algenol facility depicted in Fig. 2, is located in Fort Myers Florida and has been using an innovative design for the production of ethanol from algae. The design emphasizes the concept of growing algae in clear transparent bags. The concept of growing algae in closed plastic bags is not new, but the overall approach of producing ethanol using an innovative reactor is a real game changer for multiple sustainability objectives.



Fig. 2, Algenol facility produces ethanol in a closed bag system⁵

The development of growing algae in large transparent bags must be analyzed to explain why this progression appears simple, while in fact the technology is very innovative and sustainable. The requirement for solar energy and amount of photons that can penetrate a plastic bag has been well documented by Dan E. Robertson et al.⁶ According to Robertson, photo-synthetically active radiation (PAR) with a wavelength from 400 to 700 nm, represents 39% of the total energy directed towards the earth by the sun. However, because of moisture in the air, the ground-incident radiation for photosynthesis is increased to approximately 48% of the total solar radiation available. According to Robertson, different locations receive PAR ranging from a low value of 2380 MJ/m²/year (Cambridge, MA) for a northern climate to 3460 MJ/m²/year (El Paso, TX) located in the southern United States.

In the research performed by Robertson, the authors described that natural sunlight can have a reflective index loss of 5% for each media layer of the closed plastic bag. If the bags are made of a protective layer and inner container, then the reflective loss (Fresnel loss) could be 10% of the solar radiation. However, the use of an open pond results in a single/water interface with an estimate Fresnel loss of approximately 2%. Based on this understanding, it would seem that open ponds have lower losses for absorbing PAR.

Both the closed system and open raceway ponds receive the same PAR at a fixed location. Furthermore, it has been shown that open ponds have a lower loss of reflective radiation. However, the conversion efficiency for the closed system appears to be greater than an open pond reactor. The closed system converts more of the solar photons than the open raceway pond. The overall conversion efficiency of the closed system is reported to be seven times larger than the conversion efficiency of the open pond system. The efficiency of an algae reactor to capture solar energy appears to depend on other factors beyond reflective losses.

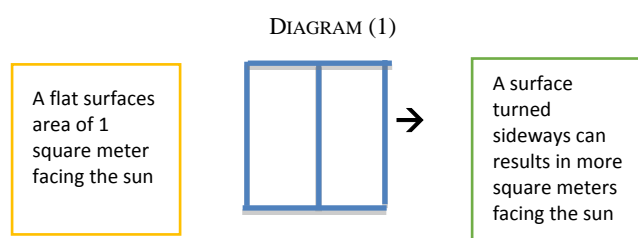


Fig. 3, Electric radiator

An attribute of designing a reactor to absorb distributed solar energy is the amount of surface area that is available for energy or photon transfer. An open raceway pond appears to offer standard growth rate for algae, but this may not be the best approach for producing ethanol from algae. A key component of designing a specialized algal reactor to produce ethanol centers on the available surface area that absorbs solar energy.⁷ In the air condition industry, we see the concept of

thin metal blades in racks that are used to distribute heat energy from the compressor. In cold northern climates, many homes use a similar approach by using radiators to distribute heat within a limited surface area. Fig. 3 illustrates the concept of long thin blades that radiate heat. Because the blades are thin and perpendicular to the area of heat release, radiation of heat occurs more quickly than using a single flat surface.

Notice in Diagram (1) that we have approximately one square meter of surface area facing the effective area. If the surface area is turned 90°, more of the surface area of the blades becomes exposed. The result is a theoretical six-fold increase in energy release from the same radiator. Diagram (1) below is a depiction of the effect of turning the flat surface of a radiator 90° or turning the blades perpendicular to allow faster transfer of radiating energy. See Diagram (1) that describes turning a flat surface perpendicular to sunlight:



If the surface area of the radiator is flat, it does not allow for fast distribution of heat. Because only one side of the surface area is exposed, only one square meter of surface area is available to distribute heat. However, with perpendicular blades of the radiator, this allows for 3 blades with a thin surface area to radiate heat. The actual surface is theoretically 6 times the surface area of a flat panel generating heat.

This is a fundamental concept that appears to occur when growing algae in flat panel-like bags that are perpendicular to the sun.⁸ Looking at this from a conventional approach we examine the basic principle of improving the surface area for algae aquaculture. Because the absorption of sunlight occurs only in the top ½ inch to ¾ of the surface of water, increasing the surface area also improves the growth rate because more sun energy can reach the algae culture per square meter. It appears that photons from strong sunlight are reflected from one flat panel and then absorbed by an adjoining panel to increase the overall absorption of solar energy for the closed bag system.

The technique of increasing the surface area appears to improve the growth of rate of algae for a fixed growing area. In a previous book published in 2009⁹, my analysis concluded that algae growth of 20 grams per square meter of surface area could not provide a strong incentive for the production of algae for commercialization. However, at a growth rate above 50 grams per square meter of surface area, the production of algae for biofuel production becomes more competitive and feasible for commercial production. The utilization of bags for growing algae promotes a sustainable production process. If the same algae with a growth rate of 20 grams per square meter are cultivated in three vertical bags, the theoretical growth rate

becomes 120 grams per square meter, because the surface area of the vertical bags is greater than the surface area of a flat raceway pond. This concept may not be appropriate for all environments or climates, but it does indicate that a flat bag panel design could increase the algae production rate for the specialized process of growing algae for ethanol. The actual growth rate will depend on the available sunlight and the angle of the algae filled bags to the direction of sunlight.

The Algenol facility reports its production rate at 8,000 gallons of ethanol per acre. This is a significant development because a typical field of corn produces approximately 420 gallons ethanol per acre. Because of the tremendous growth rate of algae, this indicates an ethanol biofuel production that is approximately 20 times greater than conventional method of producing ethanol from corn or sugar cane.

For the Algenol facility, the “growth rate” of algae should be refined to describe the “production rate of ethanol from algae” because this provides a better metric for the process. The type of algae used by the Algenol process may offer additional advantages that are not available to this author. Below is a comparison of the ethanol production for three types of biofuel methods. See Table (2):

TABLE 2, ESTIMATED BIOFUEL PRODUCTION FOR DIFFERENT METHODS

Type of ethanol production	Amount of ethanol production	Land and water requirements
Sugar Cane	662 gallon/acre/year ¹⁰ 6.192,3liter/hectare/year	Requires fresh water and farmland
Corn	420 gallon/acre/year 3.928,6 liter/hectare/year	Requires fresh water and farmland (may compete with food crop production)
Algae	8,000 gallon/acre/year 74.831,2 liter/hectare/year	Requires sea water (does not compete with food crop production)

III. LAND MANAGEMENT

Because algae can be grown in bags, this allows for bioreactors that can be installed in areas that do not require flat land. A long practice of farming has been to grow corn and other crops on land than has less than a 6% slope. Growing crops on farmland with greater than a 6% slope encourages the flow of rainwater to carry and disperse essential soil nutrients.

Because algae can be cultivated in transparent bags, algae farming occur on sandy soils, white porous sand, or any location where crops are not grown. The growth of algae as a biofuel does not need the flat ground that we see in large open raceway ponds. Many hillsides with a 10% to 15% slope could be used to grow algae in bags at an angle perpendicular to the

hill. This is type of aquiculture would be applicable to subtropical islands or land mass near the ocean that are available for non-traditional farming.

Another feature of using bags as bioreactors is the reduction of evaporation and greater control of contaminants affecting a specific culture. Research scientists grow algae in desert and parched land where groundwater is not plentiful. Near desert locations are preferred by commercial algal facilities because they are out of sight from typical farmland. However, desert locations are prone to strong winds that carry sand, which can frequently damage an open raceway pond. An example is the concept of growing algae on the coastline of a parched or arid land area near the coast line. The use of bags in closed systems eliminates sand and other contaminants from affecting the growth of the algae culture.

Other locations like Hawaii grow algae in open ponds that are susceptible to wind and water damage from severe weather.¹¹ Hurricane or torrential downpour of water can easily disturb algae growing in open ponds. The flat bag design increases the flexibility of growing algae in locations that are not otherwise feasible or environmental friendly. Because closed bags reduce the likelihood of algae contaminants from reaching the local landscape, this reduces the concern that strong wind could carry algae to location deemed environmental sensitive. An important factor is the ability to grow algae near sensitive ecological areas that have been overwhelmed with nutrient loads from the utilization of fertilizers in farming.

Aquaculture has the potential to increase the value of land not suitable for farming. The average price of farmland in the U.S. is \$5,496.¹² However, the value of poor quality soil may increase above the average price of non-farmland if it is utilized for aquaculture, providing an additional incentive for commercial production of algal biofuel.

IV. CONTROL OF CONTAMINANTS

Mainstream scientists are also concerned about preserving sensitive ecosystem and preventing contamination of the algae colony where algae is grown. The algae grown in bags could be seen as an aid in preventing the aquaculture from contaminating the local ecosystem. This approach also makes the growth of algae in a control environment more sustainable since less water is needed to produce ethanol in a closed environment. In a closed environment, the amount of water and nutrients can also be controlled.

Another area of concern is seawater contaminants that can inadvertently affect algae growing in transparent bags. Local pathogens in brackish water could affect the ethanol production of algae in the transparent bags. Local communities may have restrictions or concerns with pathogens that are accidentally added when seawater or brackish water is transferred to transparent bags. An accidentally release of concentrated pathogens enclosed in wastewater or brackish water could cause concerns for the local community, if contaminants are accidentally released to the local aquifer. Therefore, the remediation of pathogens is an important issue

TABLE 3 SOLAR RADIATION METHODS FOR REDUCING WATER CONTAMINANTS

Types of water contaminants	Hours of sunlight required to destroy contaminants	Factors that influence the neutralization of contaminants
<p><i>Bacteria</i></p> <ol style="list-style-type: none"> 1. P. aerugenosa 2. S. Flexneri 3. S. typhi 4. S. enteritidis 5. E coli 6. Sparatyphi B 	99.9% of total bacteria population can be destroyed in 5 hours of strong sunlight, assuming the water is stored in clear transparent bottles or other clear transparent container	Geographical location Clarity of the water Seasonal variations Time of day Effective range of sunlight Wall thickness of the container Shape, color or transparency of the container
<p><i>Mold and Yeast</i></p> <ol style="list-style-type: none"> 1. Aspergillus niger 2. Apeergillus flavus 3. Candida 4. Geotrichum 	It take 3 hours of strong sunlight to destroy contaminants	
<ol style="list-style-type: none"> 5. Penicillium 	It takes 6-8 hours of strong sunlight to destroy contaminants	

for local communities that are concerned with airborne or wastewater contaminants arising from commercial aquaculture production. If the water media is non-turbid, then pathogens inside the closed transparent bags could be remediated if brackish water is allowed to stand a full day in bright sunlight.

UNICEF performed a study in 1979 using solar disinfection for treating drinking water in the Middle East.¹³ The report indicated that non-saline low turbidity water could be effectively treated for many pathogens by using solar disinfection. It was concluded that many types of bacteria in water could be destroyed or controlled by the lethal effect of ultraviolet light (UV). The study revealed that 99.9% of subjected coliform bacteria population could be destroyed in 300 minutes by sunlight. The study revealed that sunlight ranging from 315 to 400 nm is the most lethal region for killing pathogens and accounts for 70% of the bacterial destruction potential. This band of wavelength is known as the near ultraviolet region and referred as black light, which is not visible by the human eye.

The visible light having a wavelength of 400 to 750 nm accounts for 30% of bacterial destruction capacity. The intensity of treating water in bottles or plastic bags happens when the intensity of sunlight is greatest between ten o'clock to two o'clock in the afternoon. The control of biological contaminants in transparent bags may not be necessary for the production of ethanol from algae. In addition, many production facilities may not be susceptible to biological contamination. However, if a local community is affected by biological contaminants from a wastewater source or seawater, then the utilization of lethal UV light treatment may offer a low cost treatment option.

In addition, seawater and wastewater could be turbid and additional filtration treatment steps could be required before solar UV radiation is used for bacteria destruction. The utilization of solar UV light is sustainable because it reduces the need for chemical disinfection.

In addition, the solar UV pathogen destruction process may be used in communities that are concerned with the water discharged after the algae is removed from the closed bags. After the algae is filtered, the remaining process water could be disinfected by solar UV treatment. A closed system UV disinfection process is sustainable and should be part of a facility that is concerned with pathogen contaminants. The results of the UNICEF study for the treatment of water by direct sunlight is described in the Table 3.

V. BENEFITS OF ETHANOL PRODUCTION

Biofuel production could be considered sustainable for several reasons if the design, construction and operation of the aquaculture is adapted to the use of the least disruptive methods. The production of ethanol biofuel from algae can provide for the long reduction of carbon emissions as described in the following reduction equation Eq. (1):



The Algenol facility has reported that they are able to produce 8,000 gallons/acre-year. For the purpose of this evaluation, it will be assumed that this technology can be distributed and applied over a 100 acre area. A 100 acre aquaculture facility is the anticipated size a commercial facility and would provide 800,000 gallons of ethanol while providing significant CO₂ reduction. Table (4) describes the amount of seawater, and carbon dioxide required to produce ethanol on a 100 acre facility. An analysis of Table (4) indicates that a 100 acre facility would produce approximately 800,000 gallons of ethanol per year. Notice the significant amount of CO₂ that can be reduced or recycled with the production of algae to ethanol. The reduction of CO₂ in the production of ethanol from algae makes this a sustainable process.

TABLE 4 PRODUCTION GOALS FOR 100 ACRE ALGAE FACILITY

Carbon reduction potential for ethanol production from algae in 100 acre - closed bag system				
Unit Type	100 Acre ethanol Facility	Sea Water (3.5% saline) or brackish water	Weight Carbon Dioxide	Weight Ethanol (100%)
US	800,000 gallons	722,870 gallons	10,076,800 lbs/year 5,038.4 US tons/year	5,267,600 lbs/year or 2,633.8 US tons/year
Metric	3.028.328 liter	2.736.300 liter	4.570.735 kg/year	2.389.354 kg/year

VI. SUSTAINABILITY

The demand for water, food and energy resources are also growing with the continuous increase in world population. Our political and industrial leaders are all working for the common good of delivering basic materials and services at the lowest price. However, without a strong focus on the concept of sustainability the goods and services provided by the industrial community may not continue for future generations.

The basic philosophy of sustainability is to ensure that natural resources are not depleted for our grandchildren and their future generations. The concept of sustainability is to improve the quality of life, so that we can all live healthier lives. Below are critical sustainability factors that are important for the production of ethanol from algae.

1. Fresh water resources are becoming more limited. The use of brackish water or seawater is a sustainable approach for algal biofuel production.
2. The utilization of fertilizer in biofuel could compete with the demand of fertilizers in farming. The use of nitrates, phosphate from wastewater or brackish water is a sustainable approach for algal biofuels.
3. Closed bag reactors for algal biofuel production do not require agriculture farmland or forest land. Fresh water requirements are reduced because of less evaporation loss. The utilization of unfertile or parched land is sustainable approach for algal biofuels.
4. The production of algal biofuels reduces carbon emissions and is a sustainable approach at biofuel production.
5. The use of solar radiation to destroy bacteria and mold reduces the need for chemical additives and is a sustainable approach for algal biofuel production.
6. The use of closed plastic bags can also reduce the potential for contamination and is a sustainable approach for the production of ethanol from algae.

The six critical factors listed above should be incorporated in the planning stages of a commercial facility. The sustainable production of algae to biofuels can be costly, and many

countries have undertaken the bold step of funding research programs on the production of liquid fuel from solar energy. Since our modern culture requires an uninterrupted need of liquid fuels, the amount of carbon in the atmosphere will surely keep increasing over the next century as people burn more fossil fuels. However, the engineering and scientific community has been working on a solution for many years. The answer is the production of biofuel using the nutrients of carbon emissions and wastewater pollutants that are the result of human activity. A large-scale facility that produces ethanol from algae must recycle the nitrates and phosphate from wastewater and carbon emissions from large emission sources whenever possible to ensure a sustainable process.

VII. COMPARISON OF ETHANOL PRODUCTION METHODS

The sustainable production of ethanol from algae appears to more sustainable than producing ethanol from sugar cane or corn. Firstly, the amount of land required for production is approximately 1/20th of the land required for corn farming. Secondly, because of the reduced amount of land required for production of ethanol from algae, almost 19 acres of land become available for absorbing additional rainfall. This is a significant savings of water resources that makes the production of ethanol very sustainable. In addition, because high slope land can be utilized for aquaculture, this process can be used on hillside and other locations that are not suitable for traditional farming methods. Also, sandy soil or land that is not fertile enough for traditional farming methods can be utilized, increasing the utilization of land that is not otherwise valuable. This technology could in theory improve the value of land in rural areas.

Furthermore, the ability to disinfect bacteria, mold and yeast in situ reduces the amount of chemical required for production. This lowers the cost of production along with reducing the amount of labor cost for maintaining a production facility. Again, the use of solar energy to neutralize contaminants makes this process very sustainable. Because algae is produced in closed bags, this reduces the evaporation of water making ethanol production more sustainable because less total water is required. Also, since the closed bag system prevents algae from contaminating the local environment, the closed system could be more appealing to a community that is apprehensive about aquaculture in their community.

Shown in Table (5) is a review of the factors that makes ethanol production from algae sustainable.

VIII. CONCLUSION

The reported high cost of biofuel for military application is the result of stringent quality assurance requirements for specific military applications. The lower cost of biofuel reported for general civilian use is based on ethanol production from algae using an innovative method where quality assurance is not as stringent. Ethanol production from algae appears to offer significant sustainability advantages that are dependent on climate, availability of land and grade of land

TABLE 5 COMPARISON OF ETHANOL PRODUCTION METHODS

Algae in closed bags system	Corn	Sugar Cane
Utilization of sea water or brackish water	Requires Fresh Water	Requires Fresh Water
Utilization of Wastewater or water from Secondary or Tertiary Treatment (high in Nitrates and Phosphates)	Requires Commercial Fertilizers Commercial fertilizers have a higher cost than using nutrients from wastewater	Requires Commercial Fertilizers Commercial fertilizers have a higher cost than using nutrients from wastewater
Utilization of land not suitable for farming. Can be cultivate on land with a grade or slope greater than 6%. Technology could be adaptable on contoured land or hill side.	Common farmland Land may have a graded slope less than 6% to prevent excessive runoff of nutrients	Common farmland near a large fresh water source ¹ Land may have a graded slope to allow growth of sugar cane near a large body of fresh water
Possibility of contamination is reduced by keeping the growth media in a closed container	Fungus, insect, mold, bacteria or fungus is possible and requires herbicides and pesticides	Fungus, insect, mold, bacteria or fungus is possible and requires herbicides and pesticides
Fresh water requirements are limited. Sea water is abundant. The bags are a closed system limiting the amount of water required to produce ethanol	Shortage of rainfall or drought could affect the growth of corn stock	Shortage of rainfall or drought or overabundance of rain could affect the growth of sugar cane
Growing algae in closed system reduces the risk of low rainfall or floods. The closed system also prevents water evaporation. Droughts or flood damage is reduced.	Corn growth cannot be applied to areas that have low availability of fresh water. Also, extreme weather or flooding could damage the corn crop.	Sugar can growth cannot be applied to areas that have low availability of water. Extreme weather or flooding could damage the sugar cane production.
Higher production rate, utilization is 1/19 th of the land requirements for corn	Lower ethanol production rate Requires 19X times more land to produce ethanol than the closed algae method	Lower ethanol production rate Requires 12X times more land to produce ethanol than the closed algae method
Because land requirements are much less than conventional, more rainwater is able to penetrate the aquifer. Process used less than 1/20 th water resources need for growing corn	Most of the rainfall is used to grow corn. Heavy downpours of rain could wash away soil nutrients	Most of the rainfall is used to grow corn. Heavy downpours of rain could wash away soil nutrients

available for aquaculture. Another factor is the limited availability of fresh water resources and low cost nutrients. Because corn and sugar cane are dependent on commercial fertilizers, the production of ethanol from these farming methods competes with food crops for the same natural resources.

Ethanol production from algae is more sustainable because of the lower demand for natural resources. The low cost production of ethanol from algae is more likely to be adaptable to communities that have arid farmland near the seacoast. The availability of ethanol production from non-agricultural land provides additional sustainability benefits for communities that are affected by climate change. Some communities may not have alternatives to farming and ethanol production from algae in a closed bag system may offer economic benefits. In addition, some communities may not have sufficient access to petroleum fuels and the sustainable production of ethanol from algae could provide drop-in liquid fuel at a competitive cost.

The production of ethanol from algae is sustainable because it can substantial reduce carbon dioxide. For every kilogram of ethanol that is produced, approximately two kilograms of carbon dioxide is removed from the environment. The production of biofuels from algae enhances the sustainability of environment because it reduces carbon dioxide in the overall environment. The recycling of carbon dioxide emission

for the production of biofuels is more sustainable if wastewater and polluted seawater is used as the primary source of nutrients for production. A biofuel facility that is able to recycle carbon emission and wastewater could be considered the best sustainable approach for long term production of ethanol when non-agricultural farmland is utilized.

The utilization of non-agricultural land for ethanol production from algae also reduces total land requirements. Algae grown in a closed system requires approximately 1/20th of the amount of land required for ethanol production from corn. The utilization of poor quality soil for algae growth opens up another method for ethanol production that is not available from corn based farming. Because algae can be grown in bags for the production of ethanol, terrain with a slope greater than 6 degrees can be utilize on land that is not currently utilized. Ethanol from algae does need the same nutrients or land requirement that are required for corn or sugar cane based farming methods and is more sustainable because it does not compete with food crops. This also reduces the amount of total fresh water required for commercial operation. When ethanol is produced from algae in a closed system, it hypothetically allows 19 acres of farmland, for crop production. This is a significant improvement in the sustainable production of biofuel that is not mentioned with other commercial production methods.

Also, because ethanol is fermented in closed bags, this reduces the need for large fermentation facilities commonly found with ethanol production from corn or sugar cane. Ethanol from algae is less susceptible to drought because brackish water and wastewater could be used for growth. Another advantage is the low cost of producing ethanol from algae because the required nutrient can be taken from wastewater while corn and sugar cane are dependent on commercial fertilizers.

Clear transparent plastic bags can be effective at pretreating process water to reduce contaminants in the closed system. The cost of treating wastewater containing phosphate and nitrates, before adding an algae culture, can be significantly reduced by using solar radiation. Using ultraviolet light to kill pathogens reduces the need for chemical additives to reduce contaminants when algae are grown in bags. The application of solar energy for treatment of contaminant in water is more sustainable because of the reduced need for sterilization of the growth environment and reduced evaporation rate. The application of low cost solar radiation with a closed system

ensures airborne bacteria, mold or yeast, which could contaminate an open raceway pond system, does not affect a local community.

Because these factors, the production of ethanol from algae grown in closed bag environment should be explored further to determine if this unique production method can be applied to different climates and environmental conditions.

CONVERSION FACTORS

- 1 U.S. Dollar = 0.72 Euros
- 1 U.S Dollar = 0.59 British Pounds
- 1 US Gallon = 3.78541 liters
- 1 gal/acre/year = 9.3539 liters/hectare/year
- Density of ethanol = .789 kg/liter
- Density of seawater = 1.025 kg/liter

REFERENCES

- [1] D. Alexander, "U.S. Force Tests biofuel at \$59 per gallon", July 15, 2012 <http://www.reuters.com/article/2012/07/15/us-usa-military-biofuels-idUSBRE86E01N20120715>
- [2] Algenol, <http://en.wikipedia.org/wiki/Algenol>, June 17 2014
- [3] U.S. Department of Energy http://www1.eere.energy.gov/bioenergy/images/nm_raceway_pond.png
- [4] J. R. Banemann, "Microalgae Biofuels and Animal Feeds: An Introduction", January 2011,
- [5] D. Markham, "Algae biofuel process by Algenol yields 8000 gallons per acre at \$1.27 per gallon", <http://ecopreneurist.com/2014/04/17/algenol-produces-8000-gallons-algae-biofuel-per-acre-1-27-per-gallon/>
- [6] Dan E Robertson, Stuart A. Jacobson, Frederick Morgan, David Berry, George M Church, Noubar B. Afeyan, "A New Dawn for industrial photosynthesis", Springer, 13 February 2011
- [7] L Wondraczek, M Batentschuk, M.A. Schmidt, R. Borchardt, S. Scheiner, B. Seemann, P. Schweizer, and C.J. Barbac, "Solar spectral conversion for improving the photosynthetic activity in algae reactors", Nature Communications 4, Article number 2047, June 25, 2013
- [8] G.c. Zittelli, L Rodolfi, N. Bassi, N. Biondi, and M. R. Tredici, "Photobioreactors for Microalgal Biofuel Production", Algae for Biofuels and Energy, Springer Science+Business Media, 2013
- [9] A. DuPont, "An American solution for reducing carbon emissions-averting global warming – creating green energy and sustainable employment", DuPont Group Publisher, n.p. p 72, 2009
- [10] C. Stillman, "Cellulosic Ethanol; a greener alternative", Citizens League for Environmental Action Now, (CLEAN), June 2006, <http://www.cleanhouston.org/energy/features/ethanol2.htm>
- [11] J. Lane, "Major changes in the algae production industry- Raceway ponds were never meant to be used for industrial algae production" press release, August 28, 2012, <http://www.prlog.org/11961418-major-changes-in-the-algae-production-industry.html>
- [12] J Bunge, "Farmland values continue to retreat", Wall Street Journal, Pg. A2, May 16, 2014
- [13] A Acra, Z Raffoul, and Y. Karahagopian, "Solar disinfection of drinking and Oral Rehydratoin Solutions" Department of Environmental Health, Faculty of Health Science, American University of Beirut, 1984



Design and performance analysis of a piezoelectric generator by Von Karman vortexes for underwater energy harvesting

用于水下能量收集的基于冯·卡门旋涡之压电发电机设计和性能分析

Andrea Perelli^{1*}, Osvaldo Faggioni^{1,2}, Maurizio Soldani² and Rodolfo Zunino¹

¹Department of Naval, Electric, Electronic and Telecommunication Engineering, University of Genoa, ITALY

²Istituto Nazionale di Geofisica e Vulcanologia, Rome, ITALY

perelliandrea@yahoo.it

Accepted for publication on 22th July 2014

Abstract—With the decrease in energy consumption of electronic sensors, the concept of harvesting renewable energy in a human surrounding, using piezoelectric technology seems promising to feed small sensors in several environments. The aim of this paper is to design a piezoelectric generator, optimized for magnetic sensors, able to work under the sea or into rivers, which can work with natural water vibrations generated by solid-fluid objects interactions (Von-Karman Vortex) and then to test the effectiveness of the device developing an electronic board to analyze the behavior of the generator.

Keywords—energy harvesting; piezoelectricity; Von-Karman Vortex; fluid dynamics

I. INTRODUCTION

From the beginning of the XXI century the increment of the World Energy Consumption (WEC) strictly related to the technological progress has highlighted the necessity to produce energy from renewable sources. By 2008 renewable energy had ceased being an alternative, and more capacity of renewable energy was added than other sources in both the United States and in Europe. In this context, piezoelectric generators seems promising for small electronic equipments, especially if used in environments where human intervention is not so easy, as for underwater applications. The principle is to harvest energy from mechanical vibrations, connected to general human activities (cars, bicycles, ecc...), or from natural effects (wind, flows, ecc...) [1]. All studies performed at present time consists of designing an oscillator, operating nearby the natural frequency and therefore maximizing the oscillations amplitude. Various attempts to generate natural vibrations from “tree like” energy harvesters have been made [2-7], whose leafs are piezoelectric thin foils, able to vibrate

because of the wind effect. When this investigation is brought into water, vibrations come from natural flow interactions [8,9]. Extensive studies about Hydrodynamic and Aerodynamic have been carried out for the last two centuries in this field.

The aim of this paper is to design a piezoelectric generator, optimized which can work with natural water vibrations generated by solid-fluid objects interactions (Von-Karman Vortexes) [10], in order to feed underwater magnetometers for port protection purposes [11], able to work autonomously for long periods; in particular, this prototype has been designed to work in combination with new magnetometer models (L.A.M.A. Project, National Plan for Military Research, Italy), designed to work inside underwater magnetic networks for harbour defence [12].

This paper introduces the theoretical principles and shows the design process of the mechanical structure, taking into account CFD and mechanical results; then considerations about the electronic aspect of the work are shown, in particular an electronic model of the system and the energy harvesting circuit for the evaluation of the performance of the generator. Finally the mounting operations and all tests campaigns are described, focusing on the results obtained.

II. MECHANICAL STRUCTURE

A. Principles of Von Karman Vortex

The first hydrodynamic aspects to be investigated is related to the interaction between a fluid and a bluff bodies submerged in the fluid itself [11-18]. This kind of study starts with Von Karman, who has described the emission of vortices generating from interaction between fluid stream and geometrical shapes,

caused by friction and dissipative forces. The intensity and dimensions of these vortices is determined by several parameters, such as velocity, viscosity and object dimensions. In order to describe this phenomenon, the Reynolds number (Eq. 1) and the Strouhal number (Eq. 2) are paramount.

$$Re = \frac{U \cdot d}{\nu} \tag{1}$$

$$fr = St \frac{U}{d} \tag{2}$$

Strouhal number allows to predict emission frequency (*fr*) of vortices around the cylinder. The emission of Vortices generated from interaction between a fluid (water or air) and the cylinder induces a vibrations in a path of cylinders downstream the first fixed cylinder.

B. CFD analysis

A first test of CFD analysis has been developed using FLUENT®. A cylindrical body has been put inside a uniform water current of 0.5 m/s, a typical velocity inside small channels or in proximity of maritime harbor gates, which will represent the typical environment for these applications. The aim of this test was to visualize the pressure field generated downstream the cylinder, and of course the behavior of vortices.

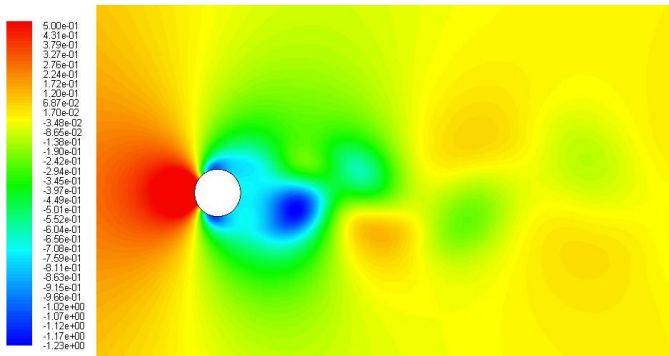


Fig. 1. Static Pressure field (Pa) around the cylinder generated by Von Karman Vortices in a fully developed stream

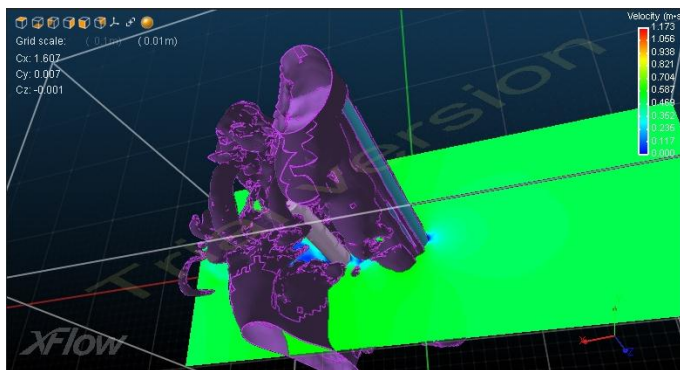


Fig. 2. Velocity simulation (m/s), showing a vortex behavior in a fully developed stream.

A second CFD test campaign, using a more innovative and powerful software, XFLOW®, has allowed the 3D analysis of the flow: the first cylinder was fixed to the structure and unable to move, the second one was allowed to oscillate vertically, so as to simulate the real behavior. The results can be seen in the following image (see Fig. 2).

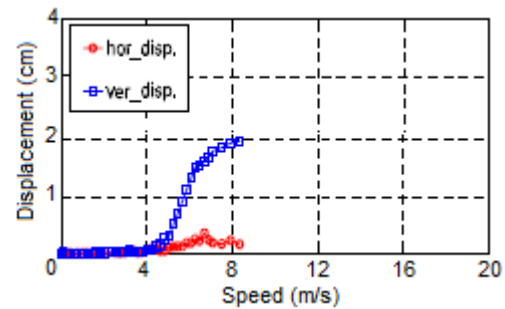
The results of both CFD studies has consolidated the result of a vibration of the second cylinder of 4-5 Hz, generally in agreement with the mathematical prediction using Strouhal number; this can be assumed as characteristic for speeds of 0.5 m/s.

C. Definition of the geometry of the structure of the prototype

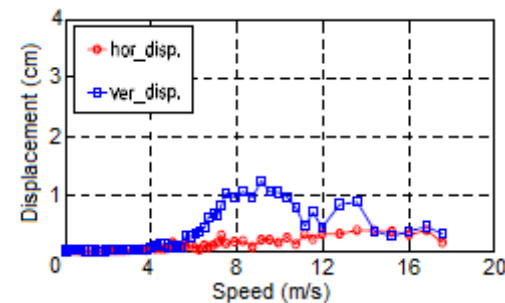
The construction of the prototype incorporates the results of previous CFD analysis, dictating guidelines of some technical solutions to maximize vibration amplitude from Von-Karman vortices, and consequently increase the energy harvesting through piezoelectric conversion.

The distance between the cylinders is a critical aspect to consider in order to compromise two opposite behavior of vortices, the full development and the subsequent dissipation for friction forces. It has been revealed from both analytical and CFD computation that the best distance is to be set at 4-5 D, with D the diameter of both cylinders (see Fig. 3).

In the schemes in Fig. 3 the trend of vibration amplitude is shown for different velocities and different distance D between the two cylinders.



A



B

Fig. 3. Amplitude of vibrations with different velocities for distances of 2D (A), 4D (B).

The vibrational structure design, as a result of all considerations made, has included the chosen shapes and a distance between the cylinders of 4D.

D. Materials

Regarding the choice of materials for the prototype realization, it is important to highlight some interesting aspects; first of all, as the oscillator must be capable of being tested both in air and in water, in order to verify the different behavior, a careful control of the two cylinders masses must ensure a not excessive difference in the two different test environments.

In addition, the cantilever bar oscillator must have a stiffness comparable to that of piezoelectric material that is to be installed: too high stiffness can dampen vibrations, and too low stiffness let the cantilever be too flexible and then to absorb itself the grand part of them, reducing piezoelectric material efficiency.

For these reasons, the cylinders were both made of carbon fiber, which in addition to possessing the required properties, is also particularly resistant to the effects of water corrosion in marine environment.

E. Mechanical modelization

An interesting aspect of vibrations behavior of the prototype is the mathematical modelization, using a second order system, commonly known as “mass - spring - damper”. The mathematical law that regulate the model behavior on the horizontal plane is the well known Eq. (3).

$$m \cdot \ddot{x}(t) + c \cdot \dot{x}(t) + k \cdot x(t) = F(t) \tag{3}$$

where m is the mass, x the displacement from the initial position, c the viscous friction coefficient, k the elastic constant of the spring and F a known external force. It is possible then trough all data collected to simulate the real behavior using the software SIMULINK.

Mass and stiffness are already known, for damper it has been chose an average value of 0.2. It is also important to consider that around the cylinder an amount of fluid moves with it during vibrations: this quantity is known in fluid dynamic as Add Mass. As it is very difficult to calculate precisely this mass, negligible for air but not for water, the total mass of the system is to increase of 20%, which will affect natural frequency of the beam, causing its reduction.

The results of the SIMULINK run are shown in Fig. 4.

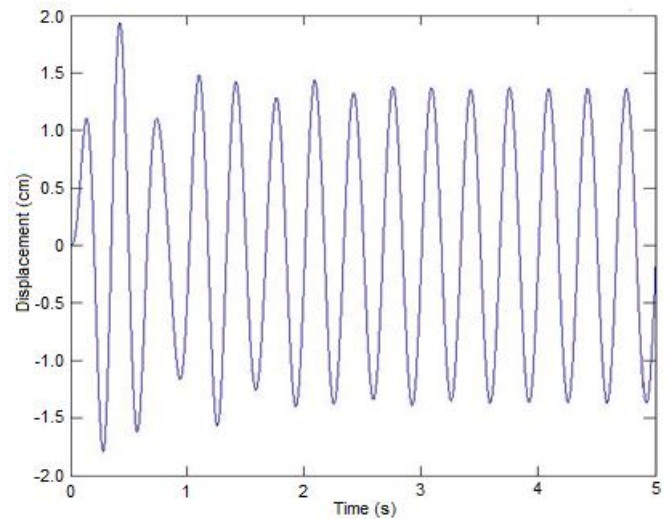


Fig. 4. Vibration of the cylinder simulated with SIMULINK.

After a brief transient, the system reach steady conditions; as it can be seen the vibration amplitude is about +/- 15 mm. These values are compatible with the test of Lunense canal.

III. ELECTRONIC ASPECTS

A. Electronical modelization

As shown in the previous Section, it is possible to model the system as a generic second order system. In particular, the equivalent of the mechanical “mass – spring –damper” model in electronic is the well known “R – L – C” circuit. By this way it is possible to simulate the behavior of the system with electronic simulation software. The equation (3) is equivalent to the following Eq. (4). in the electronic field:

$$L \cdot \frac{di(t)}{dt} + R \cdot i(t) + \frac{1}{C} \int_0^t i(t)dt = e(t) \tag{4}$$

that represents the Kirchhoff's Voltage Law (KVL) to the RLC circuit designed, where L,R and C are respectively the values of Inductance, Resistance and Capacity of the circuit and $i(t)$ is the current intensity depending from time t (s)

Considering equation (4) as a function of the electric charge Q – which is obtained for the charge conservation principle by integrating the current i between 0 and t – equation (4) can be written as equation (5):

$$L \cdot \ddot{Q}(t) + R \cdot \dot{Q}(t) + \frac{1}{C} Q(t) = e(t) \tag{5}$$

Then the schematic is composed by a generator $e(t)$, two storage elements (L and C) and a dissipative element (R) as for the mechanical one. Every single element could be compared to one mechanical element of the equation (3) and in particular:

$$L = m \tag{6}$$

$$R = c \tag{7}$$

$$\frac{1}{C} = k \tag{8}$$

$$Q(t) = x(t) \tag{9}$$

$$e(t) = F(t) \tag{10}$$

It is possible to simulate and measure the value of $x(t)$ for a particular $F(t)$. Moreover in the circuit are represented the mechanical-electronic conversion by a transformer and the capacity of the piezoelectric which is an intrinsic parameter of the component. The circuit response to a sinusoidal input is analogue to the one obtained with the mechanical model.

B. Energy harvesting circuit

By this way it is possible to include in the circuit the energy harvesting part and tests it. The first element of the harvesting circuit is represent by a rectifier and in particular by a diode bridge to obtain a full-wave rectification and a capacitor in parallel to the bridge to obtain a DC voltage from the AC rectified voltage. Then the DC voltage can be adapted to the one required by the load with the use of a DC-DC converter. The power obtained by this circuit can be stored in a storage capacitor such as a rechargeable lithium battery (see Fig. 55).

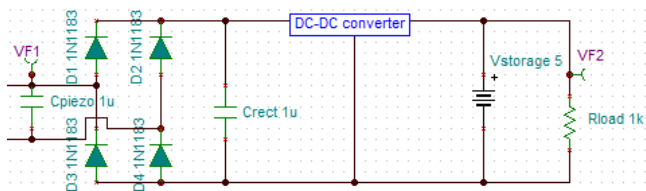


Fig. 5. Scheme of the energy harvesting circuit.

The design of electronic equipment in support has been focused with the aim of improving the generator efficiency and thereby increase the resulting power, with particular reference of power consumption of L.A.M.A. magnetometer, in order to reach longer period of autonomy of the system.

IV. EXPERIMENTAL RESULTS AND PERFORMANCE ANALYSIS

A. Prototype mounting operations

The first step has involved the realization of the external support in plexiglass and of the two cylinder in carbon fiber.

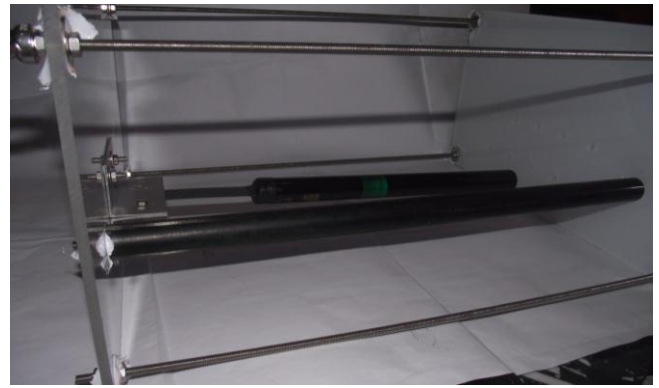


Fig. 6. Front view of the prototype

Subsequently the cantilever beam has been installed, with the piezoelectric sensor (MFC piezoelectric M2814-P2, produced by Smart Material Corp.).

B. Lunense canal hydrodynamic test

The aim of the test was to verify the prototype proper functioning, and to have experimental evidence of all results from the CFD analysis and from theoretical development of the mass / spring / damper model. The prototype has been raised with the aid of ropes and posed into the center of the canal, in order to avoid all edge contributes. To ensure complete stability of the prototype during the experiment, both ropes have been fixed at an equal height on the opposite sides of the canal (see Fig. 77).



Fig. 7. Picture during the test: the prototype in Lunense canal.

Depending on days, the water flow rate varies, but always inside a typical range of values, a characteristic that makes it usable for small device testing in all seasons. In addition, water current has an average speed that is almost constant around 0.5 m/s, thanks to floodgates

The satisfactory results are listed below:

- The prototype has demonstrate to resist to water flow in all test conditions: in particular, integrity of cylinders, cantilever and piezoelectric material have been ensured

- The vortex generator cylinder induces a velocity field downstream as predicted
- The second cylinder, after a few second of transient effects has shown a vibration around 4-5 Hz, as predicted

C. Complete prototype air preliminary test

The aim of this second test campaign was to analyze the behavior of the full prototype after piezometer installation and insertion of electrical wiring, in order to connect the device to an electronic test rectifier, and consequently verify voltage output. As the whole system was not water-proof, the experiment was conducted outside water, using an industrial dryer to obtain a steady air flow inducing vibration.

An industrial oscilloscope has been used to analyze output voltage. The whole prototype and the oscilloscope are shown in Fig. 8

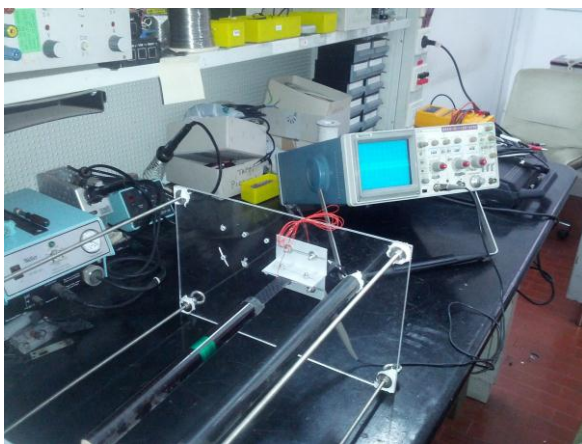


Fig. 8. The prototype during the test with the oscilloscope

As the flows of air started to interact with the device, the cantilever beam started to vibrate, with an intensity that was obviously less than that obtained with water flow in Canale Lunense, but enough to measure a moderate voltage output, with a peak of more than 30 V. The sinusoidal output is shown in Fig. 9.

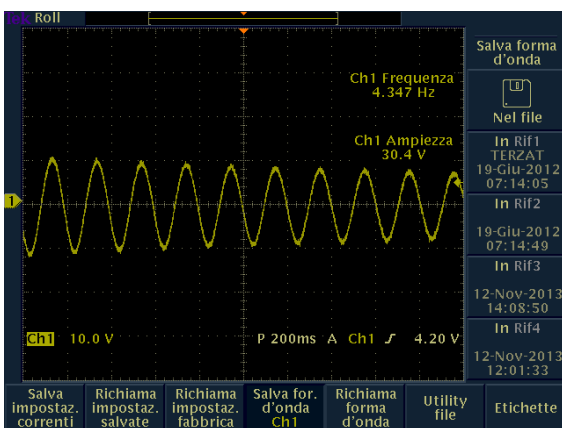


Fig. 9. Oscilloscope output screen

In the second phase of the test the rectifier has been connected to the piezoelectric thin foil, in order to obtain a DC output and supply various test LEDs. The rectifier used was a test platform, customized to select various output voltage (1.8 V, 2.5 V, 3.2 V and 3.6 V). (Fig. 10)



Fig. 10. Rectifier used for the test

After measuring the correct output with the help of a tester, a small LED of 1.6 V and an electrical resistance of 820 Ohm has been connected and the structure was forced to vibrate; after a brief transient phase, the LED remained alight.

The use of bigger LEDs led to less satisfactory results, with alternate phases of switching on and off. The use of a capacitor in support allowed to stabilize the lighting of the LED for a longer time, after a few second of recharge of the capacitor itself.

The results of this experiment are then summarized below:

- The prototype has demonstrated to successfully harvest energy from fluid-dynamic interactions
- Through the use of a rectifier it was possible to obtain a DC output to feed a small LED
- The estimated power output is 2-3 mW

V. CONCLUSIONS AND FUTURE WORKS

The aim of the project is to create a low cost energy harvesting device, which must be able to feed electrically a sensor or pack of sensors of modest power requires, especially magnetic sensors.

The actual development of this power unit has shown his real capability to-develop a synergy between the generator and the sensor-(Magneto-Variometer), with the aim of realizing an underwater systems for magnetic detection with high autonomy. All results obtained and described are encouraging.

The future objectives are to optimize the prototype in both aspects, fluid dynamic and electronic, in order to increase the power output, even with analysis of new possible configurations including multiple cylinders operating in sinergy.

REFERENCES

- [1] E. Minazara, D. Vasic and F. Costa, "Piezoelectric Generator Harvesting Bike Vibration Energy to Supply Portable Devices", in Proceedings of International Conference on Renewable Energies And Power Quality (ICREPQ'08), Santander, Spain, 12–14 March 2008.
- [2] S. Roundy and P. K. Wright "A piezoelectric vibration based generator for wireless electronics" *Smart Mater. Struct.*, vol. 13, pp. 1131-1142, 2004.
- [3] Cornell Creative Machines Lab - creativemachines.cornell.edu
- [4] J.J. Allen and A.J. Smits, "Energy harvesting eel", *Journal of Fluid and Structures* 15, pp. 629-640, 2001.
- [5] G.W. Taylor, J.R. Burns, S.M. Kammann, W. B. Powers and T. R. Welsh, "The energy harvesting eel: A small subsurface ocean/river power generator", *IEEE Journal of Oceanic Engineering* 26, pp. 539-547, 2001.
- [6] S. Adhikari, M.I. Friswell and D.J. Inman, "Piezoelectric energy harvesting from broadband random vibrations", *Smart Materials and Structures* 18, 115005, 2009.
- [7] S. Lee, B.D. Youna and B.C. Jung, "Robust segment type energy harvester and its application to a wireless sensor", *Smart Materials and Structures* 18, 095021, 2009
- [8] D.F. Young, B.R. Munson and T.H. Okiishi, "A brief introduction to fluid mechanics", John Wiley & Sons, 2001.
- [9] F.M. White, "Fluid Mechanics", McGraw-Hill, 1986
- [10] G. Sandroni, "Sviluppo e analisi delle performance della struttura meccanica di un generatore piezoelettrico stimolato da vortici di von karman per l'energy harvesting in ambiente subacqueo", Degree Thesis, Corso di Laurea in Ingegneria Meccatronica, Università degli Studi di Genova, 2013.
- [11] O. Faggioni, M. Soldani, D. Leoncini, A. Gabellone and P.V. Maggiani, "Time domain performances analysis of underwater magnetic SIMAN Systems for port protection", *Journal of Information Assurance and Security*, vol. 4, n. 6, Special Issue on Information Assurance and Data Security, 538-545, 2009.
- [12] O.Faggioni, M.Soldani, A. Gabellone, R.D. Hollet and R.T. Kessel, "Undersea harbour defence: a new choice in magnetic networks", *Journal of Applied Geophysics*, vol. 72, n. 1, 46-56, 2010.
- [13] J. H. Gerrard, "The mechanics of the formation region of vortices behind bluff bodies", *Journal of Fluid Mechanics* 25, 401-413, 1966.
- [14] P. Huerre and P. A. Monkewitz, "Local and global instabilities in spatially developing", *Annual Review of Fluid Mechanics* 22, 473-537, 1990.
- [15] A. khalak and C. H. K. Williamson, "Motions, forces and mode transitions in vortex-induced vibrations at low mass-damping", *Journal of Fluids and Structures* 19, 813-851, 1999.
- [16] A.Leonard and A. Roshko, "Aspects of flow-induced vibrations", *Journal of Fluids and Structures* 15, 2000.
- [17] E. Naudascher and D. Rockwell, "Flow-Induced vibrations", *An Engineering Guide*. Brook, A. Balkema, 1994.
- [18] A. Roshko, "On the drag and shedding frequency of two-dimensional bluff bodies", *NACA Technical Note No.* 3169, 1954.
- [19] T. Y. WU "Swimming of a waving plate", *Journal of Fluid Mechanics* 10, 321-344, 1961
- [20] R.D. Blevins, "Flow-induced vibration", Van Nostrand Reinhold, ed. 2, 1990.



Research on the local and total stability criterion of high arch dam

高拱坝局部和整体稳定性评判准则研究

Guojian Shao (邵国建)*, Jiashou Zhuo (卓家寿)

Department of Engineering Mechanics, Hohai University, Nanjing 210098, China

Accepted for publication on 15th November 2014

Abstract - It is essential for the design of high arch dams to research problems of ultimate bearing capacity and total stability of the high arch dams. On the basis of evaluation on current analysis methods of the stability in the arch dam abutment and the total arch dam, their deficiencies are pointed out. With the application of the friction theory and the vector geometry, the formula of anti-slide stability safety coefficient is presented based on the non-linear FEM analysis. In response to the stability problem of high arch dam abutment without conspicuous slide faces, the local and total stability of the high arch dams are researched using the non-linear FEM analysis. Based on quantitative disturbing energy criterion and static criterion, the quantitative standards of the latent slide face and the most dangerous slide direction and the minimum stability safety coefficient are proposed and established. The stability criterion system is perfected for the local and the total stability of the high arch dams. The mechanical foundations are laid for quantitative stability criterion on the local and the total stability of high arch dams without conspicuous slide faces. The stability computation of a high dam abutment with the height of 305m is given. According to the disturbing energy value and its isograph, the latent side faces are determined. Estimating rockmass stability by the disturbing energy method and the static method, the numerical results indicate the rationality and the feasibility of the presented method.

Keywords – high arch dam, dam abutment stability, static criterion, disturbing energy criterion, stability safety coefficient.

摘要 – 高拱坝的极限承载力和整体稳定性是高拱坝设计中的关键问题, 在总结和评价现有拱坝坝肩和坝基以及整体稳定性分析方法的基础上, 指出其中的不足之处, 针对没有明显滑动面的拱坝坝肩岩体稳定性问题, 采用三维非线性有限元理论与分析方法围绕高拱坝局部和整体稳定性问题进行针对性的研究。基于可量化的干扰能量准则和静力准则, 建立了确定潜在滑动面、最危险滑向和最小安全系数的失稳警戒指标的量化标准, 完善了拱坝局部与整体稳定性的评判体系, 从而为解决没有明显滑动面的拱坝局部和整体稳定性评判量化指标这一难题奠定了力学基础。

关键词 – 高拱坝, 坝肩稳定, 静力准则, 干扰能量准则, 整体稳定安全度。

I. INTRODUCTION

An arch dam is the structure integrally bearing and retaining water, whose load is passed to the rock body in two banks by the construction base level. The arch dam balance is an entire equilibrium problem of dam body, rock mass and the interface between them. Arch dam stability is that keep dam body, rock mass and the interface in balance entirely under powerful water load and so on. Among dam body, rock mass and the interface, if one of them becomes unstable, the whole arch dam is in instability then. In order to keep the whole arch dam in stability, the dam body and rock mass and the interface have to maintain their equilibrium status severally. At the present time, evaluating arch dam local and total stability methods include rigid limited equilibrium method^[1], geomechanical model test^[2], over loading method based on nonlinear finite element, and reduce the material strength method^[3]. Rigid limited equilibrium method obviously is limited in both conception in solving methods, based on quoting some assumptions and neglecting many factors, which lead to inexact computed results. Geomechanical model test has difficulties in finding some modeling materials which can be used to simulate dam body concrete and dam foundation completely according to similarity theory requests; in simulating high arch dams complex load mode and many nonlinear influences also.

If abutment's possible sliding mass is known in advance, anti-slide force and sliding force on sliding surface are obtained from non-linear FEM calculating results, and possible sliding mass's anti-slide stability safety coefficient can also be gained through projection. In present anti-slide stability safety coefficient computing formulae^[4], synthesis of anti-slide force and sliding force on sliding surface often adopt simple algebraic addition and leading to considerable difference in the results. Besides, if possible sliding mass is not given in advance, abutment stability cannot be estimated. Although the reference [5] adopts the point safety coefficients to judge the stability, the point safety coefficients in essence is strength condition in classical mechanics and only reflects Mohr-Coulomb strength criterion.

Under the background above, after summarizing and appraising existing analysis methods of arch dam abutment

and foundation and total stability, with the application of the friction theory, the vector geometry formula of anti-slide stability safety coefficient of three-dimension problem is presented based on the non-linear FEM analysis. According to the mechanics principle of engineering stability, the disturbing energy method of rockmass stability criterion is presented which is used to propose and establish the latent slide mass and the most slide direction and the corresponding stability safety coefficient. The judging system of the joint applied static method and disturbing energy method is promoted, which makes base for the local and total stability quantification judgment of the arch dams.

II. RIGID LIMITED EQUILIBRIUM METHOD

At present, the rigid limited equilibrium method is the conventional design method in analysis of structural and slope stability at home and abroad, it has engendered relevant safety coefficient conception based on engineering experience, and also be brought into kinds of design specification. It has been acquainted, habitual and traditional to the largeness designers. The rigid limited equilibrium method assumes that the possibly gliding mass is a rigid body of no deformation and the force system effects on gliding mass only includes the normal force and the shearing force but no bending moment. The ratio of anti-slide force and sliding force is defined as stability safety coefficient of slide mass. There are a lot of methods, the main computing equation of stability safety coefficient is

$$K = \frac{\sum N_i f_i + \sum c_i A_i}{\sum T_i} \quad (1)$$

In Eq. (1), N_i, f_i, c_i, T_i, A_i indicate respectively effective normal force, friction factor, cohesive force, sliding force of the glide direction and the area of the sliding surface on the slide mass, the subscript i denotes numbered i region of the area of the sliding surface. After getting the N_i, T_i through the projection equilibrium method of slide mass force system, then substituting them into Eq. (1), we can get the value of stability safety coefficient.

The modal of rigid limited equilibrium method is shown in Fig. 1.

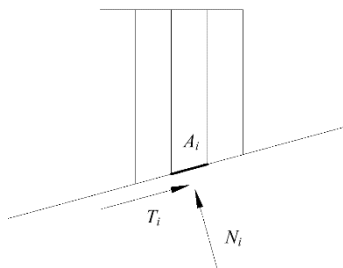


Fig.1 The modal of rigid limited equilibrium method

Because the rigid limited equilibrium method imports some assumptions and many factors neglected, the calculation results is rough comparatively and it can't reflect stress status and failure mechanism of rock mass structure or dam abutment accurately; and the stability safety coefficient we get is almost

estimated value. But the limit equilibrium method can't resolve of the stability problem of complex slide mass which have strike fault or crevassed structure, particularly to the instability problem of arch dam abutment rock.

III. THE GEOMECHANICAL MODEL TEST

There are three major ways in the model test of high arch dam total stability. They are over loading method and strength reserve method and synthetical approach. Over loading method assume the dam foundation rock mechanical parameters is unchanged and gradually increase the upstream water load until the foundation rupture instability, over loading multiple of water load is called overloading safety degree; Strength reserve method considers that the dam foundation rock itself has a certain strength reserve capacity and gradually lowers the design mechanical parameters of the rock until the foundation become instability, the lower material parameters multiples is called strength reserve safety; Synthetical approach is the combination of over loading method and strength reserve method, it not only considers the several times upstream water load in the project we may encounter, but also considers the rock and weak structure face mechanical parameter lowing on the influence of stability, the multiples of overloading times and lowing strength times is called synthetical stability safety degree.

The merit of geomechanical model test is that it is an intuitive, perceptive analysis, it can get quite obviously visualize concept, macro and quantitative indicators of safety; it can get entire arch dam damage process, such as the formation of cracks and slip face and development until rupture; it can assume the slip face for other numerical methods and provide reference frame for loading measures. The shortcoming of geomechanical model test is that it is difficult to consider earthquake, seepage pressure and temperature changes and other load factors; it is difficult to completely simulate dam concrete and model material of dam foundation according to the similarity theory. The stress mechanism of high arch dam is very complicated. The model test is difficult to simulate affects of many nonlinear factors. The problems of rationality of analysis results quantitative estimates and model test technology are worth to study further.

IV. STABILITY SAFETY DEGREE UNDER OVER LOADING

Applying finite element numerical analysis method, dam body and foundation's stress field and displacement field are obtained. Adopting over loading or abasing material strength parameter, make the system reach the ultimate balanced state, thereby, over loading stability safety degree or strength reserve safety degree is received. The criterion which makes the system reaches the ultimate balanced state is called instability criterion. It belongs to elastic plastic ultimate balanced analysis category.

There are two possible reasons which bring on arch dam abutment and foundation rock come into plastic limit balanced

state and cause instability. The first one is dam abutment and foundation rock design strength is close to actual strength, but dam meets with supernormal loads. Then we should adopt over loading method to analysis stability. The second one is under normal loading, but dam abutment and foundation holding force rock's design strength is differ from actual strength. Then we'd better adopt strength reserve method to analysis stability. When construction base face materials all give in yield and come into being slip ways, and some key points relative displacement on dam and construction base face is widened or inflexion appear at loading deformation curve, we believe that the arch dam shows the tendency to slip through construction base face, and the dam reaches the ultimate balanced state. This status is regarded as the instability criterion to arch dam.

Strength reserve method considers the material strength uncertainly and the possible deterioration, but rock characteristic of dam foundation is very complex in actual projects and it is difficult to correctly ascertain material intensity parameters, and which method is adopted to debase material strength parameters is yet to be further studied. Besides, debasing material strength parameters gradually is difficult to carry into execution by corresponding model test.

V. STATIC CRITERIONS

5.1 Revision of conventional point anti-slide stability safely coefficient

The conventional evaluation stability methods of rock mass depend on the ratio of anti-slide force and sliding force, which is called anti-slide stability safely coefficient. The conventional point anti-slide stability safety coefficient computing formula is

$$k = (c - f\sigma_n) / |\tau_n|, \quad (2)$$

where $(c - f\sigma_n)$ is shear strength of the point on the investigated face, which is anti-slide force here; τ_n is shear stress which means sliding force.

The modal of i point anti-slide stability safely coefficient is shown in Fig. 2.

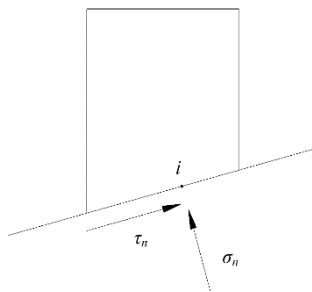


Fig.2 The modal of point anti-slide stability safely coefficient

When sliding face cannot be confirmed in advance, the minimum k_{\min} of this point usually acts as the criterion to

judge whether it is instability. If the angle between outer normal direction n and the first primary stress σ_1 is α , then σ_n and τ_n can be expressed by σ_1 and σ_3 .

$$k_{\min} = \frac{c - f\left(\frac{\sigma_1 + \sigma_3}{2} + \frac{\sigma_1 - \sigma_3}{2} \cos 2\alpha\right)}{\left|\frac{1}{2}(\sigma_1 - \sigma_3) \sin 2\alpha\right|} \quad (3)$$

Because of $\frac{\partial k}{\partial \alpha} = 0$, when k equals to k_{\min} , α is deduced as

$$\alpha = \frac{1}{2} \arccos \left[\frac{\frac{1}{2}(\sigma_1 - \sigma_3)f}{c - \frac{1}{2}(\sigma_1 + \sigma_3)f} \right] \quad (4)$$

5.2 Revision of conventional point anti-slide stability safely coefficient

The definition and corresponding computation formula of the conventional evaluation methods about point anti-slide stability safely coefficient of rock is incompatible with mathematics and mechanics general knowledge.

Point anti-slide stability safely coefficient was denoted as Eq. (2), whose essential is the strength condition in classical mechanics rather than stability condition. k_{\min} in Eq. (3) is shear strength safely coefficient of the point, which can not be used to judge the stability. The actual angle α on slip surface between outer normal direction n and the first primary stress σ_1 is not must be the value came from Eq. (4), so k_{\min} calculated by Eq. (3) doesn't reflect the anti-slide stability degree of safety.

When calculate k by point σ_n and τ_n on actual slip surface as Eq. (2), the expression is incompatible with frictional theory and space vector algorithm. Firstly, anti-slide force $(c - f\sigma_n)$ and sliding force τ_n will be both vector. Secondly, it is known by slide frictional theory that the direction of anti-slide force is opposite to the relative slip direction of this point, while it may not be at the opposite direction to the slip force vector direction. Therefore, it is meaningless to compare the two different direction force vector like Eq. (2), and it breaks vector algorithm too.

In order to establish the anti-slid safety coefficient of the point according to the original meaning of Eq. (2) and following vector algorithm, the anti-slid force can only be compare with the component in the sliding direction \mathbf{r} , and the ratio can be defined as the point safety coefficient k_s along the direction \mathbf{r} , with this amendment, the point anti-slid stability safety coefficient formula is as Eq. (5).

$$k_s = (c - f\sigma_n) / |\tau_n| \cos \beta \quad (5)$$

In Eq. (5), β is the angle between composite shear stress direction τ_n of the point and sliding direction \mathbf{r} .

Anti-slide stability safety coefficient K_s is defined by the ratio of anti-slide force and sliding force on slip surface commonly, whose precondition is that slip surface is given in advance.

Based on the understanding about the questions above, frictional theory and vector geometry concept, anti-slide safety coefficient formula and the most dangerous composite sliding direction can be deduced below.

$$K_s(\bar{r}) = \frac{\sum_{i=1}^{N_e} (c - f\sigma_{z'})_i A_i \sqrt{l_i'^2 + m_i'^2}}{\sum_{i=1}^{N_e} [l_i' \tau_{z'x'} + m_i' \tau_{z'y'}]} \quad (6)$$

In the equation, z' is the normal on some element slip surface, x' and y' are the two local coordinates in element slip surface tangential direction. l' , m' and n' are the direction cosine of the angles between the body composite sliding direction \bar{r} and local coordinate system x' , y' and z' in element i . A_i is the slip surface acreage of element i . N_e is the total number of elements on slip surface.

Despite Eq. (6) gives out the formula of the new anti-slid stability safety coefficient but still maintain the framework of traditional definition of rock project. From the mechanics, its essential still has the meanings of strength checking, it extends to the reserve safety degree of the whole slip face shear strength from the concept of strength safety coefficient of a point in the mechanics. This is not the content of stability definition. In addition, from the Eq. (6) we can get the minimum safety value and the most disadvantaged slip direction, but how to determine the most disadvantaged possible slip face is still an outstanding problem.

VI. THE CRITERION OF DISTURBING ENERGY

According to the axioms of Dirichlet^[6], the potential energy Π of the objects on the equilibrium configuration has the minimum value or the maximum value, if the Π is on the minimum value, the equilibrium configuration is stable, its mathematical expression is $\delta\Pi = 0, \delta^2\Pi > 0$; if the Π is on the maximum value, the equilibrium is unstable, its mathematical expression is $\delta^2\Pi < 0$; when the $\delta^2\Pi = 0$, the potential energy of the objects on the surface will not change after the minuteness deviation, and the equilibrium is random.

Based on the above ideas, the following relevant calculation formula can be established.

The Potential energy functional under the Lagrange system is as

$$\begin{aligned} \Pi &= \int_{\Omega} A(e_{ij})d\Omega - \int_{\Omega} f_i u_i d\Omega - \int_{s_\sigma} \bar{p}_i u_i ds \\ &= U - W \end{aligned} \quad (7)$$

In Eq. (7), the potential energy of the system is as

$$U = \int_{\Omega} A(e_{ij})d\Omega \quad (8)$$

The work of the external forces is as

$$W = \int_{\Omega} f_i u_i d\Omega + \int_{s_\sigma} \bar{p}_i u_i ds \quad (9)$$

The displacement of the equilibrium configuration is assumed as u_i^0 and the disturbing displacement is assumed as δu_i . The potential energy increment after disturbing is $\Delta\Pi$. Based on the Taylor series expansion, $\Delta\Pi$ can be expressed as

$$\begin{aligned} \Delta\Pi &= \Pi(u_i^0 + \delta u_i) - \Pi(u_i^0) \\ &= \delta\Pi + \frac{1}{2}\delta^2\Pi + \dots \end{aligned} \quad (10)$$

In Eq. (10), $\Pi(u_i^0)$ is the total potential energy of inspection body in the original equilibrium position, $\Pi(u_i^0 + \delta u_i)$ is the total potential energy of inspection body after disturbing displacement δu_i , $\Delta\Pi$ is the disturbing energy caused by the disturbing displacement.

Because the total potential energy is stationary value before disturbing, that is $\Delta\Pi = 0$. So there is the approximate relationship.

$$\Delta\Pi = \frac{1}{2}\delta^2\Pi \quad (11)$$

When do the numerical analyses, the value of $\delta^2\Pi$ can be expressed by the potential energy increment $\Delta\Pi$. The value of $\Delta\Pi$ and $\delta^2\Pi$ can also judge whether the inspecting body is stable or not, and the value of $\Delta\Pi$ can be got by numerical computation.

According to references [7], the disturbance energy nonlinear expressions in the initial stability problem can be derived by using the finite element discrete.

$$\begin{aligned} \Delta\Pi &= \sum_{e=1}^{N_e} \frac{1}{2} \{\Delta\delta^e\}^T [k_{ep}] \{\Delta\delta^e\} \\ &+ \sum_{e=1}^{N_e} \frac{1}{2} \{\Delta\delta^e\}^T [k_\sigma] \{\Delta\delta^e\} \\ &+ \sum_{e=1}^{N_e} \int_{\Omega^e} \{\Delta\delta^e\}^T [B] \{\sigma^0\} d\Omega \\ &- \sum_{e=1}^{N_e} \{\Delta\delta^e\}^T \{R_e^0\} \\ &= \Delta U - \Delta W \end{aligned} \quad (12)$$

In Eq. (12),

$$\Delta U = \sum_{e=1}^{N_e} \frac{1}{2} \{\Delta\delta^e\}^T [k_{ep}] \{\Delta\delta^e\} + \sum_{e=1}^{N_e} \frac{1}{2} \{\Delta\delta^e\}^T [k_o] \{\Delta\delta^e\} + \sum_{e=1}^{N_e} \int_{\Omega^e} \{\Delta\delta^e\}^T [B] \{\sigma^0\} d\Omega - \sum_{e=1}^{N_e} \{\Delta\delta^e\}^T \{R_e^0\}$$

$$\Delta W = \sum_{e=1}^{N_e} \{\Delta\delta^e\}^T \{R_e^0\}$$

In Eqs, (13) and (14), $\{\Delta\delta^e\}$ is the disturbing displacement. ΔU denotes the deformation energy increment which stores in the objects after disturbing, which is the factor to make the system revert to the initial position, calling disturbing internal energy. ΔW means the work that is outside force work on the disturbing displacement, which will consume the energy of the system.

According to references [7], the definition of stability safety coefficient is as

$$K_s = \frac{\Delta U}{\Delta W}$$

Owing to the disturbing energy is scalar quantity, we can give the inspecting body's disturbing energy isoline after getting the disturbing energy of each unit of the inspection body. Obviously, the minimum disturbing energy isoline (face) which also has free face is the most dangerous latent slide face, and the most disadvantageous disturbing displacement of each point on the slip face's resultant displacement vector direction is the most disadvantageous slip direction.

VII. PROJECT EXAMPLE ANALYSIS

7.1 The stability analysis of high arch dam abutment

In the middle downstream of the Yalong River in china, a high arch dam is planed to be set up. The height of the dam crest is 1 885m, the height of construction base level is 1580m, the height of the dam 305m, ranking the first in the world. By applying the three-dimensional non-linear FEM theory and the disturbing energy method and static method of structural stability evaluation, this paper established the total three-dimensional computation model of the arch dam and foundation, and carried out a research for the total stability of arch dam and left abutment.

According to the geological conditions of left abutment, four groups possible slide mass can be identified. Due to lacking of information about initial stress, here, the initial stress field is the gravity stress field.

The stability safety coefficients of left abutment rock under natural conditions are given in Table 1.

TABLE 1, VALUES OF STABILITY SAFETY COEFFICIENT OF LEFT ABUTMENT ROCK

No.	(1)	(2)	(3)	(4)
disturbing energy method	1.721	1.867	1.795	1.816
static method	1.960	1.924	2.299	2.793

From the results shown in the table above, the four minimum clipping and friction stability safety factor against sliding of possible gliding mass is 1.924 of left dam abutment after the building of the dam, all in a stable condition, but security reserves are short.

7.2 Results comparison of several projects by using disturbing energy method

The values of the total stability safety coefficient of several arch dam in china by using disturbing energy method are given in Table 2.

TABLE 2, VALUES OF THE TOTAL STABILITY SAFETY COEFFICIENT OF SEVERAL ARCH DAMS

Names of projects	safety coefficient
Left Slope of Lijiaxia	1.72
Ertan	2.17
Xiaowan	1.88
Jingping	1.64
Xiluodu	2.60

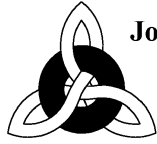
VIII. CONCLUSION

Based on the review and evaluation of the existing dam abutments and foundation and the total stability analysis method, this paper establishes the linking application of the disturbing energy method and the static method, the quantitative criterion standards and analysis of the local and total stability of arch dams, the criteria and method have been successfully applied to a number of projects. The disturbing energy method strictly abides by the basic principles of computational mechanics and gives the stability safety coefficient of local or total from the view of energy. Because the energy is a scalar, it avoids disunity of anti-slide stability safety coefficient leading by different projection methods. However, the safety coefficient got by the disturbing energy method is different from mechanism of anti-slide stability safety coefficient, the intrinsic link between them is still lack of deep study, and there isn't a stability criterion standard, they still can be a complement and reference. If combining with the disturbing energy method and the static method, especially it can be used to identify the latent slide mass and possible slide direction; combining with static method it can make comprehensive evaluation of the stability of dam abutment.

This work was supported by the National Natural Science Foundation of China (No.50978083).

REFERENCES

- [1] Yang Qiang, Zhu Ling, Zhai Ming-jie. "On Mechanism of Rigid-body Limit Equilibrium Method for Abutment Stability Analysis of Arch Dam", *Chinese Journal of Rock Mechanics and Engineering*, **24(19)**, pp3403-3409, 2005. (in Chinese)
- [2] Yang Baoquan, Zhang Lin, Chen Jianye, Dong Jianhua, Hu Chengqiu. "Experimental Study of 3D Geomechanical Model for Global Stability of Xiaowan High Arch Dam", *Journal of Sichuan University, Chinese Journal of Rock Mechanics and Engineering*, **29(10)**, pp 2086-2093, 2010. (in Chinese)
- [3] Yang lingqiang, Lian Jijian, Zhang Sherong. Chen Zuping. "Analysis of Breaking and Overloading of Arch Dams", *Journal of Hydraulic Engineering*, **3**, pp55-62, 2003. (in Chinese)
- [4] Zhang Youtian, Zhou Weiyuan. *Deformation and Stability of High Rock Slopes*, Beijing: China Water Conservancy and Hydropower Press 1999. (in Chinese)
- [5] Zhou Weiyuan. *Advanced Rock Mechanics*, Beijing: Water Resources and Electric Power Press 1989. (in Chinese)
- [6] Hill R. "On Uniqueness and Stability in the Theory of Finite Elastic Strain", *J. Mech. Phys Solids*, **5**, pp 229-241, 1957.
- [7] Shao Guojian, Zhuo Jiashou, Zhang Qing. "Research on Analysis Method And Criterion of Rockmass Stability", *Chinese Journal of Rock Mechanics and Engineering*, **22(5)**, 691-696, 2003. (in Chinese)



Defining ecological and economical hydropower operations: a framework for managing dam releases to meet multiple conflicting objectives

规划生态与经济型的水利发电运作：通过监管大坝释放量来实现多种相互冲突目标的框架

Elise R. Irwin

U.S. Geological Survey, Alabama Cooperative Fish and Wildlife Research Unit, Auburn University, Auburn, Alabama, 36849 USA

eirwin@usgs.gov

Accepted for publication on 16th November 2014

Abstract - Hydroelectric dams are a flexible source of power, provide flood control, and contribute to the economic growth of local communities through real-estate and recreation. Yet the impoundment of rivers can alter and fragment miles of critical riverine habitat needed for other competing needs such as downstream consumptive water use, fish and wildlife population viability, or other forms of recreation. Multiple conflicting interests can compromise progressive management especially with recognized uncertainties related to whether management actions will fulfill the objectives of policy makers, resource managers and/or facility owners. Decision analytic tools were used in a stakeholder-driven process to develop and implement a template for evaluation and prediction of the effects of water resource management of multiple-use systems under the context provided by R.L. Harris Dam on the Tallapoosa River, Alabama, USA. The approach provided a transparent and structured framework for decision-making and incorporated both existing and new data to meet multiple management objectives. Success of the template has been evaluated by the stakeholder governing body in an adaptive resource management framework since 2005 and is ongoing. Consequences of management of discharge at the dam were evaluated annually relative to stakeholder satisfaction to allow for adjustment of both management scenarios and objectives. This template can be applied to attempt to resolve conflict inherent in many dam-regulated systems where management decisions impact diverse values of stakeholders.

Keywords – Decision analysis; hydropower; conflicting objectives; adaptive resource management

摘要：水电大坝是一种灵活的能量来源，它可用于防洪并能以固有地产和休闲场所的形式有助于当地经济的增

长。然而，河流的拦蓄能够改变和破坏下游数英里内的其他需求所依赖的河流环境，比如下游的消费用水，鱼类和其他野生动物的种群的生存力，以及其他形式的休闲活动。多种相互冲突的利益可以通过协调形成渐进式的管理而实现，尤其是在面临诸如管理行为是否能满足政策制定者、资源管理者以及设备所有者的需求等不确定因素的情况下。以美国阿拉巴马州塔拉普萨河 R.L. Harris 大坝为例，通过运用决策分析的工具建立和实施了一个用以评估和预测水资源管理的多重应用系统的模板。该模板为决策制定提供了一个透明且有组织的框架，并能整合已知和全新的数据以满足多个不同的管理目标。自 2005 年以来，作为一个资源管理框架的成功案例，该模板已得到了相关主管部门的肯定并一直沿用至今。大坝排放量管理的成效依据利益相关者的满意度，每年进行相应的评估以便调整管理方案和目标。该模板可应用于尝试解决与水坝系统相类似的许多系统中的固有冲突，这些系统中决策的管理影响着利益相关者的各种利益。

关键词：决策分析；水利发电；冲突目标；自适应资源管理。

I. INTRODUCTION

Society's need for clean water and power is critical to human existence and progress. Hydropower represents a flexible, clean, renewable source of power that supports 20% of the world's power needs [1]. Because of the nature of river systems as societal conduits for important services such as water, transportation, food, and recreation, rivers are

inherently multiple use systems. Although hydropower facilities supply many benefits to humans, dams can have negative impacts on both upstream and downstream uses of riverine systems [2]. Allocation of uses usually via regulatory policies for dam operation do not always account for conflicting objectives for system use. These conflicts revolve around different and often competing values by land-owners, municipalities, fishers and hunters, navigation and boating interests, environmentalists and natural resource managers [3]. Although creative exchanges, negotiations and cooperative arrangements to resolve disputes are more common than “water wars” [4], transparent frameworks for water allocation decision making have been called for [5], [6].

Adaptive resource management incorporates societal needs (or values) in a transparent open forum with managers and scientists and is a special iterative form of structured decision making [7], [8]. Water allocation decision making-including dam release applications-meets the criteria for adaptive management which strives to reduce structural uncertainty over time through application of management scenarios and measurement of success of those prescriptions on stated objectives. Therefore, adaptive management frameworks allow for decision making in the face of uncertainty, can account for changes in applicable policy and environmental states, and allow for learning about effects of management actions on water management problems in question[9], [10]. In this paper, I describe the long-term application of adaptive management to a river regulated by a large privately owned hydropower facility. Multiple conflicting objectives emerged decades ago shortly after the dam was closed. In 2002, an adaptive process was suggested to alleviate litigious threats and ultimately define solutions acceptable to the stakeholders [3].

II. CASE STUDY-TALLAPOOSA RIVER, ALABAMA, USA

The Tallapoosa River below R.L. Harris Dam is a 78-km reach where river flow is strongly influenced by the daily generation schedule at the dam (Fig 1). Harris was constructed for hydropower, with other potential benefits including flood control, recreational opportunities on the reservoir created by the dam, and economic growth associated with the reservoir. The dam has two turbines (135 mega-watts) that account for about 10% of the total capacity of the 11 privately-owned hydropower dams in the eastern Mobile River drainage. Since completion in 1983, Harris Dam has been operated primarily as a hydropeaking facility, such that water is released in pulses, usually 4-6 hours in duration, through one or two turbines, each with the capacity to pass 226 cms. Historically, generation occurred once or twice daily, five days a week, and usually included no generation on weekends (i.e., pre-adaptive management flow regime). As a result of the hydropeaking operation, the flow regime was characterized by extreme low flows and high flows associated with one- or two-turbine generation (Fig 2). Comparison of pre- and post-dam flow data indicated that high flows were dampened, low flows were

lower and more frequent and seasonal shifts in flow magnitude) were quantified [3].

In addition to flow alteration, the temperature regime below the dam has been affected; whereas, during spring and summer months, temperature decreases as much as 10°C during generation events [3]. During non-generation periods, the Federal Energy Regulatory Commission (FERC) license for Harris Dam requires that flow as recorded at the United States Geological Survey (USGS) stream gage at Wadley, Alabama (#02414500; 22 km downstream from the dam) is not to fall below the pre-dam historic record low-flow of 1.27 cms.

The river below the dam is one of the longest and highest-quality segments of Piedmont river habitat remaining in the Mobile River drainage, which is one of the most biologically diverse river drainages in North America [11]. Extensive areas of rocky shoal habitat are abundant along this portion of the river. The native fish that live there number at least 57 species, including a minimum five species endemic to the Tallapoosa River system. Prior to construction of Harris Dam, the river also supported productive sport fisheries for black basses (*Micropterus* spp.) and catfishes (primarily channel catfish *Ictalurus punctatus* and flathead catfish *Pylodictis olivaris*), as well as river boating activities (D. Catchings; Alabama Department of Conservation and Natural Resources, personal communication).

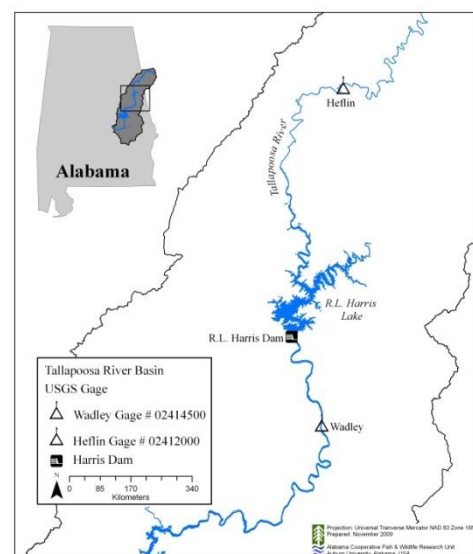


Figure 1.-Location of study site in the Tallapoosa River Basin. The river is regulated below Harris Dam, and unregulated above R. L. Harris Lake. USGS gages are maintained at Heflin and Wadley, Alabama, USA.

Declines in angler success rates and the loss of access to the river because of changes in flow regime have been major concerns since construction of Harris Dam. However, altering the peaking operation could threaten the power utility’s flexibility to provide and sell electricity on demand during periods of peak consumption. Changes in dam operation could also affect water levels and therefore values for home owners

and other recreationists that use the lakes in the system, particularly at Harris Reservoir.

Management issues in the study reach below Harris Dam were based on how dam operations impacted social values associated with power production needs, water availability for economic development, consumption, boating, angling and other recreational activities (upstream and downstream of the dam), and the general health of the Tallapoosa River ecosystem (Fig 3). These conflicting management objectives had been vocalized for many years, yet the ability of stakeholders to reach agreement over what and how to change management at the dam have not been realized.

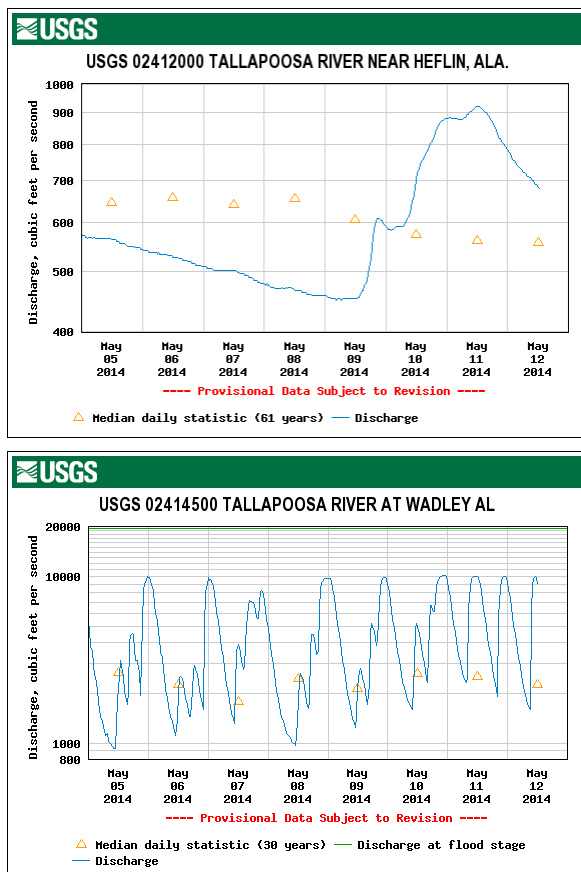


Figure 2.-Tallapoosa River discharge measured at USGS gage 02412000 (top panel-naturally occurring flows) located near Heflin, Alabama and USGS gage 02414500 (bottom panel-regulated by Harris Dam) located in Wadley, Alabama, 22km below the dam (5-12 May 2014; <http://waterdata.usgs.gov>; data reported in ft³/s).

Multiple stakeholders wanted to develop of a plan of action. One alternative was to ask FERC to reopen the regulatory license and order evaluation of dam operation with respect to competing objectives. This option was not desirable to the utility owner, particularly in light of previous experiences where a reopened regulatory license resulted in a re-negotiated flow regime developed without options to amend the license based on meeting (or not meeting) stakeholders’ objectives.

Formal discussions with stakeholders and the publication of Irwin and Freeman’s [3] framework provided a roadmap toward implementation of adaptive management below the dam. The stakeholders recognized that quantification of system function during management would assist with reduction in uncertainty related to future FERC regulations—the license is scheduled to be renewed in 2023.

III. CONFLICTING STAKEHOLDER VALUES AND DECISION ANALYSIS

To begin the adaptive management process, a workshop was conducted to determine the stakeholder objectives (see www.RiverManagement.org for transcripts of the workshop). The goal of the workshop was to implement a structured process to make a decision about providing different flows at the dam that would satisfy the most stakeholders. The participants varied from biological experts to local landowners that reside on the reservoirs and the river, but all had a common interest in making positive progress toward making the right changes. Stakeholders (23 groups participated) were polled by professional facilitators (www.group-solutions.com) using an interactive session regarding the features about the river and reservoirs that were most important to them. The 10 resulting primary values (i.e., fundamental objectives [8]) that were identified are listed below (Table 1).

Stakeholders ultimately agreed upon these equally weighted fundamental objectives as complete and representative of the interests of all parties involved. In addition, stakeholders agreed to adopt the concept of adaptive management as a framework for future discussions and management decisions.

TABLE 1, FUNDAMENTAL OBJECTIVES OF STAKEHOLDERS.

Maximize economic development
Maximize diversity and abundance of native fauna and flora
Minimize bank erosion downstream from Harris Dam
Maximize water levels in the reservoir
Maximize reservoir recreation opportunities (e.g., angling, boating, swimming)
Maximize boating and angling opportunities downstream from Harris Dam
Minimize total cost to the power utility
Minimize river fragmentation
Maximize power utility operation flexibility
Minimize consumptive water use

Objectives established at the workshop were used in a decision model to assist stakeholders in making complex decisions necessary to change the flow regime below Harris Dam. To make the initial decision, stakeholder’s objectives were incorporated into a decision network using Bayes network software [12] that incorporated probability matrices associated with projected outcomes under different management options. For example, individual stakeholders understood that if too much water was released from the dam

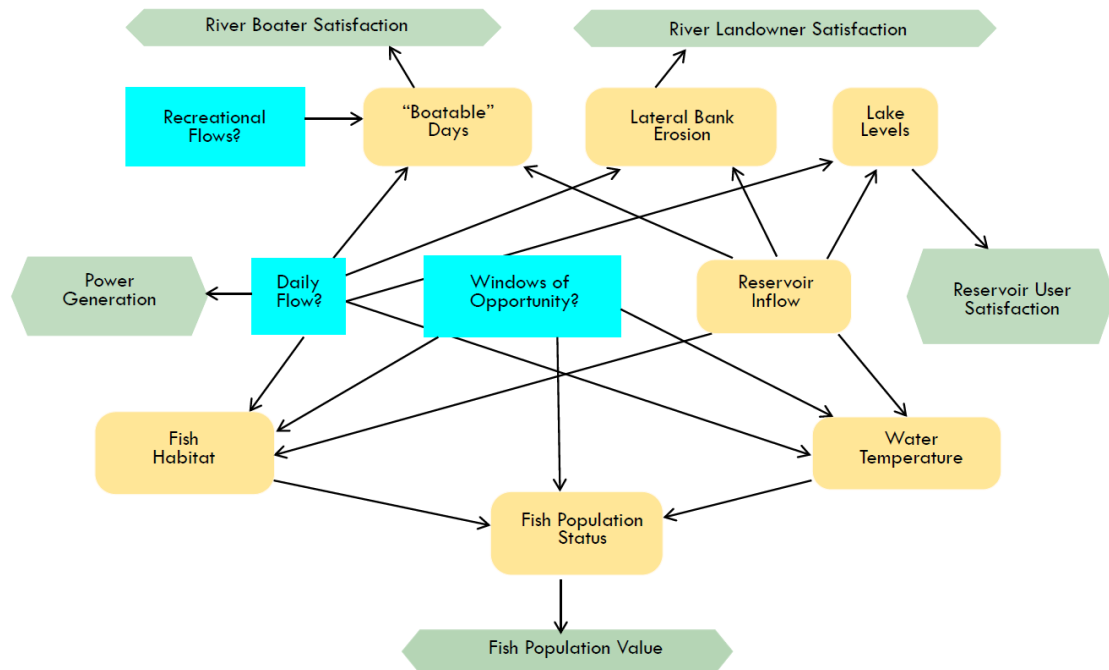


Fig. 3.-Simplified influence diagram showing the complexity of managing flows below R.L. Harris Dam. The blue rectangles are the decisions that were made about flow, the yellow ovals are stakeholder objectives, and the gray hexagons are “satisfaction” (utility) values of the different stakeholders. The initial flow management decision was the portfolio that maximized the satisfaction of the stakeholders.

for downstream needs then lake levels could be impacted. Constraints by stakeholders were defined before the model was parameterized to ensure that solutions that were completely impossible were accounted for. For example, the power utility needed to utilize peak power production procedures to maximize the flexibility of the facility to provide energy to the grid. Stakeholders then needed to find a way to evaluate tradeoffs associated with the impact of the management options on their different values; and given the complexity of the decision, the network was invaluable. Because the decision network was visual in nature (Fig. 4), the stakeholders could evaluate how their objectives were affected as different management scenarios were “tested.” The network evaluated thirty-two management portfolios that were combinations of flow regimes, spawning conditions for fish and boating conditions. The model allowed for making an initial decision while acknowledging that uncertainty because it was not possible to know everything about how the system would respond to management. A governance structure was established that dictates the rules and periodicity for decision making by a governing board that is informed by both technical committees that consist of science and engineering experts and model updates based on collection of data of system response to management.

The decision model indicated that stakeholders would be most satisfied if more water from the dam was released, October boatable flows were provided, and stable flows (in

spring and summer) were provided for fish spawning potential (blue rectangles; Fig. 4). This management portfolio was named the “Green Plan” and the daily amount of water that was released from the dam was determined by the daily volume of water at the USGS gage (#02412000; located upstream from the reservoir) on the previous day. Water was delivered through the turbines in 20-30 minute pulses or through regular power generation depending on the volume needed to meet the management target. Management was initiated in March 2005 and response to flow management on stakeholder objectives has been measured yearly (see Sec IV).

IV. REDUCING SYSTEM UNCERTAINTY

The initial parameterization of the Bayes network was conducted with both expert opinion and empirical data (see Table 2 for variable descriptions, [13]). There was uncertainty related to how certain state parameters would respond to management. In particular, management of various aspects of the flow regime under the Green Plan was hypothesized to provide habitat stability for fishes and acceptable boatable conditions while maintaining suitable lake levels above the reservoir and ensuring flexibility for the utility but we were unsure of the specific responses of these and other variables. Therefore careful evaluation of response of variables to management was critical to reduction of uncertainty in the system. This was conducted using a carefully designed

TABLE 2, DESCRIPTION OF STATE VARIABLES, DATA SOURCES AND RANGES OF VALUES FOR THE INITIAL MODEL PARAMETERIZATION (SEE FIG. 4). NOTE THAT EROSION* IS AN UNINFORMED NODE BASED ON LACK OF DATA AND RESOURCES TO COLLECT DATA AND RESERVOIR INFLOWS** HAS FIVE RESPONSE LEVELS VERSUS THREE.

State Variable	Brief Description; Source	Range		
		High	Medium	Low
Boatable Days	# consecutive weekend days discharge between 12.7 and 56.6 cms; USGS gage data	> 70 d/yr	40-70 d/year	< 40 d/yr
Erosion*	No data/Uninformed node	High	Moderate	Low
Lake Levels	# days/year that lake levels fall below rule curve; APC	< 10 d	11-20 d	> 21 d
Reservoir Inflows**	Exceedence flows (cms) for reservoir tributaries combined; USGS data	Flood > 48.1 cms Wet 42.5-48.1 cms	Normal 28.3-42.5 cms	Dry 17.0-28.3 cms Drought >17.0 cms
Flow Through Pools	Pool habitat percent with flow > 20 cm/s; Expressed for different inflows using PHABSIM model	High Normal Year > 50%	Moderate Normal Year 20-50%	Low Normal Year <20%
Shallow-fast Amounts	Shallow (<45 cm)-Fast (>45 cm/s) habitat percent; Expressed for different inflows using PHABSIM model	High Normal Year 60-100%	Moderate Normal Year 20-60%	Low Normal Year <20%
Slow-cover Amounts	Slow(>20 cm)-Cover (present) percent; Expressed for different inflows using PHABSIM model	High Normal Year 50-100%	Moderate Normal Year 10-50%	Low Normal Year <10%
Degree Days	#10-d periods where cumulative degree days exceeded 17.2°C; USGS data expressed as percent of days in growing season	High >65%	Moderate 45-60%	Low <45%
Small Fish Abundance	Number of juvenile fish in 100 samples; USGS data	High >50	Moderate 20-50	Low <20
Bass Recruitment	Number of juvenile bass in 100 samples; USGS data	High >20	Moderate 10-20	Low <10
Redbreast Sunfish Spawning	Number of juvenile redbreast sunfish in 100 samples; USGS data	High >60	Moderate 30-60	Low <30

monitoring program. Data regarding reservoir inflows and lake levels, number of boatable days and provision of spawning conditions were calculated each year based analysis of the hydrology data provided by the USGS gages or collected by the utility as part of their FERC license requirement.

The response of the biological parameters was evaluated by design and implementation of a program to quantify variation in fish occupancy in relation to system co-variates [14]. The response of fish habitat variables was evaluated by seasonal application of the post management hydrograph to a Physical Habitat Simulation Model (PHABSIM, [15]) that was developed at two of the sites.

Bayesian updating of probability distributions was performed yearly from 2005-2013 in Netica to learn how the management regime affected stakeholder objectives. The stakeholders have been apprised of the results periodically and formally through board meetings and through other methods such as publications and presentations and specific stakeholder briefings.

V. FRAMEWORK FOR LEARNING AND THE DOUBLE-LOOP

In general, most stakeholders have been somewhat “satisfied” with the outcome of the management regime; however, it appears that improvements may be possible. For example, black bass recruitment (# of juvenile bass/sample) and “boatable” days (# of weekend days where flow is between 14.2-56.6 cms) targets were not consistently met under the green plan. In addition, when the decision model was updated with new information each year (i.e., Bayesian updating), the “right” flow decision varied indicating that a different management regime may be more beneficial.

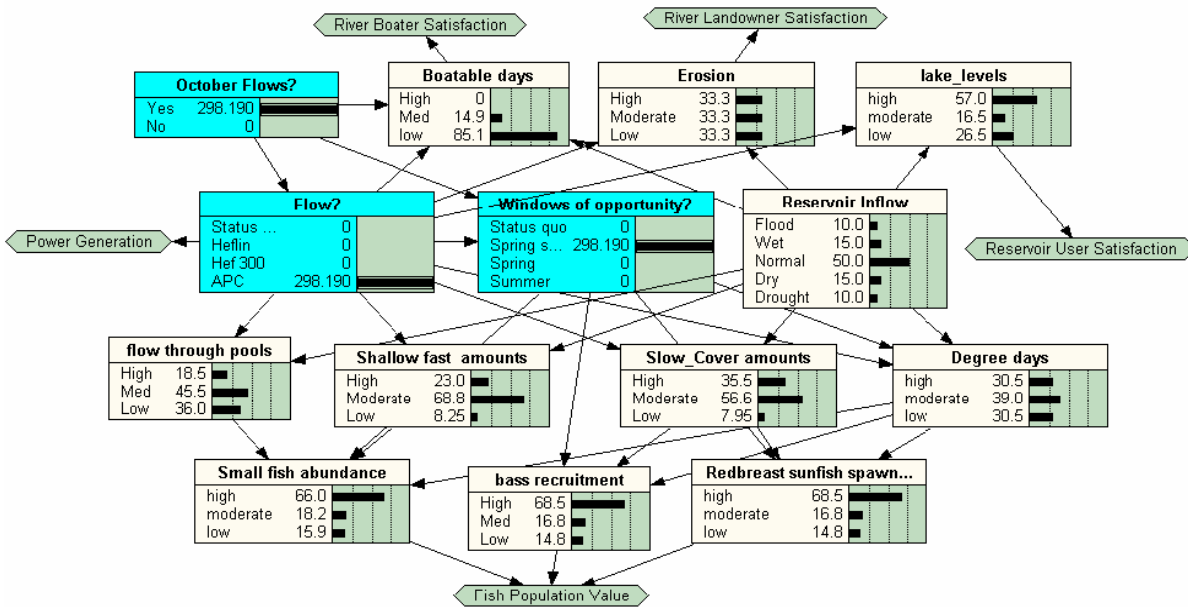


Figure 4. Bayesian decision network used to determine an initial flow prescription for adaptive management of Harris Dam, Tallapoosa River, Alabama. The initial decisions are illustrated in the blue rectangular boxes and the decision portfolio was to conduct the “APC” flow option, provide spring and summer spawning conditions (windows of opportunity) and October flows for boating. The other nodes display probability distributions for individual state variables that are attributes for the various fundamental objectives (see text for more detail). The hexagons represent utility values of the stakeholders and the decision was the one that optimized the satisfaction of the stakeholders (greatest sum of the utility values; equal to 298.190 and displayed in the three decision nodes). See Table 2 for descriptions of state variables and data sources.

The status of the project is ongoing with stakeholders considering a re-evaluation of their objectives in summer 2014. In an adaptive management context this is called double-loop learning [17] and is important because as stakeholders learn more about how a complex problem is constructed they also tend to adjust their expectations and desired outcomes. If this type of adjustment is done in a structured and transparent way then conflict over changing objectives will be minimized. Overall the project has been a success in that stakeholders have learned something about how their objectives responded to management and they remain committed to continuation of the project at least up to the time when the FERC license will be evaluated and renewed (2017-2023). In addition, the project is one of the few aquatic examples of adaptive management where the “loop” has been closed and re-evaluation will likely change future management [10].

VI. DISCUSSION

Integrated and adaptive management of water resources is becoming a global paradigm that is beginning to replace command and control approaches [5], [18]. Integrated water resource management

(IWRM) and adaptive management are different processes that have been applied to address complex management of water problems [18]. The case study presented here has elements of IWRM in that it is heavily stakeholder driven with a governance structure, while it maintains the elements of adaptive management. Because institutional barriers often derail adaptive processes [(Walters 1996)] frameworks that combine stakeholder driven cooperative management with structured decision making and learning are mechanisms for changing social-ecological systems into improved states [19]. Although the case of the Tallapoosa River is an example that only involves one dam, the complexities (and uncertainties) of the system along with the social-ecological demands are not trivial. The long-term commitment of the decision making board and the inclusivity of certain stakeholders in making management decisions together provide an excellent example of co-management that illustrates the benefits of governance structure even for seemingly localized problems at fine landscape scales.

VII. CONCLUSION

Conflict resolution where water rights are involved requires communication, cooperation and trust and these terms may not apply when conflict over water arises. Adaptive management of the flows below Harris Dam allowed for modification of flows below the dam without re-opening the FERC license which was a win-win for the stakeholders because regulatory red-tape and potential litigation does not provide a framework for testing potential solutions to the actual problem. Consequently, the adaptive management framework has been proposed to find solutions to water allocation issues below several other dams in the Southeast United States (e.g. Weiss Dam, Coosa River, Alabama; Tim's Ford Dam, Elk River, Tennessee). Success of the project is attributed to stakeholder innovation, leadership and patience through the learning process and quantification and parameterization of the decision model that allowed stakeholders to evaluate trade-offs associated with different management actions. Finally, because of population growth in the region coupled with potential changes in climate, demand for water resources may increase and additional conflict could arise. Embracing frameworks such as stakeholder-based adaptive management that consider social values and are informed with scientific findings will be important in the future.

ACKNOWLEDGEMENTS

This research was funded by the United States Geological Survey, the United States Fish and Wildlife Service, the Alabama Department of Conservation and Natural Resources, and the Alabama Power Company. The Alabama Cooperative Fish and Wildlife Research Unit is jointly sponsored by the U.S. Geological Survey; the Alabama Department of Conservation and Natural Resources, Wildlife and Freshwater Fisheries Division; the Alabama Agricultural Experiment Station, Auburn University; the Wildlife Management Institute; and the U. S. Fish and Wildlife Service. This study was performed under the auspices of Auburn University Institutional Animal Care and Use protocol # 2006-2569. Any use of trade, firm, or product names is for descriptive purposes only and does not imply endorsement by the U.S. Government.

REFERENCES

- [1] N. L. Panwar, S. C. Kaushik and S. Kothari. "Role of renewable energy sources in environmental protection: a review," *Renewable and Sustainable Energy Reviews*, **15**, pp. 1513-1524, 2011.
- [2] C. Pringle, M.C. Freeman and B.J. Freeman. "Regional effects of hydrologic alterations on riverine macrobiota in the New World: tropical-temperate comparisons", *Bioscience* **50**, pp 807-823, 2000
- [3] E. R., Irwin and M. C. Freeman. "Proposal for adaptive management to conserve biotic integrity in a regulated segment of the Tallapoosa River, Alabama, U.S.A." *Conservation Biology* **16**, pp 1212-1222, 2002.
- [4] A. Swain. "Water wars: fact or fiction?" *Futures* **33** pp 769-781, 2001.
- [5] C Pahl-Wostl, M. Craps, A. Dewulf, E. Mostert, D. Tàbara, and T. Taillieu. Social learning and water resources management. *Ecology and Society* **12**, pp 5-23.
- [6] N. L. Poff, J D. Allan, M. A. Palmer, D. D. Hart, B. D. Richter, A. H. Arthington, K.H. Rogers, J. L. Meyer, and J.A. Stanford. "River flows and water wars: emerging science for environmental decision making", *Frontiers in Ecology and the Environment* **6**, 298-306, 2003.
- [7] C.J. Walters. *Adaptive Management of Renewable Resources*. New York, MacMillan, 1986.
- [8] R. T Clemen. *Making hard decisions: an introduction to decision analysis*. Pacific Grove, California, Duxbury Press, 1996.
- [9] J. Peterson, C. Moore, S. Wenger, K. Kennedy, E. Irwin, and M. Freeman. "Adaptive management applied to aquatic natural resources" *Proceedings of the 2007 Georgia Water Resources Conference*, Athens, Georgia March 27-29, 2007.
- [10] B. K Williams and E. D. Brown. *Adaptive Management: The U.S. Department of the Interior Applications Guide*. Adaptive Management Working Group, Washington, DC U.S. Department of the Interior, 2012.
- [11] C. Lydeard, and R. L. Mayden. "A diverse and endangered aquatic ecosystem of the southeast United States," *Conservation Biology* **9** pp 800-805, 1995.
- [12] Netica 4.16 for MS Windows software. www.norsys.com, 2014.
- [13] B. Marcot, J. D. Steventon, G. D. Sutherland, and R. K. McCann. *Guidelines for developing and updating Bayesian belief networks applied to ecological modeling and conservation*.

- Canadian Journal of Forest Research 36 pp 3063-3074, 2006.
- [14] MacKenzie, D. I., J. D. Nichols, J. A. Royle, K. H. Pollock, L. L. Bailey, and J. E. Hines. Occupancy estimation and modeling: inferring patterns and dynamics of species occurrence. San Diego, California Elsevier, 2006.
- [15] Z. H. Bowen , M. C. Freeman and K. D. Bovee. "Evaluation of generalized habitat criteria for assessing impacts of altered flow regimes on warmwater fishes", Transactions of the American Fisheries Society, 127, 455-468 1998.
- [16] E. R Irwin and K. D. M. Kennedy. "Engaging Stakeholders for Adaptive Management Using Structured Decision Analysis." pp 65-68 in U.S. Geological Survey Scientific Investigations Report 2009-5049, 2009
- [17] D. Armitage, M. Marschke, and R. Plummer. "Adaptive co-management and the paradox of learning", Global Environmental Change 18 pp86-98, 2008.
- [18] N. L. Engle, O. R. Johns, M. Lemos, and D. R. Nelson. "Integrated and adaptive management of water resources: tensions, legacies, and the next best thing", Ecology and Society 16, 19-29, 2011.
- [19] C.T. Folke, T. Hahn, P. Olsson, and J. Norberg. "Adaptive governance of social-ecological systems", Annual Review of Environmental Resources 30, pp. 441-473 2005.



Numerical simulation of wave loads over a large container ship on mooring state

锚泊状态下大型集装箱船波浪载荷的数值模拟

Qiu Jin* (金秋), Tingqiu Li (李廷秋), Zaiqing Li (李再庆), Jianjian Xin (辛建建)

WUT-UoS High Performance Ship Technology Joint Centre, Departments of Naval Architecture, Ocean and Structural Engineering, School of Transportation, Wuhan University of Technology, P. R. China.

autumnjinqiu@163.com

Accepted for publication on 28th November 2014

Abstract –In this paper, the mooring dynamic loads and the motion responses of a large container ship in irregular waves with steady wind and current is investigated based on the commercial software AQWA. Comparisons between the time-history motion responses of a large container ship and the change of the mooring line tension in three different cases, non-mooring case, V-type mooring case and I-type mooring case are discussed. The result shows that there is a long-period surge and sway motion response to the large container ship because of two-order drift loading, and the two-order drift loading has a strong effect on the response of large container ship system because of close low frequency between ship and wave. Both I-type mooring case and V-type mooring case can obviously reduce the surge and sway caused by second-order drift loading in typical sea conditions; conditions that each mooring line carries too much stress can be avoided by changing the mooring configuration in sea conditions. As expected, the relevant feature can provide a valuable base for the analysis of large container ships mooring in typical sea conditions.

Keywords –Second-order drift loading, mooring line tension, motion responses.

I. INTRODUCTION

Recently, with the development of global ship transport, it has been a tendency to build larger container ship. Under this condition, the safety of large ship becomes an important research subject. Especially on mooring state, if the ship bears high environmental loading, it's highly possible to be an accident caused by insufficient strength of mooring lines.

Researches on ship motion response of large ship on mooring state and the tension of mooring line are very difficult. The typical ship motion response of large container ship on mooring system not only includes first-order response which has the same frequency as the wave, but also contains two-order drift response. Even though the value of the two-order drift force is much smaller than the first-order force, it has a strong effect on the response of the large container ship system because of close low frequency between ship and wave (Dai and Duan, 2008). As the horizontal restoring force is very small, the natural oscillation periods long, which may leads to the resonance with low-frequency wave force. Wanget al (2007) used SESAM to analyze the static force and dynamic force of ship on SPM (single point mooring) state. After calculating different combinations of wind, wave and current, they found that on SPM state the tension of mooring line is very sensitive to the variation of wind and current while the surge and sway of ship has the biggest influence on the tension of mooring line.

The time-domain 3-D potential theory and segmental catenary theory have been used and the simulation model of the mooring system has been set up. Under the typical environmental condition, the motion response and tension of mooring line are analyzed under two different mooring states to get the curves of time-domain motion response of large container ship and tension of the mooring line over time, which can be a reference for the mooring of similar ships.

II. CALCULATION PROCESS AND BASIC THEORY

Calculation Process

The computations are carried out based the ANSYS-AQWA following the process illustrated in Fig.1. Firstly, the 3-D potential theory is used to calculate first-order, second-order wave loading, added mass and radiation damping caused by wave radiation and diffraction. Then the tension of the mooring line is carried out using the elastic catenary method. Under typical ocean environmental condition, the tension of the mooring line and the time-domain motion response with coupling of large container ship and the mooring lines are analyzed to obtain motion statistics and maximum.

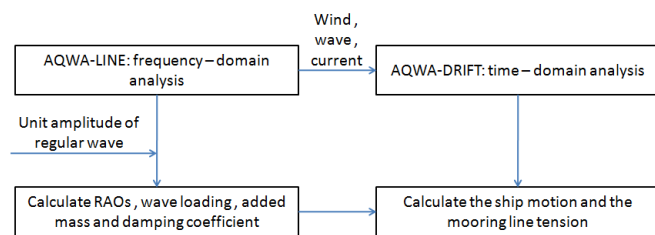


Fig.1 Calculation Process.

Basic Theory

Frequency-domain and Time-domain Motion Response Equation

The frequency domain analysis is carried out for regular waves of unit. Laplace's equation [L] is used as the governing equations. Boundary conditions are set up for lineared free surface boundary condition[F], the impenetrable body surface condition[S], the bottom condition at depth h [B] and the radition condition at infinity[R], as shown in Eq.(1).

$$\begin{aligned}
 [L] \quad & \nabla^2 \Phi(x, y, z, t) = 0, \text{ In the fluid domain} \\
 [F] \quad & \frac{\partial^2 \Phi}{\partial t^2} + g \frac{\partial \Phi}{\partial z} = 0, \quad z = 0 \\
 [S] \quad & \frac{\partial \Phi}{\partial n} = U_j n_j, \quad \text{at object plane} \\
 [B] \quad & \frac{\partial \Phi}{\partial n} \Big|_{z=-h} = 0 \quad \text{or} \quad \lim_{z \rightarrow -\infty} \nabla \Phi = 0 \\
 [R] \quad & \text{infinity radiation condition}
 \end{aligned} \tag{1}$$

The total potential function in Eq. (1) can be expressed as follows:

$$\Phi(x, y, z, t) = \phi(x, y, z) e^{-i\omega t} = \left[(\phi_I + \phi_d) + \sum_{j=1}^6 \phi_j x_j \right] e^{-i\omega t} \tag{2}$$

where ϕ_I : incident potential function,
 ϕ_d : radiation potential function,
 ϕ_j : velocity potential function caused by motion in j direction,
 x_j : motion response in j direction and
 ω : incident wave frequency.

Through frequency-domain calculation, the RAOs of structure under unit wave loading are obtained using Eq. (3) as follows:

$$[-\omega^2 (M_s + M_a(\omega)) - i\omega B + K] X(\omega) = F(\omega) \tag{3}$$

$$RAO = \frac{X(\omega)}{A} \tag{4}$$

where A : wave amplitude,
 M_s : ship mass matrix,
 M_a : added mass matrix,
 B : damping matrix ,
 K : hydrostatics stiffness matrix,
 F : wave excitation vector and
 X : motion response vector.

Time-domain motion equation is shown as follows:

$$M_s \ddot{X}(t) = F(t) \tag{5}$$

$F(t)$ refers to the total force action on float body, including the forces caused by wind, wave, current and the mooring lines.

Through impulse response method, the convolution integral form is as follows:

$$[M_s + M_a] \ddot{X}(t) + KX(t) + \int_0^t h(t-\tau) \dot{X}(\tau) d\tau = F(t) \tag{6}$$

Calculation of Second-order Wave Exciting Loading

The near field solution of second-order wave exciting force is as follows (Pinkster,1980):

$$\begin{aligned}
 F_{strc}^{(2)} = & \sum_{i=1}^N \sum_{j=1}^N \left\{ P_{ij}^- \cos[-(\omega_i - \omega_j)t + (\varepsilon_i - \varepsilon_j)] + P_{ij}^+ \cos[-(\omega_i + \omega_j)t + (\varepsilon_i + \varepsilon_j)] \right\} \\
 & + \sum_{i=1}^N \sum_{j=1}^N \left\{ Q_{ij}^- \sin[-(\omega_i - \omega_j)t + (\varepsilon_i - \varepsilon_j)] + Q_{ij}^+ \sin[-(\omega_i + \omega_j)t + (\varepsilon_i + \varepsilon_j)] \right\} \tag{7}
 \end{aligned}$$

Where P_{ij} and Q_{ij} are the in-phase and out-of-phase components of the time independent transfer function.

Supposing the sum frequency contribution can be ignored, the equation above becomes:

$$F_{strc}^{(2)} = \sum_{i=1}^N \sum_{j=1}^N \left\{ P_{ij}^- \cos[-(\omega_i - \omega_j)t + (\varepsilon_i - \varepsilon_j)] \right\} + \sum_{i=1}^N \sum_{j=1}^N \left\{ Q_{ij}^- \sin[-(\omega_i - \omega_j)t + (\varepsilon_i - \varepsilon_j)] \right\} \quad (8)$$

where ω_i and ω_j are the frequencies of each pair of waves, a_i and a_j are the corresponding amplitudes, ε_i and ε_j are the radiat ion phase angles.

According to Newman (1974):

$$P_{ij}^- = \frac{1}{2} a_i a_j \left(\frac{P_{ii}^-}{a_i^2} + \frac{P_{jj}^-}{a_j^2} \right), Q_{ij}^- = 0 \quad (9)$$

Thus Eq. (8) can be simplified to:

$$F_{sv}^{(2)}(t) = \sum_{i=1}^N \sum_{j=1}^N \left\{ P_{ij}^- \cos[-(\omega_i - \omega_j)t + (\varepsilon_i - \varepsilon_j)] \right\} \quad (10)$$

III. COMPARISON BETWEEN EXPERIMENTAL DATA AND NUMERICAL SIMULATION

Before using AQWA to analyze the problem, it's necessary to certify the validity of the theory. In this section, two cases are used to exam the theory. One is a mooring box-type floating breakwater case (Dong et al, 2009), and the other is a three anchors buoy system (Miao et al, 2003).

Experiment Parameter

CASE ONE

The box-type floating breakwater mooring system is composed of four mooring lines. The main geometrical parameters are listed in Tab. 1. The model is built in the AQWA-Line, shown as Fig.2.

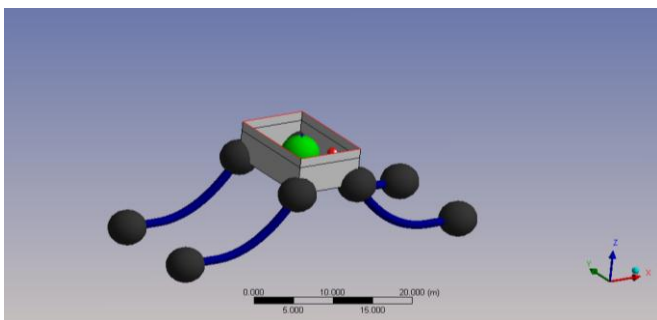


Fig.2 Box-Type Floating Breakwater System.

Table 1. The principal dimensions of floating breakwater system.

Name	Parameter	Value
Breakwater	Wide /m	0.3
	Moulded depth T/m	0.18
	Designed draft T/m	0.135
	Scale Ratio /m	1/30
Mooring line	Length/m	13.0

CASE TWO

The buoy system is composed of three parts: buoy, pontoon and the mooring lines. The main geometrical parameters and wave parameters are listed in Table 2 and Table 3, respectively. According to the offsets of the buoy system, the model is built and meshed which is shown as Fig.3:

Table 2. The geometrical characteristics of buoy system.

Item	Parameter	Value
Buoy	Diameter D ₁ /m	10.0
	Depth T /m	2.2
	Designed draft T /m	1.00
	Mooring point height /m	0.72
Pontoon	Diameter D /m	3.4
	Height H /m	1.62
	Mass M /kg	5000
Mooring line	Short anchor chain length /m	37.5
	Long anchor chain length /m	165.0
	Overall length/m	202.5

Table 3. Wave parameters.

Wave direction /°	180
Wave height /m	4.0
Period /s	1.98

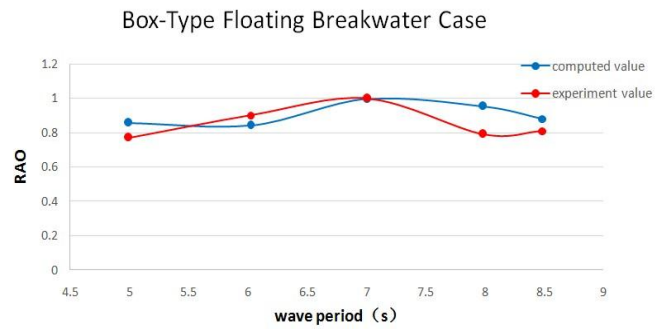
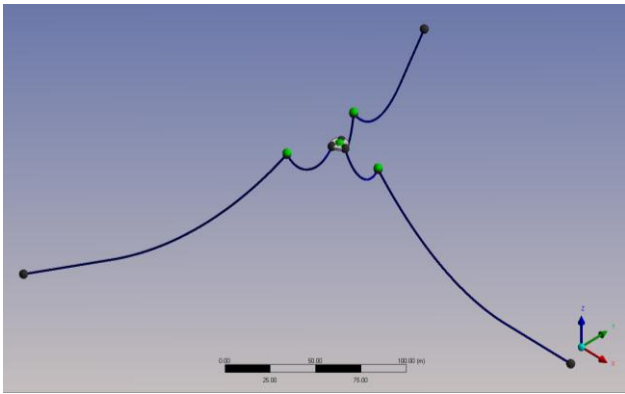


Fig.4 Box-Type Floating Breakwater System.

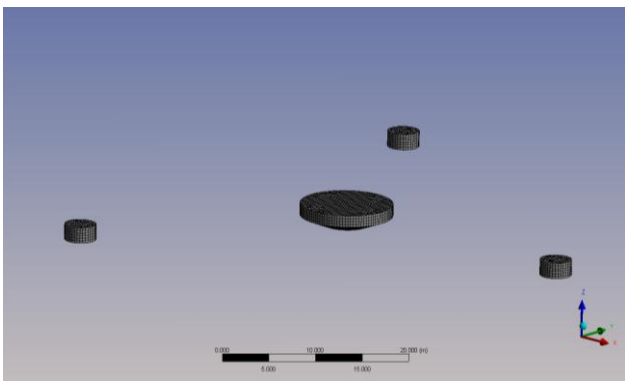


Table 5. Comparison between tested and simulation results of Buoy system in head waves.

item	measured value 1	measured value 3	surge	heave	pitch
Simulation result	0.729	1.666	3.58	1.87	9.05
Tested result	0.687	1.57	3.48	1.82	8.5
Relative error	6.10%	6.10%	2.9%	2.7%	6.50%

Fig.3 Buoy Displacement and Mesh.

Result Analysis

Comparison between experiment and numerical calculation of box-type floating breakwater and buoy motion response and mooring line tension, are listed in Tab.3 and 4, respectively. The tested and simulation results of the box-type floating breakwater system and the buoy system are shown in Fig.4 and 5. The comparison shows that the calculation results agree well with experiments. This indicates that modeling errors and settings of parameter, when using the software, are acceptable and the simulation method is feasible and reliable.

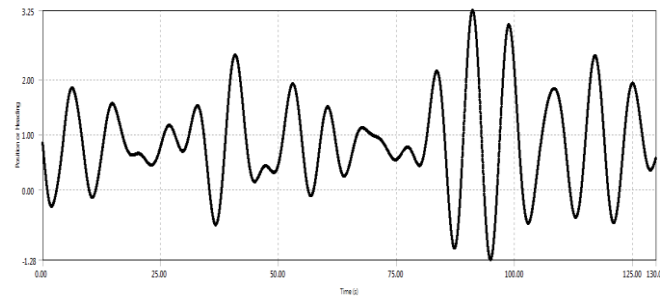


Fig.5 Time History of Buoy Heave Motion Response.

Table 4. Comparison between tested and simulation results of Box-Type Floating Breakwater System.

Period(s)	Calculated	Experimental	Error
5	0.85	0.77	10.39%
6.028	0.85	0.9	5.56%
7.0144	0.99	1	1.00%
7.99	0.95	0.79	20.25%
8.49	0.88	0.81	8.64%

IV. MOORING MODEL OF LARGE CONTAINER SHIP

In this paper, three different cases are considered, i.e., non-mooring case, V-type mooring case and I-type mooring case. The time-history motion responses and the changes of the tension of the mooring line are calculated. The mesh and displacement of fairlead are shown as Fig. 6, 7 and 8. Parameters of environmental condition and the mooring lines are as Tab. 6 and 7.

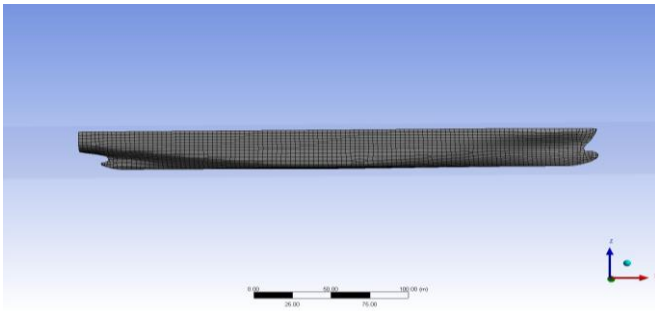


Fig.6 Mesh.

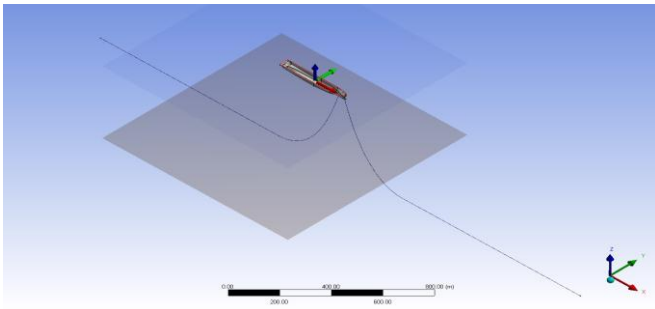


Fig.7 I-type mooring case.

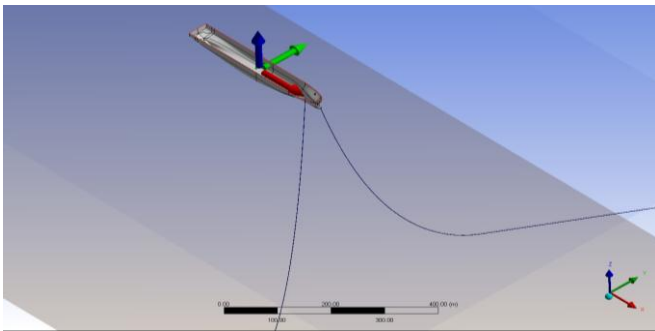


Fig. 8 V-type mooring case.

Line	Item	Value	
	Number	2	
	Overall length /m	1600	
	Length /m	400	
	Diameter /mm	108	
	Unit weight/kg·m ⁻¹	150	
Section 1	Stiffness EA/N	600000000	
	Max tension /N	7500000	
	Length /m	500	
	Diameter /mm	108	
	Unit weight/kg·m ⁻¹	120	
	Section 2	Stiffness EA/N	600000000
		Max tension /N	7500000
	Length /m	700	
	Diameter /mm	108	
	Unit weight/kg·m ⁻¹	170	
	Section 3	Stiffness EA/N	600000000
		Max tension /N	7500000

V. TIME-DOMAIN ANALYSIS OF LARGE CONTAINER SHIP ON MOORING STATE

Wave Condition of Head Sea (The angel between Ship and wave, wind, current is 180 degree.)

Analyzing the effect of second-order drift loading on large container ship, the motion response and the tension of the mooring line on different mooring state in typical environmental condition are obtained. The comparisons are shown as Fig. 9, 10 and 11. The results are listed in table 8.

Table 6. Wave, wind & current parameters .

parameter	value	
wave	Significant wave height /m	6.75
	Zero-crossing period /s	8.38
wind	Speed /m·s ⁻¹	20
current	Velocity /m·s ⁻¹	0.5
Angle between ship and wave, wind and current /°		180°& 145°

Table 7 mooring line parameters .

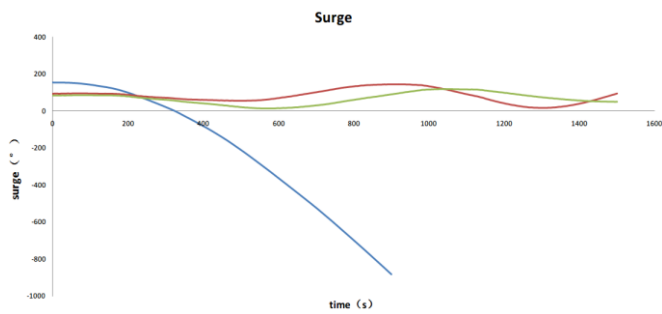


Fig.9 Ship Motion.

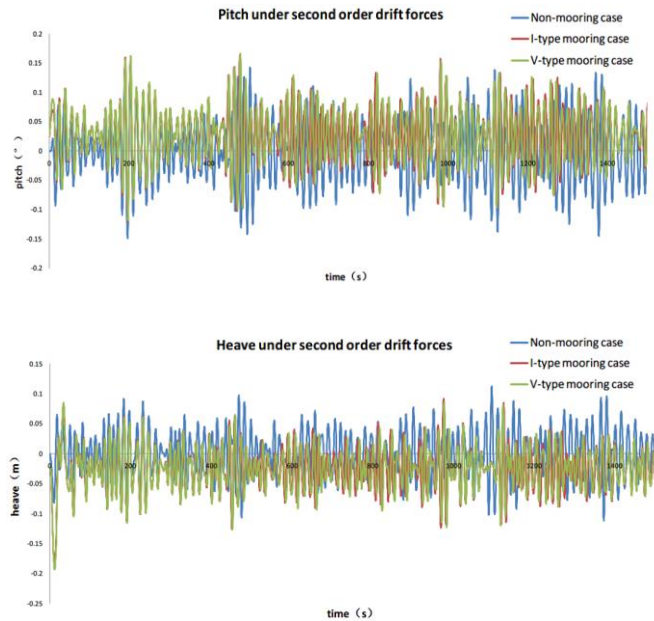


Fig.10 Ship Motion under Second Order Drift Force.

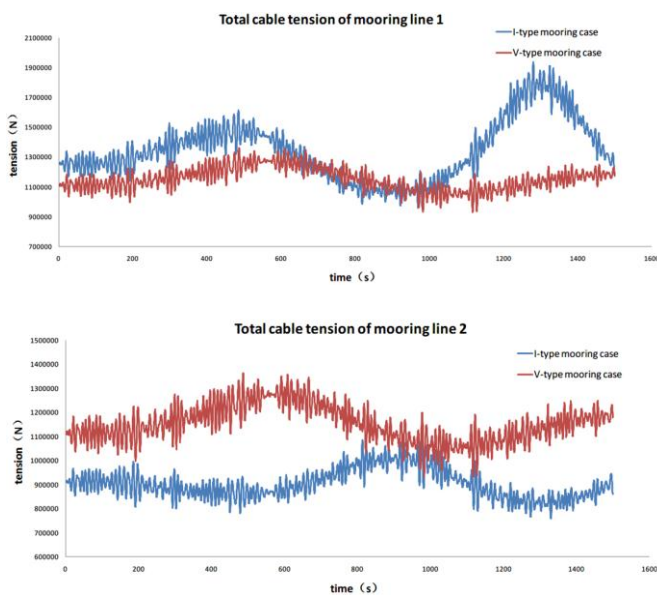


Fig.11 Mooring Line Tense

Table 8 Significant results under 180°.

	Non-m ooring case	I-type mooring case	V- type mooring case
Surge /m		34	45
Heave /m	0.443	0.444	0.441
Pitch /°	0.546	0.579	0.575
Heave under second order drift forces/m	0.055	0.027	0.026
Pitch under second order drift forces/°	0.059	0.094	0.095
Tension(line 1)/N		1760062	1240864
Tension(line 2)/N		1034329	1240222
Tension(line 1 section)/N		988000	437225
Tension(line 2 section)/N		232206	361698

Through the comparison we can get:

(1) As shown in Fig.9 and Tab.8, there is the long-period surge motion response of large container ship caused by two-order drift loading. Both of the two kinds of mooring ways can reduce the surge of ship, but I-type mooring case performs better relatively.

(2) According to Tab. 8, in head seas condition, there are almost no differences between the heave and the pitch motion whether the ship moors.

(3) In Fig.10 and Tab. 8, the influence of second-order drift loading plays nearly 10 percent proportion in motion responses on non-mooring state. V-type and I-type mooring case can obviously reduce the heave motion caused by second-order drift loading while increase the pitch about 5%.

(4) As shown in Fig.11 and Tab.8, in head seas condition, the tension of the mooring line is below the safety standard. However, the difference between two mooring line is relatively great in the I-type mooring case. It has a good chance that the dragging will happen.

It may be concluded that in head sea conditions, the V-type mooring case performs better.

Wave Condition of Bow Sea (The angel between Ship and wind, wave, current is 145 degree.)

Under the condition of bow sea, 145 degree, the comparisons of the motion response and the tension of the mooring line are as Fig.12, 13, 14 and 15. The results are listed in Tab. 9.

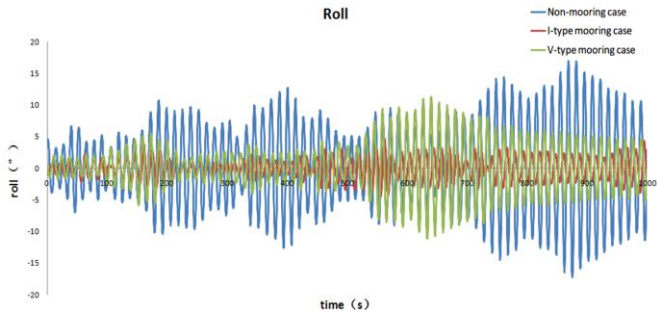


Fig.12 Ship Motion (roll).

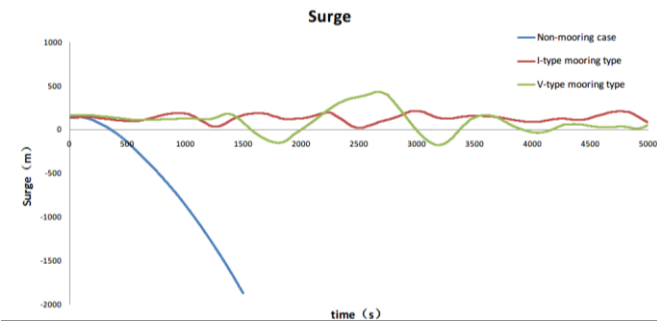


Fig.13 Ship Motion (surge and sway).

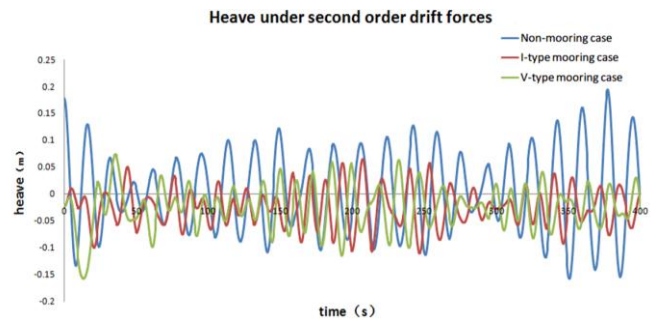
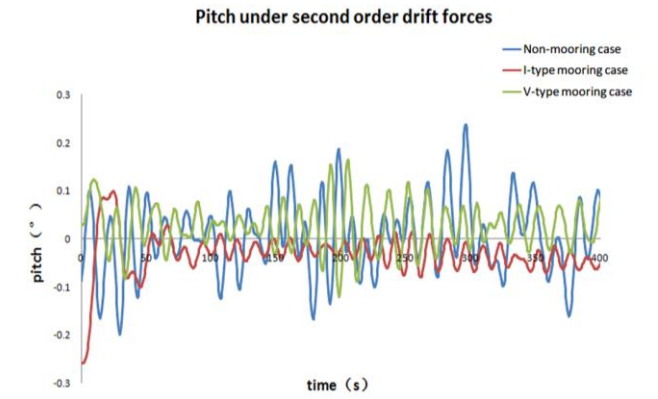
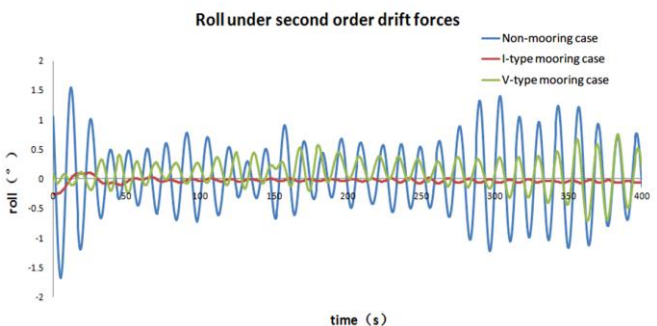


Fig.14 Ship Motion under Second Order Drift Force.

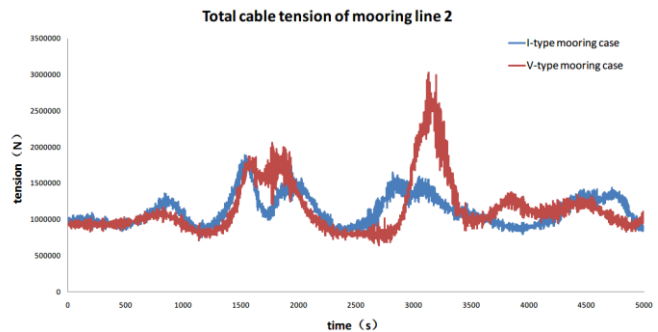
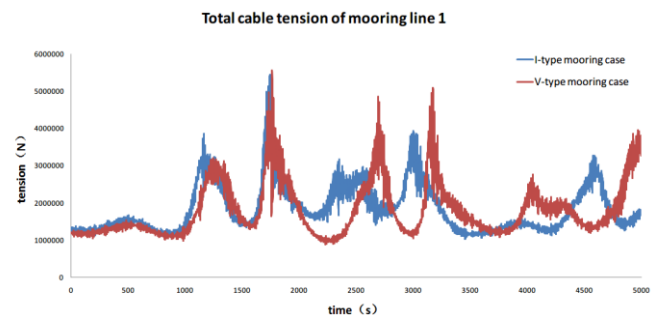


Fig.15 Mooring Line Tense.

Through the comparison it can be observed that:

- (1) According to Fig.12 and Tab.9, in bow seas condition, there is an obvious roll, so the I-type mooring case and V-type mooring case can both provide some restoring force to the ship, reducing the roll effectively. However, through the comparison of the data, it can be found I-type mooring case performs better.

Table 9 Significant results under 145°.

	Non-moori ng case	I- type mooring case	V- type mooring case
Surge /m		45	69
Sway /m		228	167
Heave /m	0.485	0.485	0.497
Roll /°	12.848	3.159	5.349
Pitch /°	0.846	0.650	0.661
Heave under second order drift forces/°	0.106	0.031	0.034
Roll under second order drift forces/°	1.573	0.10615	0.129
Pitch under second order drift forces/°	0.177	0.105	0.107
Tension (line 1)/N		2610385	2643026
Tension (line 2)/N		1381797	1551427
Tension/N (line 1section)		1878906	1911516
Tension/N (line 2 section)		590118	767629

(2) By comparing the influence of I-type mooring case and V-type mooring case on ship motion response, it's obvious that I-type mooring case performs better on reducing surge but worse on sway which are all caused by second-order drift force. The effectiveness depends on the angel between the mooring line and environmental loadings, i.e., wave, wind, current loadings.

(3) The loading conditions are almost the same between I-type mooring case and V-type mooring case. As the angle between environmental loadings and each mooring line is different in both two ways, there is always one mooring line carrying larger force than the other one in both two ways.

It can be concluded that in bow seas condition, the best mooring way depends on the specific conditions.

VI. CONCLUSION

In this article, a tentative conclusion is reached that the container ship motion response and the tension of the mooring line on two different mooring states in two different

environmental conditions, 180/145 degree between the ship and wind, wave and current.

The results are as follows:

(1) Both I-type mooring case and V-type mooring case can dramatically reduce the surge and sway caused by second-order drift loading in head sea and bow sea conditions compared with non-mooring case.

(2) Results show that the second-order drift loading in our study case plays nearly 10 percent proportion in motion responses on non-mooring state. Its impact on the ship can be highly reduced on mooring state.

(3) According to Tab.8 and Tab.9, it can be learned that when the angle between the two mooring lines is large, it can effectively restrict the ship movement in one direction (for example, I-type mooring case in both cases can effectively limit the surge motion of the ship), but also easily lead to one mooring line carries much higher environmental loading. In order to ensure the safety of the mooring line it is important to come up with an appropriate mooring way to avoid the condition that one of the mooring lines to bear too much force.

VII. ACKNOWLEDGMENTS

The present work is supported by the National Science Foundation of China (No.51139005, 51179142, 51039006) and by 111 Project (No B08031). We also thank the reference for helpful suggestions

REFERENCES

- [1] Yi-shan Dai, Wen-xiang Duan. Potential Flow Theory of Ship Motions in Waves, [M]. Beijing: National Defense Industry Press, 2008.113.
- [2] Wang, J.R., Li, H.J., Li P. and Zhou, K. Nonlinear Coupled Analysis of a Single Point Mooring System, Journal of Ocean University of China, 2007, 6(3):310-314.
- [3] PINKSTER J A. Low frequency second order wave exciting forces on floating structures [D] . Delft The Netherlands: Delft University of Technology, 1980. 53—55.
- [4] Quan-ming Miao, Min Gu, Zhan-ming Yang, De-cai Zhou, Xin Yuan. An experimental study on mooring buoy in waves. Ship Building of China, 2003. 359-366.
- [5] Huayang Dong, Yongxue Wang, Yong Hou, Yunpeng Zhao. An experimental study on hydrodynamic characteristics about the rectangular box floating breakwater. Fishery Modernization.3:7-11, 2009



Effect of PV module frame boundaries on cell stresses in solar cells

光伏模块的框架边界对太阳能电池板中应力的影响

Johannes Schicker^{1*}, Christina Hirschl¹, Roman Leidl²

¹ CTR Carinthian Tech Research AG, Europastraße 4/1, 9524 Villach, Austria

² AIT Austrian Institute of Technology, A-1220 Vienna, Austria

johannes.schicker@ctr.at

Accepted for publication on 15th November 2014

Abstract - Usually, stresses in module integrated solar cells are obtained by Finite Element (FE) calculations because these stresses can hardly be determined by measurements. Apart from the knowledge of the material properties, the FE boundary conditions have a distinct effect on the results of a FE solution for a standard mechanical pressure test. We used different simplified approximations to the complex real clamping of pv modules for simulating the deformation of the module and hence the stress-strain situation in the cells. Some deformation results could be compared to experimental findings from a standard mechanical load test. In this paper we show the bandwidth of results from variations of the assumptions which were made for the simulations. We found that particularly weak modules, i.e. thin frame and thin glass plate, show a strong dependency of cell stresses on the boundary conditions of the FE model. Hereby, the calculated stresses resulting from one assumption can easily deviate for more than 50% from the stresses using another assumption, even when the displacements are nearly equal and both lie closely to the measured values. Finally, we outline one possibility to directly in situ measure the cell strains what could help to resolve this uncertainty.

Keywords – Solar cells, mechanical stresses, standard load test, Finite Elements, boundary conditions.

关键词 - 太阳能电池, 机械应力, 标准加载实验, 有限单元法, 边界条件。

I. INTRODUCTION

The key to long term operating stability of photovoltaic (pv) modules is the integrity of the solar cells. One of the main factors responsible for the loss of cell integrity in outdoor modules are mechanical stresses due to external loads, as e.g. snow, imposed on the module. A good estimate of the arising mechanical stresses is a crucial prerequisite to estimate the fracture probability of a silicon solar cell. For a module design it is also desirable to determine the stresses in advance without time and cost extensive experiments. But even for already existing modules, due to the inaccessibility of the cells inside the module, it is hardly possible to measure the cell stresses during load application in a standard mechanical load test.

Finally, the stresses are usually obtained by simulations using Finite Element (FE) analyses.

A primary component of a realistic model is an adequate constitutive model for the materials of the pv laminate and its corresponding parameters. Aside from the laminates response to external loads, also its mounting and clamping has a distinct effect on the module's behaviour. The mounting of the laminate is usually realised by a metal frame which itself is clamped onto a metal base frame. Both are subjected to deformations. The complex clamping is hardly transferable into Finite Element boundary conditions. Hence, some simplifying assumptions must be made. The simplest boundary condition of the laminate results from the idealisation of the frame as rigid. Then the laminate can be regarded as fixed at all edges, and either it may rotate freely about the edges or it is fully restrained, depending on the character of the fitting of the laminate in the frame. Implementing into the model the ability of the frame to bend under load adds an additional level of complexity. And finally, this complexity is added for the base frame, too.

Three different types of commercial pv modules were investigated. On one hand they were subjected to a mechanical load test according to international standards (IEC 61215 sub clause 10.16) in the test facilities of AIT, while on the other hand these tests were simulated at CTR using Finite Element analyses. From the experiments the deflections at some designated points of the modules were obtained and served for calibration of the calculations. Aim of the simulations was to determine the cell stresses that arise in the modules.

The frame geometries of the modules were obtained from the manufacturers as CAD data. The laminate thicknesses (glass, EVA, cells, back sheet) were also known. The characteristics of the module clamping in the test stand had to be simplified for the simulation but still should describe the bonding condition of the test situation close enough to match the actual module behaviour. This led to a systematic study how the boundary conditions of the FE model affect the

module's overall behaviour, i.e. the deformations, and the cell stress in particular.

II. MODULE PROPERTIES

We chose three different types of pv modules for testing and modelling. They differed in size, material of the back sheet, thickness of the glass, and in the frame geometries. All frames were built of the soft aluminium alloy AlMgSi-T66. We approximated its stiffness behaviour using a bilinear hardening elastic-plastic constitutive law, whereas the geometries were taken as detailed as necessary. All cells were 156x156 mm multi crystalline solar cells with a thickness of 180 μm . We used an isotropic elastic material law for them as proposed by Hopcroft [1]. They were encapsulated by 360 μm EVA on each side. We assumed the EVA to be strain- and stress-free in the unloaded module. Although EVA is known to behave visco-elastic (see e.g. [2]), we applied a linear elastic behaviour using an initial short term stiffness as we considered the duration of the load tests as comparably short. This stiffness, however, is not known; and we found contradictory values. From a manufacturer we found a Young's modulus of 65 MPa, [3], but we doubt this to be valid for cross linked EVA. Another value was estimated by polymer experts assuming rather something about 10 MPa. For this study we used 65 MPa in the first place for all simulations, but then, we varied this stiffness in additional simulations, where we used both 6 and 0.6 MPa instead for the otherwise identical models, and compared the results. To model the sealant between laminate and frame we supposed soft sanitary silicon with an elastic behaviour with a Young's modulus of 15 MPa. All calculations were done using large deformation theory and postulated double symmetry.

Module type #1 was a 54 cell module with 3.2 mm front glass and a lean and low built frame, whereas module types #2 and #3 had 60 cells and higher and stiffer frames. Module type #2 had 4 mm front glass and module type #3 again had a 3.2 mm thick front glass. The back sheet of module types #1 and #2 was a standard TPT foil (a Tedlar/PET/Tedlar composite), whereas module type #3 had a pure polyamide foil (Icosolar[®] AAA 3554, Isovoltaic AG). The TPT foil is stiffer than the polyamide AAA foil, a Young's modulus of 1.3 GPa and 5 GPa, respectively, can be assumed. Furthermore, the cavity in the frame where the laminate is to be fitted in varied between the frames. It was higher and less deep in the frame of module type #2 than in the two others. The free height after inserting the laminate in module #2 was 2 times 775 μm , whereas in type #1 only 2 times 150 μm , and in module type #3 2 times 225 μm were filled with sealant. In contrast the embedment depth of the laminate was only 5 mm into the cavity of the frame type #2, whereas it was 10.5 mm into the frame of module #1, and 11.3 mm into frame #3. Fig. 1 shows the three frames in their respective relative size and the embedment of the laminates.

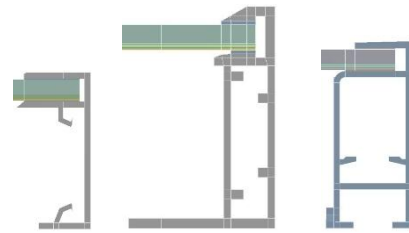


Fig.1, Sketches of module frames and their respective relative sizes. From left: module types #1, #2, and #3.

In all simulations a uniform pressure load onto the glass of the module was applied. For comparability, we only applied the lowest load that was not disturbed by secondary effects in any of the modules. This load was 2400 Pa, since the backside of module #1 was pressed against the base frame at a pressure just above 2400 Pa, see Fig. 2. In addition, the frame of module type #1 showed plastic yielding next to the mounting point at higher loading, whereas both other frames still behaved elastically at this load.



Fig.2, At a load higher than 2400 Pa the back sheet of module type #1 is pressed onto the supporting beam.

III MOUNTING SYSTEM OF PV LAMINATES AND FE BOUNDARY CONDITIONS

Industry provides different mounting systems for solar modules. Most consist of a base frame of metallic beams with a second frame of beams mounted crossways on the first beam layer. Then, the module's frame is clamped onto these upper bars. The laminate of glass, solar cells, encapsulant, and back sheet was already inserted in the frame cavities and sealed and fixed by soft silicon at delivery of the module.

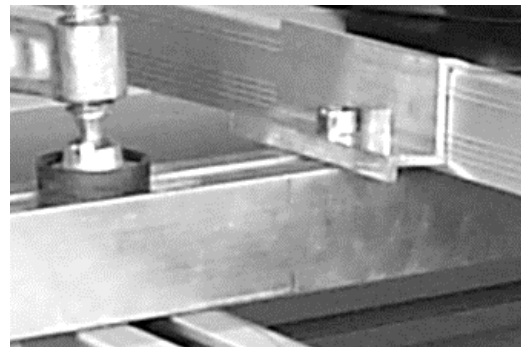


Fig.3, Clamping of the frame to the supporting beam and of the beam to the base frame.

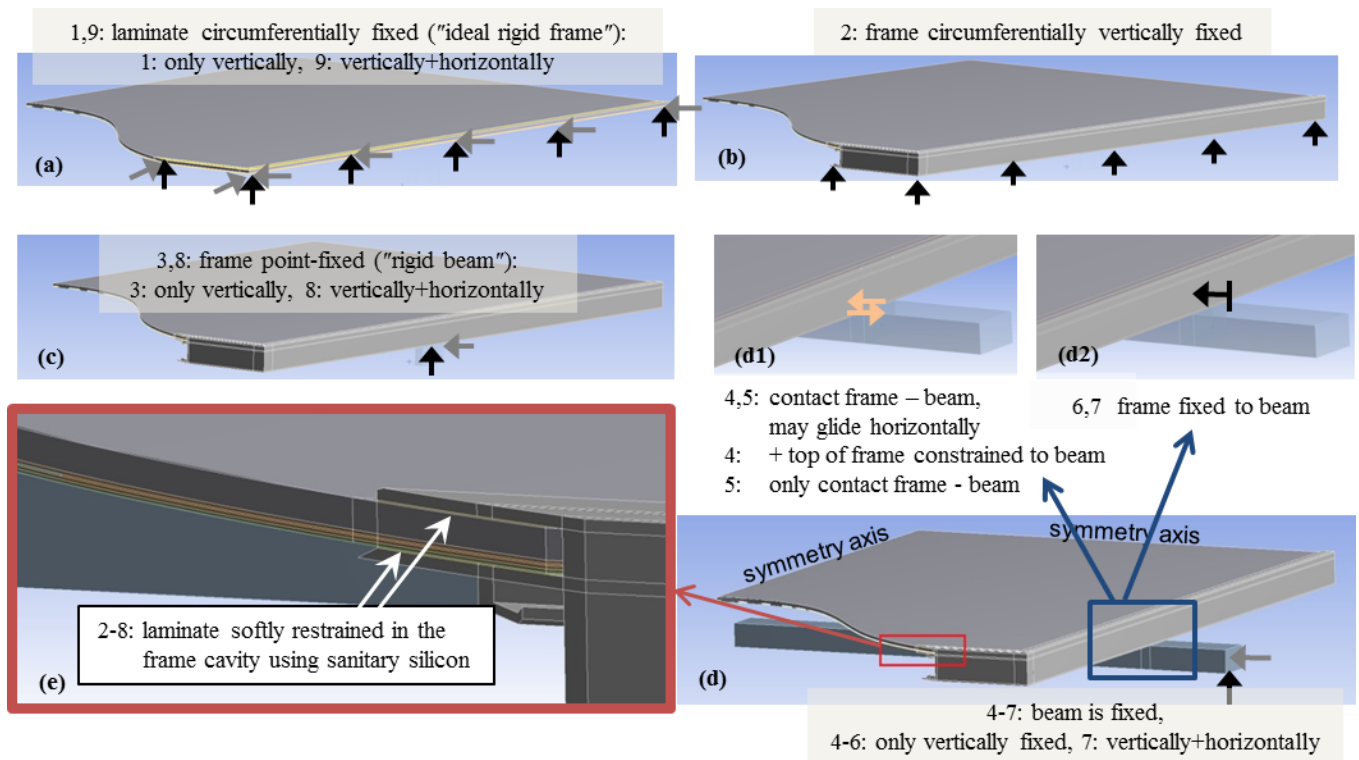


Fig.4, Laminates bonding conditions: (a) Models 1 and 9: pure laminate bonded circumferentially, (e): in all other models, i.e. 2-8, the laminate is restrained in its respective frame. (b) shows a circumferentially fixed frame, (c) shows a frame that is fixed in space at its supporting point to the beam, (d) shows the frame on its supporting beam where the protruding end of the beam is fixed. (d1) and (d2) symbolise the beam-frame interaction of model (d), i.e. models 4-7. The lighter, horizontal arrows in (a), (c) and (d) are active restraints only in the models

The mounting system used during the laboratory tests is designed to emulate a customary mounting system. It consists of an almost rigid base frame, a pair of standard profiled aluminium beams used in pv applications is screwed to this base frame and the module is clamped to the profiled bars. For clamping, a S-shaped piece of aluminium presses the top face of the module frame down so that the frame’s lower surface has frictional contact to the profiled bar, see Fig. 3.

The attempt of modelling this scenario in a Finite Element analysis revealed several unexpected difficulties and disadvantages. First of all, the requirement for modelling several separated contact problems increases the calculation costs immensely. Then, without knowledge of the pre stress of the clamps, it can not be expected to get realistic results. Therefore, we began with a simple approximation to the real mounting situation and successively refined it. In the following we use the term “model” to address the different refinements of the FE assumptions for the module bonding problem. Fig. 4 sketches the following explanations.

For the laminate bonding we used two general refinements in the Finite Element simulations: first, the pure laminate was bonded circumferentially at its edges, addressed as **model 1**, see Fig. 4(a), and second, the laminate was softly restrained in the cavity of its frame by entirely filling the gap between the laminate’s surfaces and the frame with 2 layers of soft sanitary silicon, Fig. 4(e). The following models, except model 9, base on the latter and only the kind of bonding of the frame is varied. Obviously, bonding the laminate without a frame is just

a fictitious construct and model 1 just serves for the purpose of comparison as representation for an infinite stiff frame.

The simplest assumption for the frame bond is to circumferentially fix the frame’s bottom faces in space. This varies the idea of a stiff frame but the frame may twist when the off-centred laminate is loaded. This is addressed as **model 2**, see Fig. 4(b). The next model, **model 3**, represents a frame on a rigid beam. Here, the frame is only fixed in space where it is supported by the beam whereas the remaining lower surface of the frame stays unsupported, Fig. 4(c). In a further refinement step, we also modelled a flexible supporting beam that protrudes from the module frame by about 90 mm before it is supported by the base construction, compare Fig. 3. The beam is only fixed at the protruding end where it is supported by the base frame, Fig. 4(d). The module frame is then fixed on the beam, Figures 4(d1) and (d2). In this constellation, the module frame may be displaced as a whole when the module is pressed down and the beam is bent. But in addition, the module may also be twisted at contact to the deformed support. In **Model 4** the top of the frame is constrained to the bar by using a constraint equation to simulate the clamp. The contact between the bottom of the frame and the supporting beam was assumed to be frictionless. This model was modified by **model 5**, in which we removed the constraint equation for better convergence of the calculation and only the pressure contact remained.

Models 1 to 5 have in common, that only the vertical directions are fixed, whereas the horizontal movements of the

module are restrained by symmetry conditions for the module. Accordingly, the frame boundary conditions allow for a horizontal movement along the beam axis of the frame bond when the module becomes bent. This horizontal movement is small but increases with the height of the frame. The real clamping, however, restrains this movement partially by friction. To check the influence of this mobility, some models where added that also restrain the horizontal movement where the frame is supported. **Model 6** is the variation of model 5 in which the contact area between beam and frame is replaced by common nodes. **Model 7** adds to model 6 a horizontal restraint at the contact area between supporting beam and base construction. **Model 8** corresponds to model 3, i.e. a small part of the frame’s lower surface is now totally fixed in space. Finally we applied a total horizontal constraint to the pure laminate edges, i.e. we modified model 1 to **model 9**. In Fig. 4(a), (c) and (d) lighter arrows mark these additional constraints. There is also a **model 10**, which is a modification of model 9 for cross-checking the results. It will be explained later.

Only the first 6 models were applied to all three module types. The models 7 and 8 were only tested with the weak module type #1. Model 9 was only used as comparison to model 1, and, since in both models no frame is involved, one calculation seemed sufficient. This was done with the laminate of module type #3, for which also model 10 was adapted.

The supporting beam in the tests was a thin walled profiled bar. Instead of modelling it in detail, we tested the elastic deformation vs. force of the beam separately. In the simulations we then substituted it by a massive bar with the same elastic behaviour.

IV. SIMULATION RESULTS

The most obvious difference of the module behaviour for different bonding conditions can be seen in Figures 5 and 6. Here the deformations are shown for the models 1 and 3, resp., i.e. an ideal rigid frame and a flexible frame bonded only at the contact point to the supporting beam. Both figures use an identical colour translation to the size of the module deflections. Due to the deformation of the frame the deflection in the centre of the module for model 3 is about twice as high as for model 1.

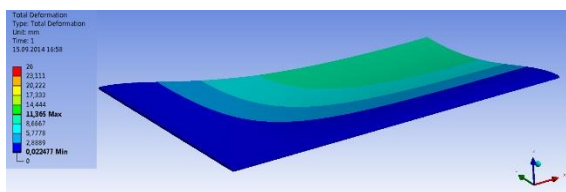


Fig.5, Total deformation of model 1 (¼ module)

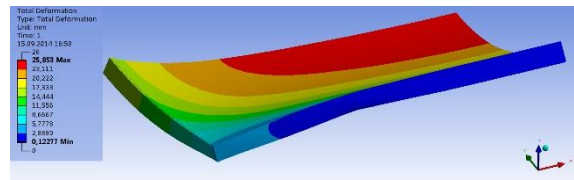


Fig.6, Total deformation of model 3 (¼ module)

The deformation of model 3 as it is shown in Fig. 6 is in good agreement with the observed deformation of the frame and module. In general, all calculations assuming a flexible module frame that is punctually supported agree with the behaviour of the tested modules, i.e. the frame buckles where it is punctually supported, and the outer frame part is deeper than the middle part. The absolute displacement values of the tested modules, however, were not achieved due to the fact that all of the simulations display slight stiffer module behaviour than the test modules. The displacement measurements, however, scattered widely from module to module even for the same module type. As most likely reason we identified the corner joint of the modules, which is not as monolithic as modelled. In the real modules, the corner joints are stuck together and the joint is movable to some extent. The scatter of the measured deformations is higher than the differences between the calculated values of all models of one module type. From comparing the measured module displacements it can therefore not be decided which model is best suited to approximate the real clamping situation. Only clear is that models 1 and 2 violate the basic deformation criteria of the clamped real modules.

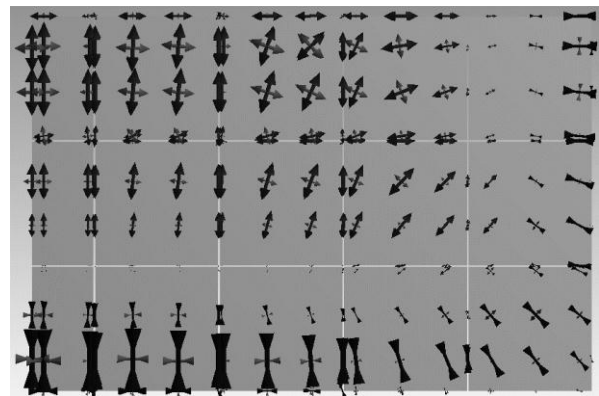


Fig. 7; Directions of the principal stresses from model 1, i.e. of a pure laminate panel circular bonded normal to the panel plane, calculated at 2400 Pa pressure. The symmetry planes are on the left and upper side, resp.; the bonded sides are right and at the bottom.

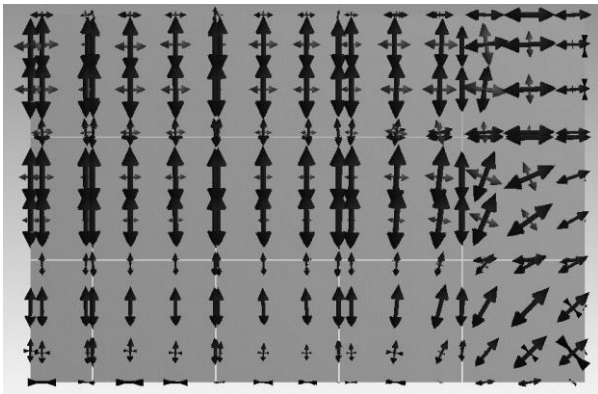


Fig.8: Directions of the principal stresses from model 3. i.e. a laminate panel fixed in its frame and the frame bonded at the position of the supporting beam, calculated at 2400 Pa pressure. The symmetry planes are on the left and upper side, resp.; the framed sides are right and at the bottom.

Figures 7 and 8 show the directions of the calculated principal stresses on the bottom side of the cells for model 1 and 3, respectively. The position of the supporting beam and a numbering convention for the cells can be seen in Fig. 9. It also shows schematics of the two different types of module-dimensions, a 54 cell module and a 60 cell module, viewed from below. The drawing shows modelled quarters of the double symmetric modules with the supporting beams.

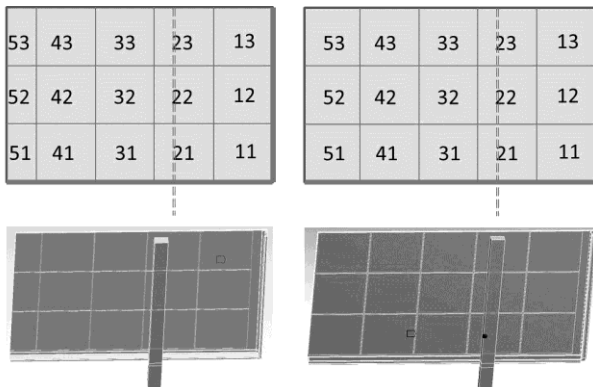


Fig.9, Cell numbering of the quarter modules, viewed from below, and position of the supporting beam: left a module with 54 cells, right a module with 60 cells.

The assumption of a rigid frame as it is represented by model 1 leads to pressure stresses (inverted arrows) along the supported laminate, see Fig. 7, with their maximum direction normal to the edges. But, considering a punctually supported flexible frame as in model 3, see Fig. 8, leads predominantly to tensile stresses (outward arrows). Furthermore, the direction of the principal stresses changes abruptly after the first column of cells. Inside the module part between the supporting points all arrows go parallel to the shorter frame side. In all the models 3 to 8 the principal stresses in cell 11 are tensile stresses having an angle of approximately 45° against the frame, whereas in cell 13 the maximum principle stresses are

parallel to the longer module edges. The bus bars, which were not modelled, should go along the longer module edges, whereas the steeper deflection goes perpendicular to the bus bars direction. The maximum principle (tensile) stresses in the centre of the module are orientated in this direction.

The stresses in the test modules could not be determined, but electroluminescence pictures of modules with broken cells after cycles of loading and unloading were taken. The cells are fracturing brittle and most theories postulate that brittle fracture is due to the maximum tensile stresses, where cell breakage usually occurs normal to the direction of the maximum tensile stress. In the test modules we observed a crack pattern that is in agreement with the orientation of the maximum principal stresses of Fig. 8 of the punctually supported module, i.e. we found cracks in the corner cells under an angle of 45° and in cell number 21 under an angle of approximately 20° against the longer frame side.

To compare the different models to each other, we focus on the maximum principal stresses in three cells. Nearly all simulation models of all three module types show the highest principle stress values in cell 53 or sometimes in cell 22. In very few calculations the highest value can be found in cell 43, but then, the value is only insignificant higher than in cell 53. The corner cell, number 11, is of interest because of its pronounced 45° direction of the principal stresses. In the Figures 10 to 12 the maximum principle stresses in these three cells are compared for all variations of the FE boundary conditions we applied to the three module types. The massive bullets, corresponding to the right y-axes of the graphs, show the corrected deflection values in the module centre for comparison. The corrected deflection value is obtained by subtracting the vertical displacement of the frame at its fixing point from the vertical displacement in the module centre. The stress values are all evaluated in the centre of the respective cells, although specifically in cell 11 and cell 22 sometimes the highest values were not found in the middle of the cell. For the benefit of legibility the scales of the axes differ in the diagrams.

In Fig. 10 for module type #1 a strong dependency of the overall stress level and module deflections on the boundary conditions in the Finite Element analysis can be seen. The general picture of the simulation shows that the module deflection and the stress levels are increasing when the number of restraints decreases. The least deflection corresponds to the least stresses if only the pure laminate is considered, model 1. The highest deflection yields the highest stress level with model 5, where we included the supporting beam as a deformable component and allowed both the frame and the beam to move along the beam axis. This movement, however, was very small and hardly noticeable by the eye. The horizontal movement was calculated to be 1.4 mm for the frame and 0.14 mm for the beam. Comparison of models 6 and 7 with model 5 shows that the most important constraint is the constraint of the frame to the beam in model 6, whereas the constraint of the beam itself is not adding much effect. Both restraints yield about the same effect as a vertical restraint at the mounting point of the frame, model 3. Only model 8, where the frame's mounting point is fully fixed in space, shows a

further significant decrease of deflection and stress level, but it still does not reach the smaller values calculated for the unbending frame of the models 1 and 2.

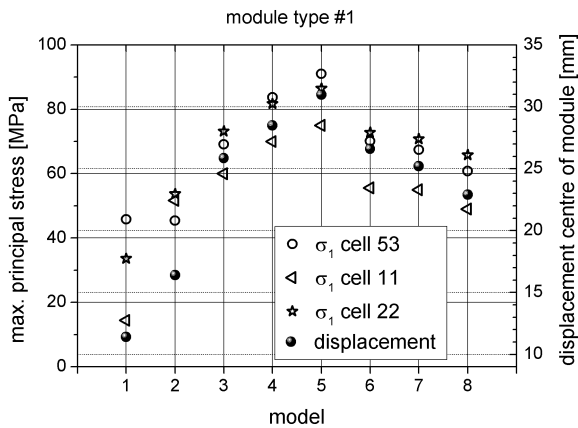


Fig.10, Stresses and deflections in dependency of various Finite Element boundary conditions for module type #1.

Considering the larger module type #2 we observe a very similar dependency, namely an increasing stress and deflection level with the decrease of restraints, see Fig. 11; only model 1 does not fit in the picture. Here, the deformation becomes smaller when adding a frame, model 2 corresponds to the framed model 1. The explanation can be found in the stiff frame of module type #2. Here, the pure laminate is stiffened by the frame, whereas the soft frame of module type #1 adds additional flexibility.

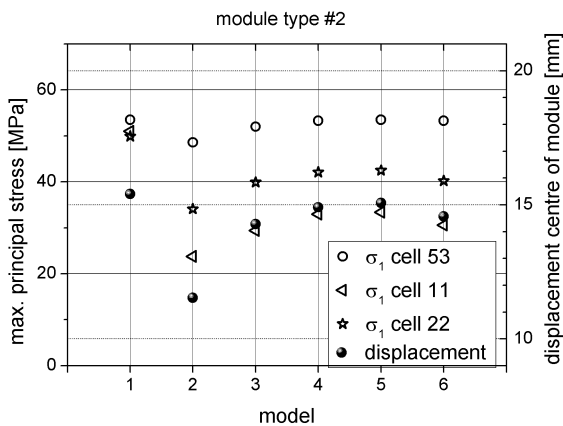


Fig.11, Stresses and deflections in dependency of various Finite Element boundary conditions for module type #2

Another observation for the stiffer module can be made: in Fig. 10 for module type #1 the stresses in cell 22 are nearly as high as the stresses in the centre cell number 53 and even higher in some boundary models. Module type #2 has a pronounced ranking of stresses: The stress in the centre cell is always significant larger than the stress in cell 22 and this itself has a pronounced larger value than cell 11. Only the frameless model 1 shows a higher value in cell 11 than in cell 22. Since

there was not much difference in the results of models 6, 7, and 8, at the weak module type #1, calculation of models 7 and 8 had been omitted for this module type. However, it can be seen in Fig. 11 that the stiff module leads to the comfortable situation that neither of the punctual support models 3 to 6 yields much difference, neither in the deflections of the centre of the module nor concerning the stresses.

Module type #3 is also a large module, i.e. 60 cells, with a stiff frame that is comparable to frame #2, but with the same glass thickness (3.2 mm) as module #1. In this module, the frame adds stiffness to the pure unframed laminate as already observed in module type #2, compare models 1 and 2 in Fig. 12. But different from module #2, in module type #3 the stiffness of the frame only reduces the cell stress in the corner cell number 11, whereas the stress in cell 22 increases from model 1 to model 2 and the stress in cell 53 only decreases slightly. We conclude this to be an effect of the thinner glass: the frame stiffens only the adjacent part of the laminate. Thus, the reduced displacement in the centre of the module is a result of the shorter distance in which the laminate is bent.

As in the other modules the cell stresses and module deflections increase with the number of bonds that are unrestrained. Here, we added model 9 to the simulations to verify this trend. Model 9 is a pure laminate without frame, but instead of bonding the edges only vertically, as in model 1, they are restrained horizontally, too. It can easily be noticed, that both, the vertical displacement of the module centre and all stresses decrease from model 1 to model 9.

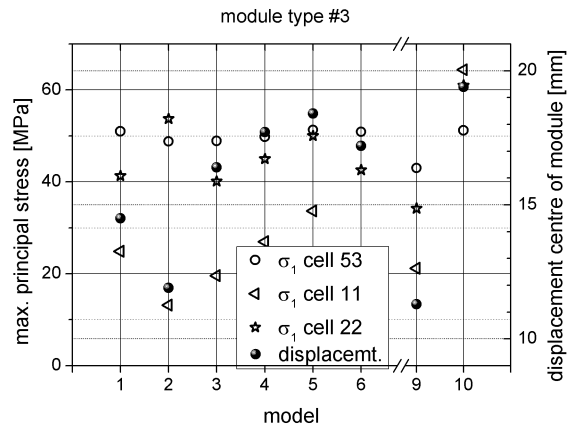


Fig. 12: Stresses and deflections in dependency of various Finite Element boundary conditions for module type #3

Finally we wondered why the pure laminate of module type #3 has approximately the same deflection and cell stress as the laminate of module #2 although it has a much thinner glass. After close examination we realised, that the embedment depth into the frame was different: module type #3 is 11.3 mm deep embedded into the frame whereas module type #2 has only 5 mm depth. When bonding the pure laminate, we used the embedment depth for applying the edge bonding, i.e. we fixed the vertical displacements of the laminate in the area where the laminate is embedded in the frame. To check, that the reason for an approximate equal deflection in both laminates, i.e. that

with the thinner glass and that with the thicker glass, is the different depth of bedding we implied **model 10**, an artificial boundary condition, where we reduced the area of constraint of module type #3. Model 10 has now the same embedment depth of 5 mm as model 1 in module type #2 has. As expected, now, the model with reduced depth of bedding, model 10, has a much higher deflection and also higher cell stresses than model 1 of the same module type. Now, the comparison of pure laminates between the thinner glass, module type #3, and the thicker glass, module type #2, meets the expectation.

V. INFLUENCE OF THE EVA STIFFNESS

Until this point, we calculated all results using a rather high value for the EVA stiffness. This value was an arbitrary choice when we started these simulations, and was maintained for the sake of comparison. Now, we examine the question whether the principle statements we found still hold if the EVA stiffness is significantly different from the assumed value.

It is obvious that the module deflections depend on the EVA stiffness, because without EVA only the glass would contribute to the bending stiffness of the laminate. A very weak EVA can not transmit much force to the cells and hence their stresses tend to zero. On the other hand, a very stiff EVA transmits bending forces to the cells which are located in the tensile zone of the composite plate and, hence, the cells can contribute to the bending stiffness of the laminate. Therefore, the cell stress must depend on the EVA stiffness.

We applied different values of the EVA stiffness to the models 3 and 5 of the precedent simulations of module type #1, without changing anything else. The results are depicted in Fig. 13.

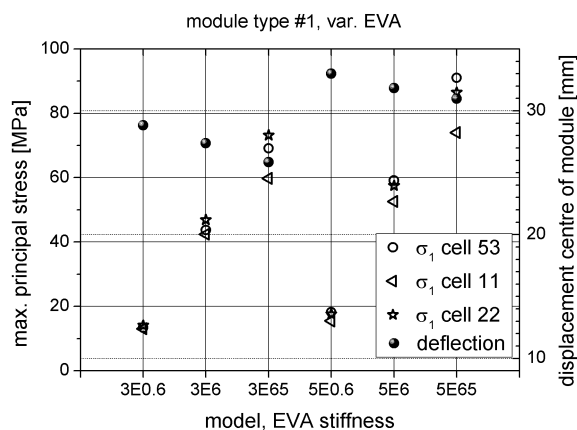


Fig.13, Dependency of module deflection and cell stress on the stiffness of EVA for otherwise identical simulation models: left in the drawing are shown results for model 3 using an EVA stiffness of 0.6, 6.0, and 65.0 MPa, and right in the drawing are shown the results using model 5.

We named the models 3E0.6, 3E6, and 3E65 to express model number 3 with EVA stiffness 0.6 MPa, 6 MPa, and 65 MPa, respectively, and 5E0.6, 5E6, and 5E65 for model 5 with EVA stiffness 0.6 MPa, 6 MPa, and 65 MPa, respectively.

With stiffness the Young modulus is meant. Clearly, 3E65 and 5E65 are already shown in Fig. 10. As it can be seen, the deflections of the modules become larger and the cell stresses decrease with decreasing stiffness of the EVA. The displacements and stresses of model 5 are higher than those of model 3 for each equal EVA stiffness. The stress values in the different cells approach each other and tend to zero with decreasing EVA stiffness. We conclude, that the previous findings stay valid for all stiffnesses of EVA, namely that with increasing number of unrestrained module bonds the cell stresses and module deflections increase

VI. ABOUT IN SITU MEASUREMENT OF CELL STRAINS

We have shown that the stresses of the solar cells in pressure loaded modules depend on various factors. Even with good knowledge of the true behaviour of EVA uncertainties remain concerning the true frame behaviour and the appropriate boundary conditions in a FE analysis to obtain a good estimation of the resulting cell stresses. Measuring these stresses directly in situ at the strained cells seems inevitable to validate the simulation results. Our expectation is that this can be achieved using strain sensors that are applied to the rear faces of the cells. The solar cells are very thin and normal pressure loading conditions on modules lead basically to stress states in the cell plane. Hence, a plane stress state is a reasonable proper assumption. Further on, since the cell strains of undamaged silicon are considered to be small, a linear Hook's stress strain constitutive law for the cells can be assumed so that stresses and strains can interchangeably be considered. This justifies the suitability of in-plane strain sensors for monitoring cell stresses.

We suggest attaching 45° strain gauge rosette micro-strain sensors (RY89-3/350, HBM GmbH) to the backside of the respective cells. These sensors consist of three independent strain gauges to capture the normal elongations in three coplanar directions of a field of about 5x5 mm. From these data the three independent components of a plane strain tensor can be determined. Electrically, each sensor leg has to be part of a full Wheatstone bridge circuit for optimal sensitivity. The connecting cable is then fed through the EVA and the back sheet to an external measurement device. Using this layout, we expect to be able to determine the cell strains directly while the module is loaded in the test stand and thus get the possibility to compare the measured strains to those obtained by Finite Element calculations.

VII. CONCLUSION

We identified three major influencing factors that stiffen a module and, hence help to reduce module deflection and thus cell stress. These are the glass thickness, the frame stiffness, and the embedment depth of the laminate in the frame. The deflections and stresses of the module depend strongly on the stiffness behaviour of EVA. But also with valid material properties of EVA it is inevitable for a realistic simulation of the module deformation by Finite Element analysis, to include

the frame behaviour in the model and to find a boundary condition that is a well suited approximation to the real bonding situation. Finally, one should be aware of the fact that a small variation of the Finite Element boundary conditions may result in a disproportionate larger variation of stresses, especially when either frame or laminate or both are weak.

We further expect that we can measure the cell strains by applying strain gauge rosette micro-strain sensors to the cells and can calibrate the calculation model with it.

ACKNOWLEDGEMENTS

This work was conducted as part of the K-Project *IPOT* within the Austrian R&D programme *COMET - Competence Centres for Excellent Technologies*. Funding by the Federal Ministries of Transport, Innovation, and Technology (BMVIT), of Economics and Labour (BMWA) and the Provinces of Carinthia and Styria, managed

on their behalf by the Austrian Research Promotion Agency (FFG), is gratefully acknowledged.

REFERENCES

- [1] M. A. Hopcroft, W. D. Nix, and T. W. Kenny. "What is the Young's Modulus of Silicon?", *J. Microelectromechanical Systems*, **19**, **2**, pp. 229-238, 2010.
- [2] U. Eitner, M. Pander, S. Kajari-Schröder, M. Köntges, and H. Altenbach. "Thermomechanics of PV Modules including the Viscoelasticity of EVA", Paper *26th European Photovoltaic Solar Energy Conference and Exhibition Proceedings*, pp. 3267-3269, Hamburg, Germany, Sept. 5--9, 2011.
- [3] <http://www.kern.de/cgi-bin/riweta.cgi?nr=1451&lng=1>
[Ethylen/Vinylacetat \(E/VA\) / Mechanische Eigenschaften](#)



Policy impact on concentrated solar power technology deployment: experience of global environment facility

集中式太阳能技术普及：全球环境基金的经验

Ming Yang (杨明)^{1*}, Hang Yin (尹航)²

¹Senior Climate Change Specialist, Global Environment Facility, Washington DC, USA

²Intern, Global Environment Facility, Washington DC, USA

myang@thegef.org

Accepted for publication on 27th November 2014

Abstract - Concentrated solar power (CSP) is a renewable energy technology that is advancing from the technology demonstration stage to the technology deployment and commercialization stage. With the current available CSP technologies and economy scale, the cost of CSP power production is in the range of US\$0.18 to US\$0.35/kWh. This cost is projected to drop to US\$0.12-0.15/kWh in 2020 with appropriate energy policy initiatives and further technology advancement. This paper introduces the current CSP technologies and renewable energy policies for CSP technology development in the US, China, the EU, the Middle East and North Africa region, and South Africa. It also presents case studies on CSP finance in South Africa, Morocco, and Egypt. These case studies show that international funding sources are important to reduce risks for the private sector in CSP technology investments. National government policies are also necessary to develop new financial models and mechanisms that would attract private investments in CSP. The objective of this paper is to share Global Environment Facility (GEF)'s experience in policy development for CSP investments. This paper concludes that with appropriate national energy policies and with large-scale investments in CSP technologies, the production cost of CSP will be competitive to conventional fossil-fired power by 2020.

Keywords - New Renewable Energy Policy, Finance and Investments, Technology Development.

摘要 - 集中式太阳能 (CSP) 是一种正从技术示范阶段向普及阶段发展的新能源技术。根据现有的技术和经济规模, 生产集中式太阳能的成本在每千瓦时 0.18 到 0.35 美金之间。若有适当的政策推动和技术发展, 这个成本预计在 2020 年降至 0.12 到 0.15 美金之间。这篇论文介绍了现有的集中式太阳能技术以及在美国、中国、欧盟、中东和北非地区以及南非等国家的技术发展状况。文章还通过南非、摩洛哥和埃及的集中式太阳能融资案例分析发现, 来自国际范围的资金对于降低私营部门在集中式太阳能技术投资领域的风险起着重要的作用。本国政府政策对于发展新的融资模式和机制用以吸引私人投资也是非常必要的。这篇文章是为了分享全球环境基金 (GEF) 在针对集中式太阳能的政策推广的经验。这篇文章的结论是, 若有合适的

国内能源政策以及大规模的集中式太阳能技术投资, 能源的生产成本将可以在 2020 前和传统的化石能源相竞争。

关键词 - 新能源政策, 融资与投资, 技术普及。

I. INTRODUCTION

Concentrated solar power (CSP) technologies use mirrors and lenses to concentrate solar thermal power to heat fluid, generate steam, and eventually power. CSP technologies depend on direct-beam irradiation, and their maximum benefits for power generation are restricted to arid and semi-arid areas with clear skies. The most promising areas for the use of CSP technologies are located in the Middle East and North Africa (MENA), Australia, South Africa, the United States, Chile, Spain, India, and the Gobi Desert in China.

CSP technologies stand out owing to their energy storage ability. Thermal storage is relatively easy to be integrated into CSP projects, and allows CSP plants to generate electricity at peak time for the grid. On top of conventional power generation, CSP can be applied to industrial processes to desalinate water, produce hydrogen, and generate heat.

Commercial CSP technologies have been developed over the past four decades. The first commercial CSP plant with 10 MW capacity started operating in 1982 in the US. Afterwards, a wave of CSP construction followed in the US, Spain, MENA, South Africa, India, and China. However, CSP capacity has not increased as fast as expected, because of the economic and financial crises in the 1990s and 2000s, and the rapid cost reduction of solar photovoltaic (PV) technologies. By the end of 2012, global CSP capacity reached 2.8 GW, and major CSP plants were installed in Spain, the US, the MENA region, and South Africa (IRENA, 2013a).

Spain has been leading the world in CSP since 2010. By the end of 2012 Spain had installed over 2 GW of CSP, which accounts for more than three-fourths of the world's CSP

capacity (REN21, 2013). Most of the CSP capacity came forth with the tailoring of the feed-in tariff in 2004 and the key decree signed in 2007—Royal Decree 611 (ESMAP, 2011). So far there are 50 CSP plants in Spain (NREL, 2014). Spain has made concrete plans to deploy a total of 2.5 GW CSP by 2015 (CSP World, 2013).

The US was the first country in researching, developing, and deploying CSP technologies. By the end of 2013, the total installed CSP capacity had reached 918 MW in the US (SEIA, 2014). In 2013, the US Treasury Department 1603 Renewable Energy Grant authorized the payment to developers of qualified renewable energy facilities of grants equal to 10% or 30% of their capital expenditure, depending on the project technology. With strong financial support from the US government, it is expected that that additional 20 GW of CSP will be installed in the US by 2020.

India has recently made progress to research and develop CSP technologies. In 2010, the Ministry of New and Renewable Energy (MNRE) of India announced Phase I of the National Solar Mission (NSM). The NSM has proven to be very effective in creating a strong national solar PV industry, but it has been not so successful in CSP. By the end of 2013, there was only a 3 MW pilot CSP project by the Indian Institute of Technology, which has been in operation since 2011. In early 2014, the MNRE announced Phase II of the NSM, including two CSP pilot projects, 50 MW each. It also announced to establish a CSP research and development center opening in 2015 (Beatriz, 2014).

China started developing CSP technology in the 2010s. The first tower-type CSP plant with 50 MW power generation capacity was connected to the grid in July 2013 in the Qaidam Basin of Qinghai. Between 2010 and 2011, five CSP plants with total installed capacity of 343 MW were approved by different national administrations. In April 2014, Rayspower, a CSP mirror manufacturer, announced that it could offer lower costs for CSP mirrors, with similar performance (Solar Thermal Energy News, 2014).

Australia is home to about 56 MW of three CSP plants in total nowadays. A 44 MW plant is under construction to feed steam to an existing coal facility. Kogan Creek Solar Boost project is set to become the largest solar-coal hybrid power plant in the world. Moreover, Novatec, the Australian solar energy technology developer and manufacturer, has a 9 MW solar boiler, which acts as a fuel-saver by feeding steam into the existing coal fired power plant (NREL Website, 2014).

The MENA region has a fast-growing demand of energy consumption with 7% of growth rate each year (World Bank, 2012a). The region also has abundant solar resources available. In 2013, the region pledged an ambitious program to create a 1 GW CSP network in five countries: Egypt, Morocco, Algeria, Tunisia, and Jordan (CIF, 2013). As one of the five participating countries, Egypt now has 20 MW of CSP capacity integrated in a 120 MW combined cycle power plant in Kuraimat, which became operational in June 2011. Meanwhile, the Egyptian government approved the Egyptian Solar Plan in July 2012, which set a target for 2.8 GW of CSP by 2027 (REN21, 2013).

Morocco has 184 MW of CSP capacity by the end of 2013 (NREL, 2014). A consortium of power companies including ACWA Power, Acciona, Sener and TSK, developed a 160 MW parabolic trough CSP plant in Ouarzazate, Morocco, which was the largest CSP plant in the world as in July 2014. The plant was in part of the Moroccan government's Solar Plan, launched in November 2009, which aimed to produce 2 GW of solar electricity by 2020 (EPIA, 2012). Along with its great success, Morocco also established the Moroccan Agency of Solar Energy (MASEN), which is notable in offering a successful institutional model for all other CSP projects in the MENA region.

Algeria has a CSP plant with 25 MW capacity using Integrated Solar Combined-Cycle (ISCC) technology in Hassi R'mel, Algeria (NREL, 2014). The energy generated by solar power would in part replace fossil fuel consumed in the power plant. The whole facility was composed by a 150 MW gas and steam combined cycle power plant and a 25 MW solar thermal plant. Besides, Algeria has set a target of 325 MW of CSP capacity to be achieved by 2015, and 7.2 GW by 2030.

South Africa started its CSP technology development at the end of last century. The first CSP feasibility study project was financed by the Global Environment Facility (GEF) between 1999 and 2001. In the early 2010s, Eskom, the national state-owned utility of the country, started construction of two CSP plants with a total capacity of 150 MW. In addition, the government of South Africa has introduced a Renewable Energy Independent Power Producers' Procurement Program, which allows private developers to bid for CSP investments. Under the program, two CSP developers—Abengoa and Bokport CSP—won a bid for three projects with a total capacity of 200 MW (SASTELA, 2012). Looking forward, South Africa aims to build 3.3 GW of CSP by 2030 (CPI, 2014).

Since 1990, the GEF has financed five CSP projects in South Africa, Egypt, Mexico, Morocco, and Namibia with governments, multilateral development banks and agencies, and private investors. One of the major achievements of GEF funding in these projects is the development and implementation of government policies to foster CSP investments. The objective of this paper is to share GEF's experiences in policy development for catalyzing CSP technology investments in developing countries. This article concludes that the government should develop and implement policies that will incentivize private investments. These may include (1) policies to establish national risk guarantee funds to reduce risk for private investments, and (2) policies to reform power tariffs for countries, and (3) policies in concessional use of government owned land for the private sector investments in CSP technologies.

II. METHODOLOGY AND DATA

An empirical methodology is used in this study. The methodology includes data collection and documentation, cost-benefit analysis, project case studies, in-depth interviews, experts' opinion, and walk-through surveys.

Data collection and documentation: Documents were gathered to enable understanding of the historical processes and developments in CSP related issues and technologies. The documents included the design and constructions papers of CSP, annual reports, mid-term review reports, and project terminal evaluation reports of selected GEF CSP projects. Government policy papers and reports on CSP technology related feed-in tariffs, technology development and project financing were also collected. This approach of data collection was used for triangulating data and helping to counteract the biases of other approaches such as in-depth interviews and experts' opinions and supplementary sources of information.

Cost-benefit analysis: Cost-benefit analyses were conducted to identify financial viability of new CSP projects. The analyses involved detailed economic and technology data collection that are specifically related to individual CSP projects. Financial criteria such as annualized net present value and internal rate of return of the project investment were calculated for overall CSP technologies as shown in the section of cost-effectiveness of CSP technologies.

Case studies: While carrying out these case studies, the GEF project implementing and executing agencies conducted more than 20 in-depth interviews with multiple stakeholders of CSP technology owners and government officers in different countries. These case studies, employing in-depth-structured interviews at CSP plant sites, tend to provide a qualitative, multi-aspect and in-depth study of selected cases. The multi-source data of case studies accurately captured real-life CSP related technologies, policy issues, and barriers. The case studies built a complex and holistic picture, and detailed views of the CSP stakeholders on technology development, investment, and deployment.

Experts' opinions: In this study, experts' opinion was a structured process of collecting and distilling knowledge from a group of experts through email communications, questionnaires, meetings and conference calls. Some data, energy efficiency outputs of the CSP plants for example, were not certain or accurate for some projects. To finalize those data, workshops and seminars were held to get opinions from a group of CSP stakeholders and experts. These brainstorm meetings were to gather ideas and wisdom from a group of experts and to improve data quality.

Walk-through surveys: The authors and their colleagues conducted walk-through surveys with a few CSP plants. These included inspections on the CSP plant premises to assess the solar energy resources, solar energy storage, electricity generation, and power transmission lines and grids.

The following sections briefly present the technology data, economic/financial data, policy achievements, and other results from the analyses mentioned above.

III. CSP TECHNOLOGIES

A CSP technology generally consists of three parts. The first part includes collectors and convertors of solar energy to

thermal energy, such as parabolic troughs and the receiver. The second part refers to thermal energy storages including storage tanks. The third part converts thermal energy to electricity, consisting of thermal turbines, power generators, steam condensers, and power transmission grids.

While four technologies exist, two dominate the market: parabolic trough and solar tower. Other technologies such as dish sterling systems or Fresnel collector systems are less mature. With parabolic trough technology, which is the most mature today (Figure 1), solar energy is concentrated by parabolically curved, trough-shaped reflectors onto a receiver pipe running along the inside of the curved surface. Within the pipe, solar energy heats transfer medium (e.g. oil or molten salt) to approximately 400°C. The average operating efficiency of parabolic trough plants ranges from 9% to 14% (Viebahn et al, 2008).

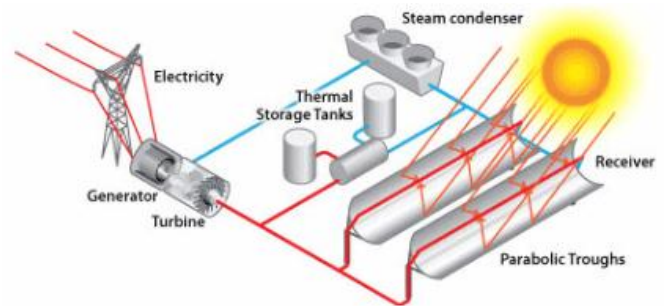


Figure 1 Diagram of a Parabolic Trough Technology. Source: (Hamilton, 2013)

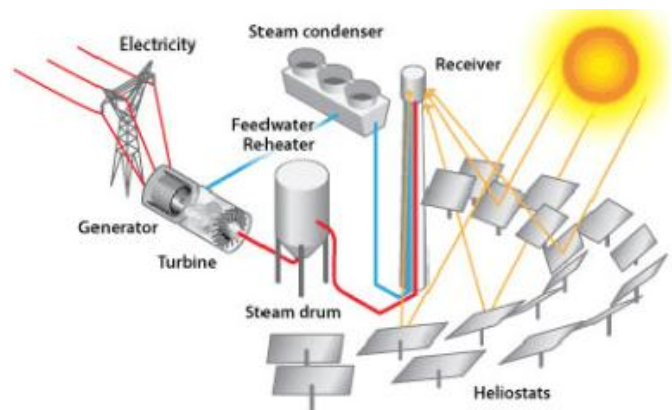


Figure 2 Diagram of a Solar Tower Technology. Source: IEA (2011)

The second widely used CSP technology is solar tower that utilizes numerous large sun-tracking mirrors (heliostats) to focus sun light on a receiver at the top of a tower (Figure 2). A heat transfer fluid heated in the receiver up to temperatures of 500–1000°C, is used for steam generation. The steam is then stored and fed to a conventional turbine generator to produce electricity. Steam, molten salt or air is used as heat transfer media. Since heat transfer is limited to one point of the process, solar tower systems have higher efficiency in harnessing solar energy with overall efficiency ranges from 13% to 18% (Viebahn et al., 2008).

IV. COST-EFFECTIVENESS OF CSP TECHNOLOGIES

CSP technologies are currently not as cost-effective as some other new renewable energy technologies. Today the costs of CSP technologies are three or four fold as high as those of other renewable technologies such as wind and biomass power technologies (IRENA, 2013b). High capital investment costs result in high production costs. Table 1 compares the levelized cost of energy (LCOE) calculation results and capital costs of biomass, wind power, solar photovoltaic (PV), and two representative CSP technologies. While on-shore wind power and biomass power technologies can provide electricity at a LCOE of US\$0.05/kWh that is competitive to electricity generated from fossil fuels, CSP technologies provide electricity at a LCOE of US\$0.18/kWh. As for the capital costs, CSP technologies could reach as high as US\$10,000/kW, which exceeds the capital cost range of other renewable energy technologies on a large extent, as shown in Table 1.

Due to these higher production costs of CSP, developers and investors have been reluctant to finance CSP technologies. This has hindered expansion to economies of scale, limited the cost reductions of the technologies in the market, and increased complexity and risks related to securing finance.

TABLE 1, COST COMPARISONS BETWEEN RENEWABLE TECHNOLOGIES

Technology	LCOE range USD/kWh	Capital Costs range USD/kW
Wind onshore	0.05 – 0.15	1000 – 2500
Wind offshore	0.15 – 0.25	4000 – 4500
Solar PV	0.15 – 0.35	2000 – 5000
CSP Parabolic Trough	0.18 – 0.38	3500 – 10000
CSP Power Tower	0.18 – 0.28	7000 – 10500

These high LCOE costs of CSP technologies have also been acknowledged by the International Energy Agency (IEA). Figure 2 shows that the CSP technologies have not matured in the energy market, falling into the stage of technology deployment where there is a high cost gap between CSP and more mature technologies. To succeed, CSP technologies need reliable support from the public sector and multilateral financing institutions such as the GEF to fill the high cost gap and to attract investments from the private sector.

V. CSP PROJECTS FINANCED BY THE GLOBAL ENVIRONMENT FACILITY

The GEF unites 183 countries in partnership with international institutions, civil society organizations, and the private sector to address global environmental issues including climate change. Since 1991, the GEF has performed a catalytic, innovative, and cost-effective role; led in financing new and emerging low-carbon technologies; and pioneered market-based approaches and innovative instruments. The

GEF has provided over US\$4 billion in more than 600 climate change projects and programs in 157 countries, leveraged more than US\$27 billion in co-financing, avoided 2.6 billion tonnes of CO₂ eq through project development and finance, and catalyzed the reduction of 6.8 billion tonnes of CO₂ eq through market transformation.

The GEF's support for climate change projects includes financing for CSP technologies. In partnership with the World Bank, the GEF completed a feasibility study in South Africa, and developed a portfolio of four CSP demonstration plants in Mexico, Morocco, Egypt, and Namibia. These projects laid out a road map for CSP development in participating countries, and built approximately 70 MW of solar power in the fields as part of hybrid gas-turbine plants. Table 2 highlights these projects. In the following sections with case studies, this paper compares and analyzes policy components in three GEF financed projects and derives the most effective government policy that facilitates investments in CSP technologies.

VI. CASE STUDY: GEF MOROCCO CSP PROJECT

RATIONALE AND OBJECTIVES OF THE GEF PROJECT

With a growing population and economic development, Morocco's electricity demand has been increasing rapidly. Between 1983 and 2003, electricity consumption grew at an average rate of 6% per year and was satisfied by domestic production and imports from Spain and Algeria. The need for additional power capacity and public spending control led the Moroccan government to tap private investments for support.

Morocco took initiatives and managed to gradually meet some of the important milestones that were previously set up in its national plan to develop renewable energy. To achieve these goals, the government created the Centre de Développement des Energies Renouvelables (CDER), to hold responsibility for new renewable energy development and investments. Besides, CDER played an important role in the implementation of promoting reduction of greenhouse gas emissions. The GEF financed CSP project was in the national least-cost power expansion plan of the Office National de l'Electricité (National Electricity Utility, or ONE). The project also fitted well with the energy sector development plans by the government of Morocco (GOM). Morocco had a great potential to achieve the diversification of energy type, therefore the GEF project contributed to the national plan by increasing the share of renewable energy.

GEF's strategy in Morocco was to support policies and investments that encouraged public and private capital investments in environmentally-friendly technologies and projects. The GOM took important steps to improve the performance of the power sector through restructuring and private sector participation and to develop the use of renewable energy. The GEF project addressed key issues in the government strategy such as increasing institutional capacity and reliance on renewable energy, while meeting growing demand for electricity.

Table 2 Highlights of GEF financed CSP projects

	Period	Partners	GEF Grant	Co-financing	Project outputs	Major policy components	Environment impacts
South Africa	1999-2001	World Bank, Eskom, and NREL, USA	US\$230,000 (56%)	US\$180,000 (44%)	Feasibility study, technology identification, and leveraging public and private investments in CSP	Feed-in tariffs, and tax incentives	Leading to large scale investments in CSP technologies in the country
Morocco	2007-2012	The World Bank and Office National De L'electricite	US\$43.9 million (8%)	US\$524 million (92%)	Build 225 kV power lines, a 225 kV substation, and an access road	Power sector privatization; Electricity tariff reforms	Install 20 MW of solar power; generate 37.5 GWh per year; and reduce 450,000 tonnes of CO ₂ eq in 20 years
Egypt	2007-2011	The World Bank and Egyptian Electricity Holding Company	US\$49.8 million (15%)	US\$278 million (85%)	Integrated solar combined-cycle with a capacity of 150 MW including 20 MW from solar	Feed-in tariffs; Tax incentives on CSP; Land use policy.	Generate 852 GWh per year including 33.4 GWh per year from solar energy; and reduce 20,000 tonnes of CO ₂ eq annually
Mexico	2008-2011	The Federal Commission of Electricity of Mexico and the World Bank	US\$49.4 million (14%)	US\$299 million (86%)	Integrated solar combined-cycle with a capacity of 271 MW including 29 MW from solar	Reform tariffs, subsidies, and cost-recovery goals	Generate 80 GWh per year; and reduce 149,975 tonnes of CO ₂ eq in 25 years
Namibia	2013-2014	The UNDP, Ministry of Mines and Energy (MME) of Namibia, Renewable Energy and Energy Efficiency Institute (REEEI)	US\$1.72 million (66%)	US\$0.87 million (34%)	Construction and commissioning of a 50 MW commercial CSP	Form policy issuance of CSP concessions to IPPs	Generate 175.2 GWh annually, and reduce 4.8 million tonnes of CO ₂ eq (with energy storage) or 2.4 million tonnes of CO ₂ eq (without energy storage) over 10 years

Source: GEF PMIS (2014)

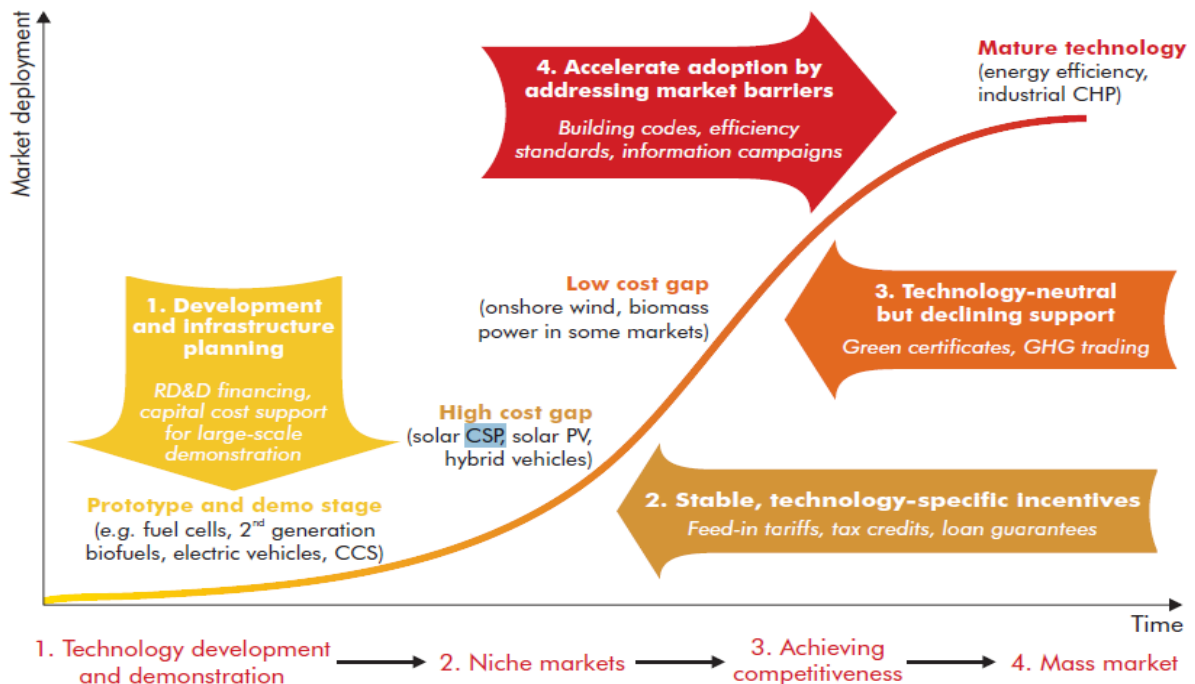


Figure 3. CSP in Clean Energy Technologies Value Proposition. Source: IEA, 2010

The goal of this GEF project was to reduce greenhouse gas emissions from anthropogenic sources by increasing the market share of low greenhouse gas emitting technologies. The project was also designed to contribute to the global learning of the CSP technology to drive down its costs to commercially competitive levels through economies of scale and innovation. A US\$43.2 million GEF grant was allocated to cover the costs of policy development, private sector engagement, and the incremental cost of the plant arising from the addition of the solar field.

GEF's support for the proposed project was critical for the following reasons: (a) it helped mitigate the high financial and technical/operational risks of grid based solar technology that were usually high in developed countries as well as relatively advanced middle-income countries such as Morocco; (b) the success of the proposed pilot project was a critical step in the gradual but global approach for adapting and developing grid based solar technologies on a large scale, and GEF involvement would leverage technical knowledge and international best practice to ensure the success of the project; (c) it helped confirm that Morocco and the Mediterranean region in general had a large potential market for dissemination of the technology; (d) the potential for cost reduction was high because of the significant size of the market for this type of technology, not only in the region but also worldwide; and (e) the GEF support accelerated the dissemination of grid based solar energy in the power market of Morocco, and ultimately achieved a very large quantity of reduction in greenhouse gas emissions.

MAJOR PROJECT COMPONENTS

There were three major project components: (1) policy improvement for Morocco to facilitate private investments in renewable energy technologies; (2) the integration of a solar trough collector field (of about 151,000 m²) producing a minimum energy output with a traditional natural gas-based power generating unit, namely a hybrid power plant; and (3) economic and financial analysis for the project.

PROJECT ACHIEVEMENTS

Three achievements were expected from the project. First, the project was expected to facilitate the development of competitive bidding procedure for CSP power investments from both public power utilities and independent power producers (IPPs) with government policy support. The competitive bidding received a limited number of responses from the IPPs. The Morocco's public power utility decided to finance the CSP plant itself. The ONE thus became the owner of the plant. Second, a solar trough collector field (of about 151,000 m²) was completed to produce energy. The solar energy production system was integrated with a traditional natural gas based power generating unit to make the whole power plant a hybrid one. The CSP station had a capacity of 20 MW and could produce 37.5 GWh of solar energy per year. The total hybrid power plant installed capacity was 472 MW. Third, an economic and financial analysis of the project was performed. The net present value and internal rate of return of the project were US\$305 million and 16.6%.

POLICY DISCUSSIONS

The government of Morocco embarked on a program to reform the energy sector and to promote private investments in infrastructure. The energy policy of the government was to continue the privatization process. Open competitive bidding was carried out among reputable IPPs and the bidder offered lowest price among the responsive proposals was selected in order that net economic and financial benefits could be maximized. In the power sub-sector, the government took important steps to secure private investors to operate the sector's generating and distribution facilities, including (1) the September 1997 financial closure for the Build, Transfer, and Operation (BTO) of the Jorf Lasfar power plant (4x330 MW); (2) rationalization of electricity tariff structures combined with increases in tariff levels; (3) concession for the operation of the power and water distribution systems of the cities of Casablanca; and (4) creation of the CDER which is responsible for undertaking studies and research addressed to promote and develop the utilization of mini-hydro, solar, and wind technologies. When the GEF project was under preparation and implementation, the main issues confronting the power sector included lack of regular adjustment of electricity tariffs, the magnitude of the arrears owed by some of the Régies (the municipal utilities) to ONE, the high level of taxes imposed on the fuels used for power generation, the lack of proper regulation and a regulating agency.

The GEF project in Morocco focused on one important policy issue: increasing private investments in renewable energy. The project supported private participation in the power sector, especially on the generation side. It also promoted the development of environmentally sustainable energy production. The proposed GEF grant supported the government policy to further develop renewable energy and to promote private participation in the energy sector as well as actions underway which complemented private participation, such as the reform of the sector's regulatory framework and practices. The project contributed further to increasing institutional capacity and reliance on renewable energy, widening private sector participation, and meeting growing demand for electricity (World Bank, 2006).

The approach to promoting private investments in CSP was open bidding for the CSP project. Bidding the project with single contract for the construction, operation and maintenance of the plant achieved smooth operation of the plant. The GEF Morocco project involved the financing of only one contract, jointly financed by the ONE, the World Bank and African Development Bank. The project went through international competitive bidding and had its procurement actions advanced and completed before the World Bank's Board approval of the grant. The ONE, with the support of its technical advisor Fichtner Solar, dealt with only one contractor, Abengoa, which introduced simplicity to an already complex project. However, the bidding did not effectively involve the private sector. The reason was that the electricity market condition in Morocco was not attractive to private investors at that time. Feed-in tariff policy and company corporate tax exemption policy were not available in the market. The private sector did not have guaranteed return.

VII. Case Study: GEF South Africa CSP Project

RATIONALE AND OBJECTIVE OF THE GEF PROJECT

Solar thermal electricity was considered as an attractive energy supply option for South Africa, since this country has abundant solar resources, available land and a technical infrastructure that could support extensive deployment of CSP technologies. However, many barriers such as high up-front capital investment costs and insufficient incentives for private investments, were preventing CSP technologies from deploying and developing. Given this background, from 2000 to 2001, the GEF, the World Bank, and the National Renewable Energy Laboratory (NREL) of the United States jointly financed the first CSP study project in South Africa: Concentrating Solar Power for South Africa Study.

The goal of the project was to support South Africa in developing renewable energy technologies and mitigating greenhouse gas emissions. The objectives of the project were to (1) evaluate the leading solar thermal electric technology options with regards to their current and future potentials for South Africa; (2) conduct a broad site assessment to identify the most attractive areas for potential plants; (3) identify preferred system(s) that could be economically feasible for Eskom to implement in the coming decade; and (4) identify specific policy and other constraints that need to be addressed to attain a sustainable deployment of solar thermal electric systems in South Africa.

MAJOR PROJECT COMPONENTS

The major project components included (1) evaluation of CSP technology options according to certain criteria; (2) identification of a reference site to provide information for technology assessment; (3) conceptual designs for promising technologies; (4) performance figures for simulated plant operation; (5) estimation of capital cost, operation and maintenance (O&M) figures and life-cycle costs; (6) evaluation of environmental and social impacts; and (7) evaluation of the viability of CSP implementation under the new national policy.

PROJECT ACHIEVEMENTS

The major project achievements included: (1) two CSP technology options were identified and evaluated according to the international CSP technology criteria for the government and power utility of South Africa; (2) a reference site at Upington in South Africa was identified for CSP technology assessment; (3) based on the current state-of-the-art CSP technologies, a concept was designed to meet the region's power dispatch requirements; (4) an operation of 140 plant designs were simulated and evaluated by using international standard modelling and assessment software packages; (5) capital cost, O&M costs, and life-cycle costs of a future CSP plant were estimated; (6) the environmental and social impacts on the region, due to the implementation of CSP technologies were assessed; and (7) through consultation with manufacturers and suppliers, and national policy makers, a policy reform to facilitate CSP investment was proposed.

POLICY DISCUSSIONS

This project was successful in two policy areas. First, the project produced a policy for development of CSP generation in South Africa. In early 2000s, the commercial exploitation of South Africa's renewable energy sources, including CSP, was very limited, but it was clear that the cost of renewable energy would continue to decline as technologies mature. Government policy supports to CSP technology development and investment should include government capital support and other financial incentives to the development of new renewable technologies. These policies may cover (1) feed-in tariff mechanisms for renewable energy generation; (2) portfolio quotas with or without tradable certificates; (3) tax incentives; and (4) green pricing. Eskom has confirmed their interest in proceeding project development with the government CSP policies. As a measure of their interest and commitment, they have decided to proceed with the next phase (detailed design) without accessing further GEF support.

In addition, the GEF first CSP project in South Africa transferred knowledge and built up initial CSP development capacity to the country. In 2005 after the GEF project was completed, the government of South Africa established Renewable Energy Finance and Subsidy Office. The office's mandate included the management of renewable energy subsidies and provision of advice to developers and other stakeholders on renewable energy finance and subsidies, including size of awards, eligibility, and procedural requirements.

With the new CSP investment policy and locally-developed capacity in CSP development through the GEF project, in the 2010s, South Africa built two CSP power plants: (1) Khi Solar One with a capacity of 50 MW in the Northern Cape Region, using solar tower technology; and (2) KaXu Solar CSP 100 MW in Pofadder Sudáfrica, using parabolic trough technology. These two CSP plants will mitigate 498,000 tonnes of CO₂ eq each year when in full operation.

VIII. Case Study: GEF Egypt CSP Project

RATIONALE AND OBJECTIVE OF THE GEF PROJECT:

The electricity demand was increasing rapidly in Egypt with an average rate of 7% in the late 1990s and 2000s. The strategy of the government of Egypt was to continue implementing gas-fired power plants, with a long-term strategy to increase the share of renewable energy power in the generation mix. The government was targeting 3% of its electricity to be generated from renewable energy sources by 2010; and 20% by 2020. Egypt is endowed with abundant solar resources and favorable geological locations. To achieve the ambitious goal, successful demonstration of the operational viability of hybrid solar thermal power generation with CSP technologies would be the key to achieve the learning effect and economies of scale, as the use of the technology expands.

The objective of the GEF project was to increase the share of solar-based electricity in the Egyptian energy generation mix, and also to contribute to the government's objective of

increasing the share of renewable energy. Besides, this project ran parallel with the objectives of GEF's programming of reducing, over the long-term, the costs of energy technologies with low greenhouse gas emissions.

Many sites in Egypt comprised an uninhabited flat desert area with high intensity of direct solar radiation and were eligible to be selected to implement the projects. The Kureimat site was selected due to the minimal additional infrastructure required because of its proximity to water resources (the Nile River) and its proximity to the 750 MW El Kuriemat Power Plant Combined Cycle.

MAJOR PROJECT COMPONENTS

The project was implemented through three components: (1) The design, construction and initial operation of the proposed ISCC Plant; (2) Capacity building to New and Renewable Energy Authority (NREA) through consulting services for management during the construction, testing and operation of the plant; (3) Environmental and Social Impact management component.

PROJECT ACHIEVEMENTS

The project achieved the objectives of increasing the share of solar-based electricity generation (20 MW) in Egypt and diversifying electric power generation. These included: (1) the construction of the integrated solar combined cycle power plant in Kureimat with total electricity of 35.1 GWh per year generated from solar sources, accounting for 4.1% of the total energy produced in the hybrid plant; (2) the demonstration of a new technology with prospects for scale up through learning and dissemination; and (3) greater awareness of this technology in Egypt, the region, and the world.

POLICY DISCUSSIONS

In line with the Egyptian structural adjustment policy, the power sector, operating under the direction of the Ministry of Electricity and Energy (MEE), was unbundled and reorganized in 2001. Power operations were organized under the Egyptian Electricity Holding Company (EEHC) that included five generation companies, seven regional distribution companies, a single transmission company, and IPPs. A regulatory board were established, chaired by the Minister of Electricity and supported by other ministries and consumers. With this policy adjusted structure, the government of Egypt intended to incentivize private investments in CSP technologies, but two government policies actually discouraged the private sector to invest in CSP technologies.

First, the government foreign currency repayment policy negatively affected CSP technology investments in Egypt. In the 2000s, Egypt had a rapidly expanding economy that was based on the availability of reliable and low cost electric power. The rate of growth of electricity demand in Egypt exceeded 6.5% per year and was expected to remain in the 6-7% range over the next 10 years. Three private sector generation projects were implemented in Egypt adding a capacity of 1,950 MW to the national grid. While the government strategy was very much to continue to award

contracts to private investors in order to meet the need for additional capacity, the drop in the Egyptian pound to major foreign currencies resulted in a significant financial burden on the EEHC, since many of its loans were denominated in foreign currency. In Egypt where local currency was in high inflation (11.0% in 2007, 11.7% in 2008, 16.2% in 2009, and 11.7% in 2009), if a utility company borrowed US\$1 from a foreign bank in any of the year between 2007 and 2011, the firm needed to pay more than US\$1.1 back to the bank to clear the debt even without paying the interest. With fixed electricity sale prices, the power utility cannot make enough revenue to cover the costs. As a result, the government foreign currency policy for private investments caused private interest in power infrastructure in Egypt to evaporate.

The failure of the government foreign currency policy was confirmed by a survey that was conducted by an independent consulting firm with former investors who had previously expressed interest in developing the CSP project as IPPs. In this survey, 31 IPP investors were contacted. Only one company filled out the requested questionnaire; another 21 responded by stating that they were either not interested in general or not interested given the policy change. Three firms contacted were no longer in existence, and six responded that they would be interested in principle, but did not fill out the questionnaires and thus were not considered serious. The survey concluded that the change of government policy in foreign currency repayment for local firms greatly reduced the interest of private investments in CSP technologies in Egypt.

Electricity tariffs in Egypt did not favor CSP investments. Electricity tariffs in Egypt remain uniform across all distribution companies. The weighted average tariff was piaster 12.8/kWh (US\$0.02/kWh) in the late 2000s. There were significant cross subsidies in the tariffs, and thus for most consumer groups the tariffs were substantially below marginal cost. For the two key consumer groups, households and the agriculture sector, tariffs were estimated to be half of the marginal cost. Until the GEF project was under implementation, subsidized tariffs remained an obstacle for large-scale private sector involvement, especially in the distribution business and also for the development of large-scale commercial renewable energy operations. However, the government announced its intention to gradually increase tariffs to allow for better cost recovery and reflection of true cost of electricity service delivery.

Having gained knowledge and experience from the GEF CSP project, the government has committed to sector reforms and has been facilitating renewable energy development through specific policy interventions. The Supreme Energy Council of South Africa announced in March 2010 the key policy steps of wind and CSP scale-up in the country that were proposed under the new electricity law. These policy steps included (World Bank, 2012b):

- acceptance of foreign currency denominated Power Purchase Agreements (PPAs) and confirmation of central bank guarantees for all Build Own Operate (BOO) projects;

- approval of the need to cover additional costs for renewable energy projects through tariffs;
- approval of zero customs duty on wind and CSP equipment;
- finalization of the land use policy for wind and CSP developers; and
- permitting support for developers with respect to environmental, social and defense permits.

These new policies will assist the private sector in (1) de-risking from foreign exchange; (2) allowing higher electricity tariffs for electricity produced from CSP technologies; (3) incentivizing private investments by tax exemption in CSP technologies; and (4) giving favorable permits for CSP technology investors in land use.

IX. Barriers in GEF Investments in CSP Technologies

Several barriers were found among the GEF CSP Projects. First, capital costs for CSP technologies were higher than expected. Host countries were required to address additional costs for the projects that could not produce the rated power on a firm basis. Among the GEF funded projects, the incremental costs exceeded the GEF's grants. Countries had to provide significant cash subsidies to operationalize the plants. To resolve this issue, government feed-in tariff policies should be effective to guarantee reasonable return of the CSP technologies.

Second, institutional capacity for CSP projects in developing countries was necessary for successful demonstration and deployment of CSP technologies. Even though the projects were intended to be demonstrations, it proved difficult for developing countries to adopt technologies that were not fully commercialized. Insufficient market viability for CSP technologies in developed countries was associated with low institutional capacity development in developing countries. To resolve this issue, government policies need to be developed to foster capacity building and institutional development for CSP technology deployment in developing countries.

Third, the projects were not mature enough to attract financing from the private sector. The co-financing resources for the GEF projects were from the government, international organizations, and multilateral development banks. Commercial banks have not yet been involved in CSP financing for GEF projects. To resolve this issue, more public funding or grant is needed to overcome cost gaps for private investments, or mass investments are needed to scale-up CSP technologies and therefore reduce the capital investment and production costs.

Fourth, an undeveloped power transmission infrastructure makes it difficult for CSP development in developing countries. Access to electricity market added complexity and reduced private sector interest. Governments in developing countries should have policies that request power grid companies to purchase CSP energy mandatorily. Without a

reformed government policy and regulatory framework, which encourage local grid utilities to purchase renewable power at reasonable prices, the private sector would not have incentives to invest in CSP technologies.

X. Future Policy Direction to Unlock Barriers

The GEF has a unique position to unlock the aforementioned barriers. First, the barrier of high capital investment cost per kilowatt can be unlocked by an international joint policy effort. If countries can jointly develop and deploy 15 GW to 30 GW of CSP plants, it will form a large economic scale. In addition, CSP technology breakthrough as announced by China would substantially cut manufacturing costs of CSP technologies in these developing countries. With rich experience in CSP investments in developing countries, the GEF will continue its catalytic, innovative, and cost-effective role in developing policy, building capacities and facilitating reforms on energy tariffs and energy systems in these countries. To do so, the GEF is in cooperation with the Clean Technology Fund (CTF) on financing a CSP program in the Middle East in the period of 2014-2018. The objectives of this program are to develop energy policies that foster CSP technology investments in developing countries, and to install 710 MW of CSP in the region, including 460 MW in Morocco, 100 MW in Jordan, 100 MW in Egypt, and 50 MW in Tunisia. The CTF is planning to finance US\$650 million for the program. The first project under this program has been approved for Ouarzazate-I in Morocco. The GEF and its partners are on the way to assist developing countries and countries with economies in transition in scaling up CSP technologies and reducing capital investment costs.

XI. CONCLUSIONS AND POLICY RECOMMENDATIONS

CSP technologies are promising due to their capabilities to store renewable energy and to be developed at a large scale. However, these technologies are not competitive in the current energy market because of several barriers including high front cost per kilowatt investment, lack of government incentives, low electricity tariffs in the energy market, and lack of local capacity in technology development. These barriers can be unlocked by more effective national government policies and international joint policy effort.

Governments of developing countries need to enact appropriate energy policies to support the development and deployment on a competitive market basis. These policies should:

- (1) provide sufficient financial incentives to the private sector to make sure that private investments in CSP could make a profit at the average rate of return of the market;
- (2) ensure that these financial incentive policies are sustained long enough to cover capital investments of the private sector. Meanwhile, the designed policies should reflect decreasing investment cost of CSP over

time. This is to avoid over investments in CSP in the future.

(3) establish national risk guarantee funds to reduce risk premium of a commercial bank loan to private investments in CSP technologies;

(4) reform power tariffs from flat power tariffs to time-of-use power tariffs. This is to remunerate the flexible power supply provided by CSP to more accurately reflect its benefit to the energy system; and

(5) provide concessional use of government owned land to the private sector in a reasonably long-term. This is to reduce risk for private investors who want to acquire land and use it for renewable energy technology development.

International policies are also needed to support and deploy CSP technologies on an international market basis. These policies may need to:

(1) transfer CSP technologies from countries with successful experiences to countries in need;

(2) develop standards and codes that are particularly suitable for CSP technology development in developing countries; and

(3) involve multiple countries jointly in investing, developing, and deploying large scale CSP plants.

REFERENCES

- [1] G. Beatriz. *Slow development of CSP industry in India caused by policy approach*, 2014. <http://social.csptoday.com/markets/slow-development-csp-industry-india-caused-policy-approach>
- [2] CPI – Climate Policy Initiative (2014) *The Role of Public Finance in CSP Case Study: Eskom CSP, South Africa*, June 2014, Venice, Italy.
- [3] CSP World (2013) *Spain's Government Changes Rules for CSP... Again* <http://www.csp-world.com/news/20130202/00730/spains-government-changes-rules-csp-again>
- [4] EPIA – European Photovoltaic Industry Association (2012) *Global Market Outlook: For Photovoltaic Until 2016*, May 2012, Brussels, Belgium.
- [5] ESMAP – World Bank Energy Sector Management Assistance Program (2011) *Regulatory and Financial Incentives for Scaling Up Concentrating Solar Power in Developing Countries*, June 2011, Washington D.C.
- [6] GEF PMIS - Global Environment Facility Project Management Information System (2014), a database of the GEF for project management. Cited 5 July 2014.
- [7] Hamilton J. (2013) *Careers in Solar Power*, The Bureau of Labor Statistics, accessed on November 18, 2013. http://www.bls.gov/green/solar_power/
- [8] IRENA (2013a) *Concentrating Solar Power Technology Brief*, IEA-ETSAP and IRENA E10 – January 2013. www.etsap.org
- [9] IRENA (2013b) *Renewable Power Generation Costs in 2012: An Overview*. (2013b) www.irena.org/DocumentDownloads/Publications/Overview_Renewable%20Power%20Generation%20Costs%20in%202012.pdf
- [10] IEA - International Energy Agency (2010) *Technology Roadmap. Concentrating Solar Power.*, Paris. http://www.iea.org/publications/freepublications/publication/csp_roadmap.pdf
- [11] IEA - International Energy Agency (2011) *Solar Energy Perspectives*, ISBN 978-92-6412-457-8, Paris, France.
- [12] NREL – National Renewable Energy Laboratory: *Concentrating Solar Power Projects* <http://www.nrel.gov/csp/solarpaces/> Cited 12 July 2014
- [13] SEIA - Solar Energy Industry Association (2014) *U.S. Solar Market Grows 41%, Has Record Year in 2013*, March, 2014. <http://www.seia.org/news/new-report-us-solar-market-grows-41-has-record-year-2013>
- [14] Solar Thermal Energy News (2014) http://www.helioscsp.com/indice_tags.php?tag=China
- [15] UNDP (2012) *Concentrating Solar Power Technology Transfer for Electricity Generation in Namibia*, Request for CEO Endorsement/approval. Re-submission: December 10, 2012. GEF Project Management Information System
- [16] Vagliasindi M, and Besant-Jones J (2013) *Power Market Structure: Power Market Structure, Chapter 6: Arab Republic of Egypt*, World Bank Publications, March 2013.
- [17] P. Viebahn, S. Kronshage, F. Trieb, and Y. Lechon (2008) *Final Report on Technical Data, Costs, and Life Cycle Inventories of Solar Thermal Power Plants*. Deliverable 12.2—RS Ia of EUIP-NEEDS. www.needs-project.org
- [18] World Bank (2006) *Morocco GEF Project Document, Integrated Solar Combined Cycle Power Project*, November 2006 . Report No: 36485.
- [19] World Bank (2012a) *Implementation Completion and Results Report (TF-91289)* Report No: ICR2173.
- [20] World Bank (2012b) *Egypt and Morocco: Concentrated Solar power* <http://go.worldbank.org/2R0W5H1010> Cited 5 July 2014
- [21] SASTELA - Southern Africa Solar Thermal and Electricity Association (2012), *CSP in South Africa*. <http://www.sastela.org/csp-in-south-africa.html> Cited 5 July 2014.



**Journal of Energy Challenges
and Mechanics**

ISSN 2056-9386

<http://www.nscj.co.uk/JECM/>

Editor:

Dr. Henry Tan
University of Aberdeen, Scotland, United Kingdom

Scope:

Since James Watt, a Scottish inventor, improved efficiency of the steam engine, human civilization relies more and more on a steady supply of energy. Today we are at a transitional age. On the one hand, we see technology advances in the exploration and development of oil and gas, a depleting resource; we see growth in handling aging and decommissioning. On the other hand, we see ideas and plans for new energy infrastructure. This journal is about energy challenges and the underlying mechanics, involving multiple disciplines in science, technology, management and policy-making. Mechanics, fundamentally, is about force and the related behaviours, where force is about relationships, including those physical, human and social. For mechanics, the journal covers interactive boundaries with many other disciplines. For energy, topics include both fossil fuels and many different forms of renewable energy; also, issues related to energy economy, energy policy, efficiency, safety, environment and ecology will also be covered.



Cove Bay, Aberdeen, Scotland, United Kingdom